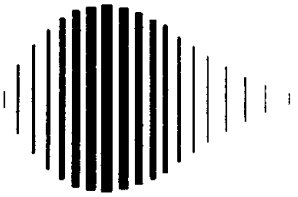

NATIONAL CENTER FOR EARTHQUAKE ENGINEERING RESEARCH

State University of New York at Buffalo

INELASTIC THREE-DIMENSIONAL RESPONSE ANALYSIS OF REINFORCED CONCRETE BUILDING STRUCTURES (IDARC-3D)

PART I - MODELING

by

Sashi K. Kunnath and Andrei M. Reinhorn

Department of Civil Engineering
State University of New York at Buffalo
Buffalo, New York 14260

Technical Report NCEER-89-0011

April 17, 1989

This research was conducted at the State University of New York at Buffalo and was partially supported by the National Science Foundation under Grant No. ECE 86-07591.

NOTICE

This report was prepared by the State University of New York at Buffalo as a result of research sponsored by the National Center for Earthquake Engineering Research (NCEER). Neither NCEER, associates of NCEER, its sponsors, the State University of New York at Buffalo, nor any person acting on their behalf:

a. makes any warranty, express or implied, with respect to the use of any information, apparatus, method, or process disclosed in this report or that such use may not infringe upon privately owned rights; or

b. assumes any liabilities of whatsoever kind with respect to the use of, or the damage resulting from the use of, any information, apparatus, method or process disclosed in this report.

INELASTIC THREE-DIMENSIONAL RESPONSE ANALYSIS OF REINFORCED CONCRETE BUILDING STRUCTURES (IDARC-3D)

PART I - MODELING

by

S.K. Kunnath[1] and A.M. Reinhorn[2]

April 17, 1989

Technical Report NCEER-89-0011

NCEER Contract Numbers 86-3032, 87-1005, and 88-1005

NSF Master Contract Number ECE 86-07591

1 Research Assistant Professor, Department of Civil Engineering, State University of New York at Buffalo

2 Associate Professor, Department of Civil Engineering, State University of New York at Buffalo

NATIONAL CENTER FOR EARTHQUAKE ENGINEERING RESEARCH
State University of New York at Buffalo
Red Jacket Quadrangle, Buffalo, NY 14261

PREFACE

The National Center for Earthquake Engineering Research (NCEER) is devoted to the expansion and dissemination of knowledge about earthquakes, the improvement of earthquake-resistant design, and the implementation of seismic hazard mitigation procedures to minimize loss of lives and property. The emphasis is on structures and lifelines that are found in zones of moderate to high seismicity throughout the United States.

NCEER's research is being carried out in an integrated and coordinated manner following a structured program. The current research program comprises four main areas:

- Existing and New Structures
- Secondary and Protective Systems
- Lifeline Systems
- Disaster Research and Planning

This technical report pertains to Program 1, Existing and New Structures, and more specifically to system response investigations.

The long term goal of research in Existing and New Structures is to develop seismic hazard mitigation procedures through rational probabilistic risk assessment for damage or collapse of structures, mainly existing buildings, in regions of moderate to high seismicity. The work relies on improved definitions of seismicity and site response, experimental and analytical evaluations of systems response, and more accurate assessment of risk factors. This technology will be incorporated in expert systems tools and improved code formats for existing and new structures. Methods of retrofit will also be developed. When this work is completed, it should be possible to characterize and quantify societal impact of seismic risk in various geographical regions and large municipalities. Toward this goal, the program has been divided into five components, as shown in the figure below:

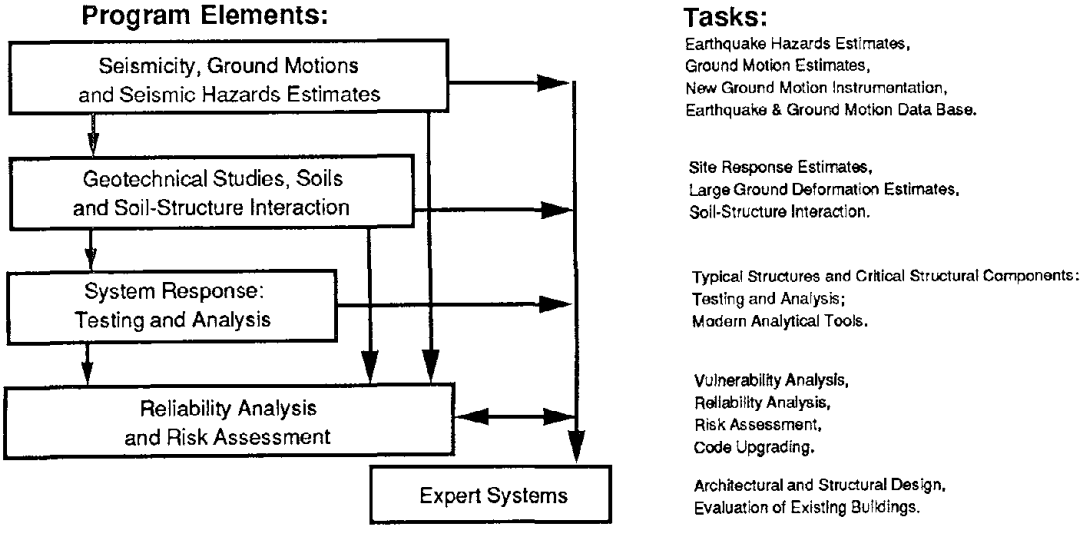

System response investigations constitute one of the important areas of research in Existing and New Structures. Current research activities include the following:

1. Testing and analysis of lightly reinforced concrete structures, and other structural components common in the eastern United States such as semi-rigid connections and flexible diaphragms.
2. Development of modern, dynamic analysis tools.
3. Investigation of innovative computing techniques that include the use of interactive computer graphics, advanced engineering workstations and supercomputing.

The ultimate goal of projects in this area is to provide an estimate of the seismic hazard of existing buildings which were not designed for earthquakes and to provide information on typical weak structural systems, such as lightly reinforced concrete elements and steel frames with semi-rigid connections. An additional goal of these projects is the development of modern analytical tools for the nonlinear dynamic analysis of complex structures.

The interaction of analytical and experimental studies of structural systems forms a key aspect of the Existing and New Structures Program. The research summarized in this report is a step toward general nonlinear analysis of reinforced concrete buildings and it strongly relies on experimental evidence provided by other NCEER projects. In turn, the computer program developed in this work aids in the design and interpretation of experiments. The idealization and analysis of three-dimensional reinforced concrete buildings, reported here, have several new features. In addition, this work has proposed an improved damage model which is needed in risk analysis and studies of possible code improvements.

ABSTRACT

A comprehensive modeling scheme is developed to evaluate the inelastic response of *three-dimensional (3D) reinforced concrete buildings* under the action of seismic loads. The structural model integrates 3D *inelastic biaxial column elements* with *inelastic uniaxial beam and shear wall components* to represent a realistic model of overall structural behavior. The motivation for such a modeling scheme is based on observation and past experimental verification which indicates that biaxial bending interaction is significant primarily for column elements.

Component modeling is established through the development of element macro-models (columns, beams, shear-walls) which incorporate the essential characteristics of reinforced concrete behavior. A *distributed flexibility model* with a varying contraflexure point is used for the stiffness formulation. The finite size of connecting joints is accounted for in constructing element stiffness matrices.

A *visco-plastic force-deformation model* which is derived from the modified Bouc model and includes the effect of *biaxial bending interaction* is developed for the column elements. Parametric studies are carried out to identify parameters which describe *strength and stiffness degradation* based on experimental data. For uniaxial behavior, a nonsymmetric trilinear envelope is used in conjunction with an available hysteretic model which permits the modeling of stiffness degradation, strength loss, and bond-slip.

A step-by-step incremental dynamic analysis of the assembled macro-models is performed by direct integration using an explicit algorithm based on Newmark's constant-average-acceleration method. The moment-deformation history is monitored at critical sections to update hysteretic parameters. A single step *force equilibrium correction* is

implemented to prevent error accumulation due to unbalanced loads, and an approximate scheme for *stiffness updating during unloading/reloading* is formulated. *P-delta effects* are included by considering eccentric floor-weights due to inter-story drift.

A new *seismic damage model* is proposed to assess response statistics following earthquake action. The model is both an extension and a generalization of existing models. The formulation accounts for damage contributions arising from permanent deformation and strength-loss (expressed as a function of dissipated energy).

Several *numerical examples* are presented (1) to *validate* the *models* developed in this study, and (2) to demonstrate the effectiveness of the modeling schemes to *simulate experimental results*. Comparative studies with existing analytical models are also carried out.

All developments are incorporated into a new modular computer code *IDARC-3D*. In addition to standard analytical capabilities for response evaluation, the program is designed to facilitate interpretation of experimental testing: (1) *cyclic loading with force or deformation control* (2) "**time-series**" testing in which *sequential dynamic loads* may be applied and "initial-stress" levels of previous analyses may be recovered and/or modified. Program input will be facilitated through a 3-dimensional *interactive graphical preprocessor*. Program features with a user guide, and details of the graphical interface, will be published as a separate Technical Manual.

ACKNOWLEDGEMENTS

This report is based in part on the Ph.D dissertation of the first author completed under the supervision of the second author.

The authors wish to express their thanks to Professor M. Constantinou for his suggestions on the biaxial model formulation, and to Professor J.B. Mander and Joseph Bracci for their contribution in the development and implementation of the damage model presented in this report.

Funding for this work was provided through the National Center for Earthquake Engineering Research (NCEER) Contract Nos.86-3032, 87-1005A, 88-1002A, 88-1005B under the National Science Foundation Master Contract No.86-07591 and the State of New York. The support is gratefully acknowledged.

TABLE OF CONTENTS

LIST OF ILLUSTRATIONS

LIST OF TABLES

SECTION 1

INTRODUCTION

The aftermath of the 1968 Tockachi-Oki earthquake in Japan and the 1971 San Fernando earthquake in California changed forever the concepts in reinforced concrete (R/C) modeling. The realization that earthquakes can be catastrophic, and that a *reliable* evaluation of structural safety against severe random load reversals was essential, fueled research efforts both in Japan and the United States to arrive at a more comprehensive understanding of the mechanics of inelastic R/C behavior. Until then, the modeling of R/C behavior was but a simple extension from well established steel material laws, while the modeling of structural response was dominated by the convenience of the finite element method.

In defining the nature of nonlinearities associated with R/C structural analysis, it must be stressed that only low to medium rise buildings are of significant concern in the context of the present study since they fall into a class of structures that are particularly vulnerable to seismic excitation. Consequently, geometric nonlinearities, in terms of the deformed configuration of the system, do not come into play in either *serviceability limit* or *moderately damaged* states of the system. However, P-Delta effects due to inter-story drifts, do influence the response of the building in the region near *collapse* and must be taken into account. On the other hand, nonlinearities which arise from material behavior dominate the inelastic response of R/C components. The mechanics of material nonlinearity, however, has proved to be so complex that even the efforts of more than a decade of analytical research and experimental testing has not afforded a realistic scenario of three-dimensional (3-D) structural response. This fact can be evidenced by the recently completed phase of the U.S.-Japan Cooperative Research Program (Wight, 1985) which examined both full-scale psuedo-dynamic tests and scaled model shaking table studies on a 7-story frame-wall structure of realistic size and complexity. Among other findings, the limitations and drawbacks of analytical modeling schemes found in most existing computer programs became evident (Charney and Bertero, 1982).

Despite the development of sophisticated models into which are incorporated the mechanics of micro-level behavior, and the enhancement of available computational tech-

niques, the field of R/C structural analysis still lacks an integrated tool which is capable of realistically modeling 3-D structures at the global level while still capturing the essence of component behavior. At the same time, there is also the need for both an *engineering* understanding of complex component behavior and a *qualitative* interpretation of the overall inelastic response of structures to earthquake action. The inability of available analytical models to translate response parameters into physically meaningful quantities has recently brought the concepts of damage and damageability of reinforced concrete structural systems into the forefront of analytical modeling procedures. A rational prediction of damageability, however, requires a definition of damage that can be quantified and incorporated into a general analysis program and an analytical tool that is capable of reproducing the inelastic response of R/C structures and their components with reasonable accuracy. The role of the latter is considerably more significant since the parameters that are generally used to establish damage levels depend almost entirely on the results of the inelastic dynamic response analysis. Hence, the present study will focus primarily on analytical approaches to successfully model inelastic behavior of R/C buildings. The use of a damage model then serves as a qualitative indicator of damage and energy-reserves in the overall structural system.

The investigation of modeling schemes for 3-D R/C buildings, both at the structural and the material levels form the central focus of this report. The proposed schemes that arise from the study have encompassed the reliability of material behavior and the mechanics of R/C structural response. The resulting response quantities are further represented in an engineering sense where capacity, demand, and damage can be delineated.

The remainder of this introductory chapter is divided into three sections. The first section reviews briefly the advantages and disadvantages of micro-modeling techniques as opposed to a macro-modeling approach for analysis of R/C building structures. This assessment serves to justify the use of macro-models for characterizing component behavior. Next, a comprehensive state-of-the-art review on modeling schemes for R/C analysis is carried out. The review focuses on two aspects; component modeling and hysteretic modeling. A separate section is devoted to the review of biaxial column bending since it is a relatively

recent development in R/C component modeling, and also because it forms the highlight of the 3-D modeling scheme developed in this study. The concluding section in this chapter sets forth the scope and objectives of this research report.

1.1 Micro vs. Macro Modeling

The advent of the finite element method for analysis of structural systems proved to have a dominant effect on modeling techniques developed for most materials. Reinforced concrete was no exception. Three-dimensional beam elements can still be used effectively for the *elastic* analysis of frame structures. The introduction of infills or shear walls complicate the modeling task but by no means restrict the capability of the method. Apart from finite element schemes, other micro-modeling techniques are still used, especially for the analysis of single components. One such method is the *fiber* or *filament* model representation of the component which offers even more flexibility than FEM procedures (such as the incorporation of distributed plasticity).

Micro modeling schemes, however, are unsuitable for inelastic analysis of entire structural systems primarily because of its immense demand on computational needs. Besides the enormous amount of computational resources required, the microscopic interaction of steel and concrete and the inter-play of flexure, shear and bond-slip (not merely for one component but for multiple members) are extremely difficult to model. Moreover, any cyclic stress-strain description is bound to be approximate, in part due to simplifications which are introduced to aid numerical algorithms. Thus, any step toward refined micro-modeling without a compensating improvement in reliability is of little practical value.

Macro-modeling schemes, on the other hand, offer an attractive alternative both in the economy of computation and in the flexibility of modeling. It is possible to account for almost any type of behavior pattern in an *equivalent* sense. This ability of a macro-model to capture the overall behavior pattern using simplified extensions from the micro-level makes it ideal for R/C modeling. In fact, almost all analytical schemes in use today for the inelastic analysis of R/C structures are based on macro-modeling techniques. The present study continues to adhere to this approach.

1.2 State-of-the-Art Review on Modeling of R/C Elements

This section reviews briefly the state-of-the-art in structural and hysteretic modeling schemes. At the structural level, both component modeling and global structural modeling are reviewed. At the material level, available restoring force models for both uniaxial and biaxial excitation are discussed. This review serves as the basis and the justification for the modeling schemes presented in this report.

1.2.1 Component Modeling

In the member-by-member modeling of structures, a component can be treated as a single element, or be discretized longitudinally and/or across the depth of the section. The first option leads to procedures in macro-modeling, while the second forms the basis of filament models and micromodeling schemes. The following discussion deals primarily with techniques for macro-modeling of structures.

Early attempts to study the earthquake response of multistory buildings were based on shear-beam idealizations (Penzien, 1960) in which an assembly of beams and columns that constituted a story level was represented by a single nonlinear spring with one lateral degree-of-freedom per floor. This approach obviously failed in the presence of shear walls. Also, failure mechanisms at the story level could be detected only if the structure was of weak-column, strong-beam type, a practice discouraged in earthquake-resistant design.

Berg and DaDeppo (1960) were among the first to develop procedures for the analysis of regular plane frames. They formulated solution schemes of the dynamic equations of motion using both Runge-Kutta and Milne's Predictor-Corrector methods. Heidebrecht et al. (1960,1964) devised a discrete procedure for the solution of continuous systems in which the effect of gravity loads was also included. Though these formulations were used essentially for steel structures, the concept of representing the members of a structure by line elements which in turn could be modeled discretely or by springs, set the stage for the development of models specific to handling reinforced concrete elements.

A multi-component approach to modeling was introduced by Clough et al. (1965) wherein each member is subdivided into two fictitious parallel elements, one elastic-perfectly-plastic and the other elastic (Fig.1.1). The first accounts for yielding while the second

introduces strain hardening. The member stiffness matrix in this case is simply the sum of the stiffnesses of the two components. Aoyama and Sugano (1968) extended this idea to a multi-component representation (Fig.1.2) which allowed for two unique elasto-plastic springs at ends thereby permitting different yield levels. An additional merit of the model was the fact that the end rotation was a function of both end moments, hence accounting for the stress variation along the member.

The main problem with the above approaches was the lack of representation of actual R/C behavior in the inelastic range. Inelastic behavior in R/C sections do not concentrate at joints, instead they spread into the member toward the contraflexure point. This inability to account for varying stiffness or to incorporate such effects as stiffness degradation led Giberson (1969) to develop a general single-component model (Fig.1.3) in which all inelastic deformations are modeled by a pair of rotational springs. However, it was demonstrated later by Takizawa (1973) that the Clough-Aoyama formulations could also lead to similar generalizations.

Variations of the discrete single-component model have also been suggested to account for the spread of inelastic deformations into the member. The initial idea came from Wen and Janssen (1965) who discretized a member into smaller elasto-plastic segments; Powell (1975) proposed using inelastic springs at connections (Fig.1.4a). A more refined alternative was proposed by Takayanagi and Schnobrich (1977) who used distributed stiffnesses for the discretized segments (Fig.1.4b). But the most significant contributions toward the idea of distributing flexibility across member lengths came from Takizawa (1976) and Otani and Sozen (1972). Otani and Sozen (1972) recognized the need to monitor the inflection point based on the stress history. Takizawa, on the other hand, assumed a parabolic distribution (Fig.1.5) with an elastic flexibility at the inflection point. Though the nature of distribution of the inelastic deformation is questionable and the implementation somewhat tedious, it was the first truly varying stiffness model.

Implementations of multi-component modeling can be found in computer programs such as DRAIN-2D (Kanaan and Powell, 1973) and ANSR (Mondkar and Powell, 1975 and 1979). Another program (SAKE) with features similar to DRAIN was developed at Illinois (Otani, 1975). Like the later version of DRAIN (Powell, 1975), it included a Takeda-type

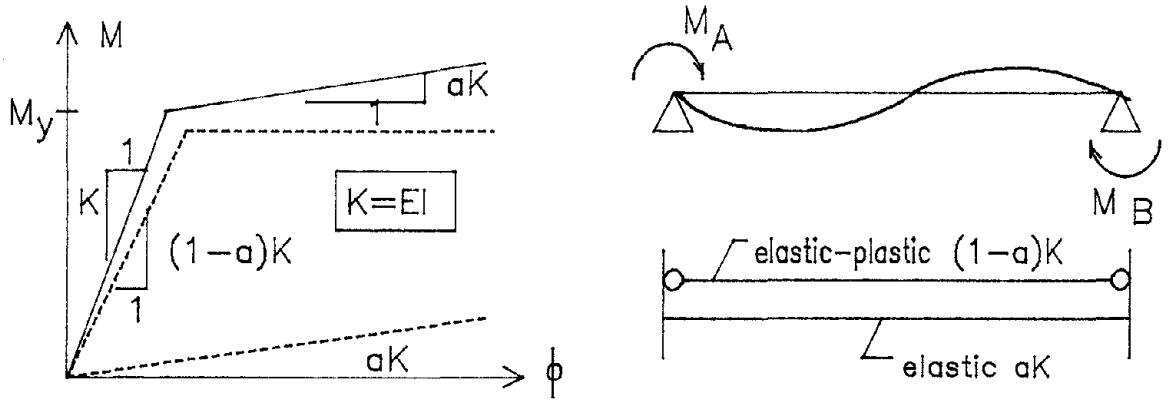

FIGURE 1-1 Two Component Model (Clough et al.,1965)

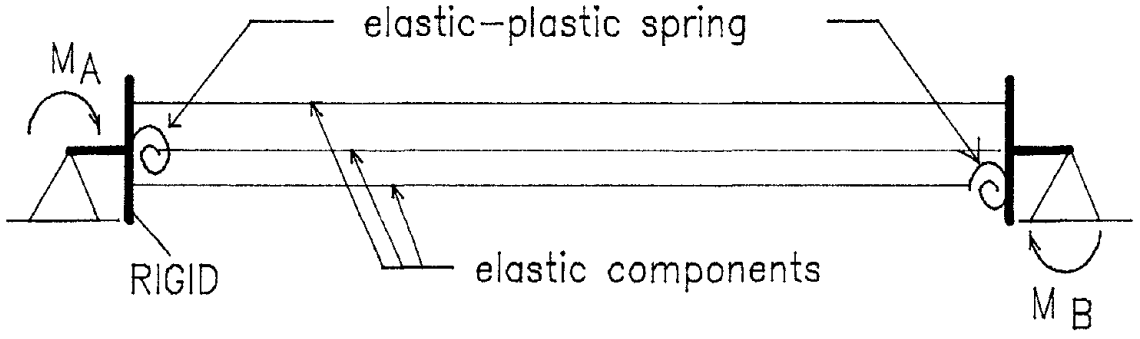

FIGURE 1-2 Multi-Component Model (Aoyama and Sugano, 1968)

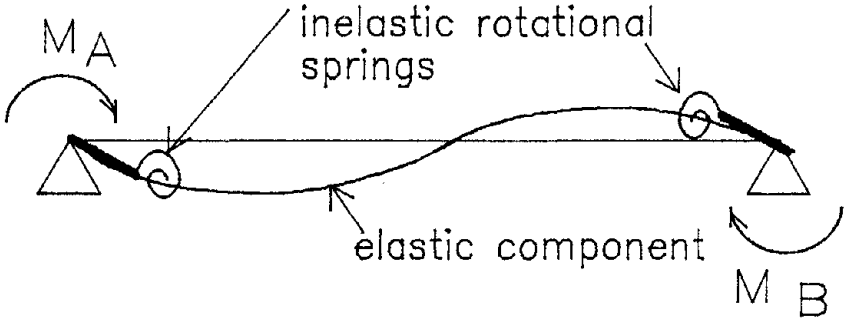

FIGURE 1-3 General Single Component Model

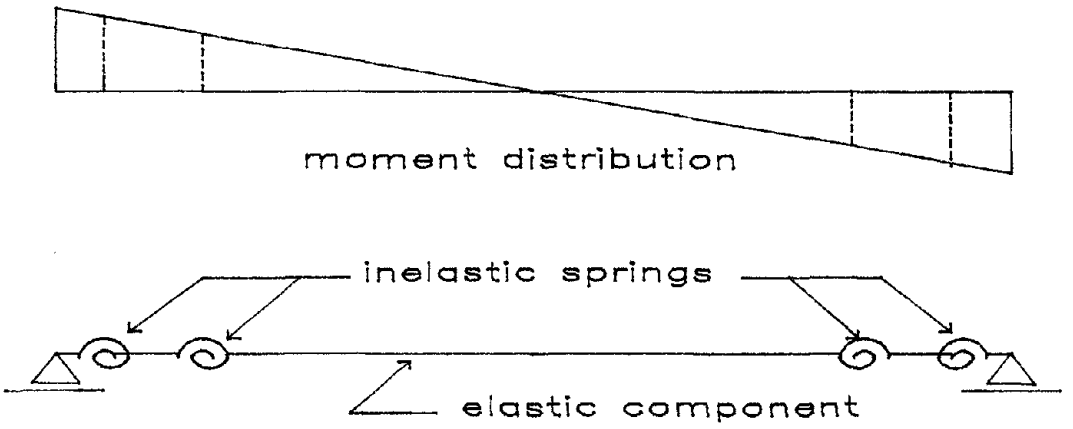

(a) lumped model

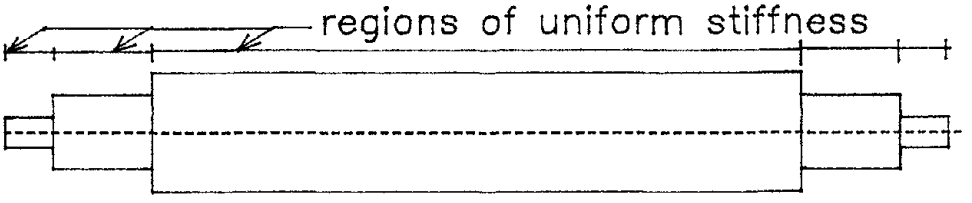

(b) distributed model

FIGURE 1-4 Discrete Element Models

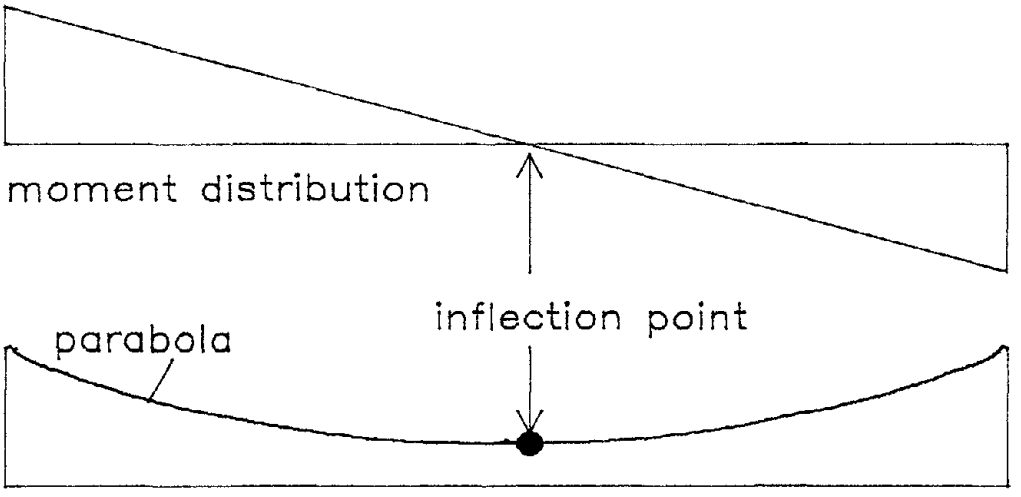

FIGURE 1-5 Distributed Flexibility Model

model (Takeda et al., 1970). Its improvement over DRAIN consisted of the recognition of stiffness changes due to cracking of concrete and yielding of the reinforcement respectively. However, the element stiffness matrices are developed on a flexibility distribution approach which assumes the point of contraflexure to be at the mid-point of sections, rendering it unsuitable for shear-wall structures.

Among the recent works to be found in the literature are several models for inelastic analysis of R/C structures which adopt new variations of earlier schemes. The first of these is by Roufaiel and Meyer (1987) who include the finite size of plastic regions at the ends of the member. But they still use a bilinear hysteretic model in which the initial stiffness must be modified to simulate the idealized behavior. Also, the construction of the envelopes curve using the conventional filament model cannot adequately account for the true deformation characteristics in R/C components where the effects of inelastic shear and bond-slip must be considered. On the other hand, LPM/I, a computer program for lumped parameter models by Ewing et al.(1987) was developed primarily for masonry structures and reports the availability of 11 different spring elements. It offers immense flexibility in modeling though only one of these springs seem suitable for R/C elements. However, the spring characteristics do not allow for non-symmetric envelopes or for the distribution of flexibility. Finally, Zeris and Mahin (1988) propose a fiber displacement model for use with finite element schemes. Despite its effectiveness to represent softening behavior, such a model is unsuitable for global modeling of entire structures or even for single components which experience inelastic shear and/or pinching under earthquake-like loading reversals.

In all of the above models, the effect of variation of axial force during the response has been ignored. In general, the yield capacity of columns and shear walls is significantly affected by the magnitude of axial force. Some attempts in this direction have been made: Takayanagi and Schnobrich (1977) modified the discrete element model to include axial force-moment interaction for the analysis of coupled shear walls; Keshavarzian and Schnobrich (1985) developed a nonlinear column element which used a similar interaction diagram to modify yield levels of the inelastic zones of the member.

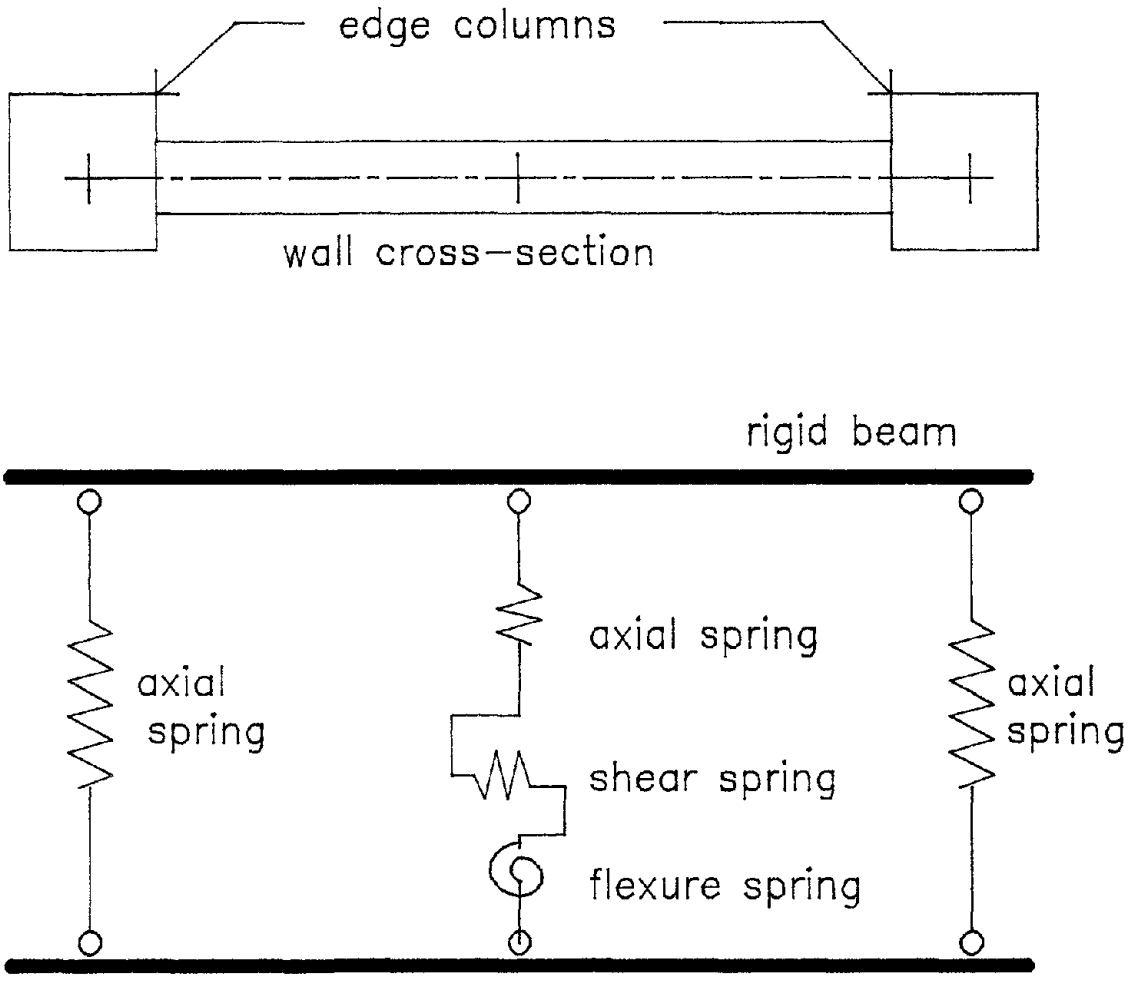

FIGURE 1-6 Three Element Wall Model

Not discussed thus far is the modeling of shear walls which are used extensively in earthquake-resistant design. Until recently, walls were modelled either as equivalent columns with inelastic rotational springs to account for flexural deformations, or as equivalent trusses which had the added capability to account for stress redistribution due to diagonal cracks. Both models were incapable of reproducing shear wall behavior though several ad-hoc changes were incorporated to account for related effects such as shear and axial force fluctuations. In particular, the detection of shear-type failure, a critical failure mode in walls, could not be simulated. Then, during the U.S.-Japan Cooperative Research Program, Kabeyasawa et al.(1983) developed a 2-D wall model which was used in analytical simulation studies. The shear wall, in this model, is composed of three line elements connected by rigid beams at the top and bottom (Fig.1.6). The central element is modeled by means of axial, flexural and shear springs while the edge elements (used only in the presence of edge columns) is modeled using inelastic axial springs. This model was used successfully to simulate results of a full-scale 7-story frame-wall building (Wight, 1985). It, therefore, continues to be the preferred approach to reliable macro-modeling of walls.

1.2.2 Hysteretic Modeling

Given the improbability of analyzing structures at the microscopic level, there arises the need to develop analytical models of macroscopic member behavior. The models summarized below are based on observed characteristics of inelastic behavior of reinforced concrete.

Bilinear elastic-perfectly-plastic models (Fig.1.7a) were among the first to be used mainly because of their simplicity both in concept and numerical implementation. The prescription of a small post-yield stiffness renders it a bilinear model. The inability of the model to handle stiffness changes during unloading and reloading made it unsuitable for analyzing R/C sections.

The break from steel-type modeling was accomplished with the proposal of a degrading stiffness approach (Clough and Johnston, 1966). Here, the unloading line upon crossing the force axis was made to target the previous maximum point thereby producing smaller hysteresis loops (Fig.1.7b). A more refined model was later developed by Takeda et al. (1970) which included stiffness changes at cracking, yielding, unloading and reloading, and also strain

hardening characteristics. Fig.1.7c shows an example of Takeda loops. This soon became the dominant model for inelastic structural analysis of R/C systems as is evident from its implementation in programs such as DRAIN-2D and SAKE.

The above models, however, are suited primarily for flexural behavior. Three other behavior patterns need to be addressed: shear, bond slip, and strength deterioration. Sections under the action of significant shear were shown to produce marked pinching of loops (Celebi and Penzien, 1973). The slip model (Fig.1.7d) accounts for this behavior. Also observed was the significant rotation at a beam end due to slippage (pullout) of the beam's main longitudinal bars at the joint (Bertero and Popov, 1977). Since this behavior is similar to pinching, the slip model is adequate to capture both phenomena. Finally, all R/C sections show considerable loss of strength upon repeated cycling at the same deformation level (Fig.1.7e). Modeling of strength deterioration has been achieved either through considerations of ductility (Baber and Wen, 1981; Ozdemir, 1976) or energy dissipation (Park et al, 1987).

Numerous variations of the above basic models can also be found in the literature, for example, the T-Beam model which accounts for the biased loop behavior of T-sections which have different force-deformation envelopes in compression and tension (a variation of Takeda's model); and the origin-oriented model used for shear springs in wall sections in which the unloading and reloading slopes target the origin point (a variation of degrading unloading stiffness).

Experimental studies have shown that the hysteretic behavior of R/C components is dependent upon numerous structural parameters such as concrete strength, steel content, axial stress level, shear span ratio, etc. These parameters greatly affect the deformation and energy-absorbing characteristics of the components (Park et al., 1972; Otani and Sozen, 1972; Kustu and Boukamp, 1973; Atalay and Penzien, 1975). It is, therefore, important to recognize that in order to reproduce closely the hysteretic behavior of various components, a highly versatile model is required. Such a model should include several significant aspects of R/C hysteretic loops, viz., stiffness degradation, strength deterioration, pinching behavior, and the variability of the hysteresis loop areas at different deformation levels under repeated loading

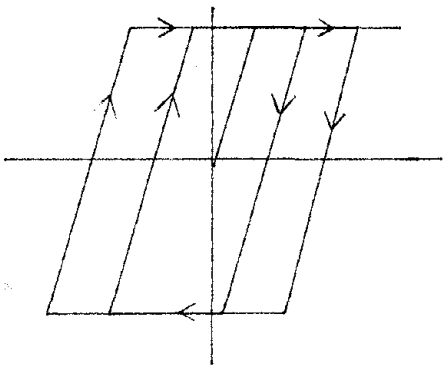

(a) Bilinear hysteresis

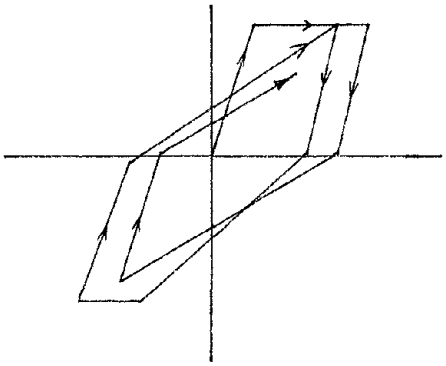

(b) Clough's degrading model

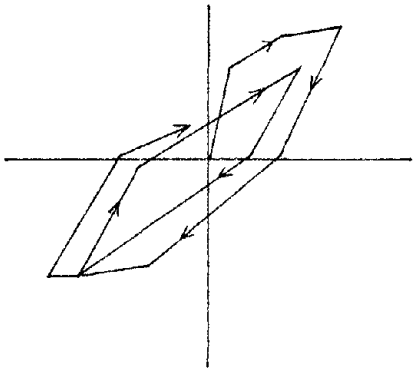

(c) Takeda model

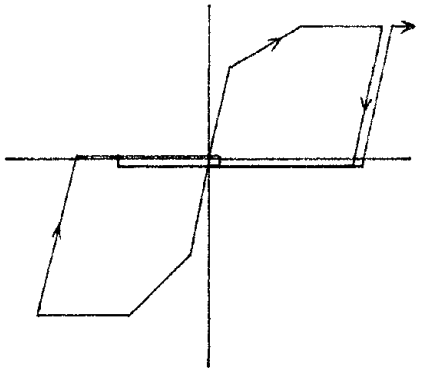

(d) Slip model

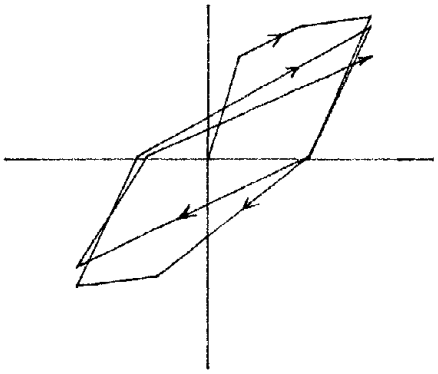

(e) Strength deteriorating model

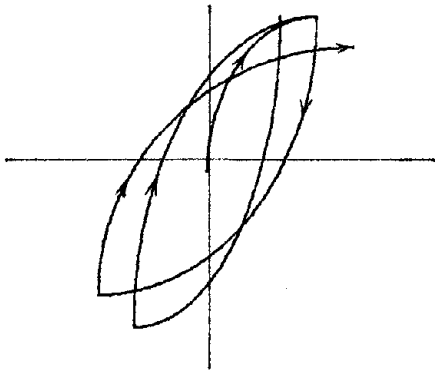

(f) Smooth hysteresis model

FIGURE 1-7 Basic Hysteretic Model Types

reversals. However, the model should also be simple to implement since a large number of inelastic springs are generally required to model an entire structure and too many parameters to describe a complex hysteresis loop.

An evaluation of existing models relating to their versatility and complexity was reviewed in a recent report (Park et al.,1987). It appears that most of the available models are suitable for particular components only and, therefore, fall short of the versatility required for modeling practical buildings having a large number of different components.

1.2.3 Biaxial Modeling of R/C Columns

A realistic formulation of the out-of-plane behavior of a structure is crucial to the understanding of seismic damage and failure. Given the random six-dimensional nature of earthquake loading, it is important to consider at least the effects of biaxial bending interaction (assuming that the structural configuration is not so irregular as to allow presence of significant torsional modes). Tests (Takizawa, 1976; Li et al., 1988) have shown that columns loaded in two perpendicular directions decay in stiffness and strength at a rate faster than that for uniaxial loads. It has also been shown that the inclusion of P-delta effects in conjunction with bi-directional loading is important (Umemura and Takizawa, 1982).

Initial concern for the effects of biaxial loading began with observation of crushing and spalling of concrete when components were loaded in a diagonal direction. The objective of biaxial testing at that time was the establishment of interaction equations at yield or ultimate moment in terms of the two components of lateral load under different levels of axial compression. The first of the yield surface models for concrete was thus established. Developed by Bresler (1960), a simple mathematical relationship of the following form was used:

$$\left(\frac{M_x}{M_{ox}}\right)^a + \left(\frac{M_y}{M_{oy}}\right)^a = 1 \qquad (1.1)$$

where M_x, M_{ox}, M_y, M_{oy} are the moments and yield moments about the x and y axis respectively. The parameter a is recognized to lie between 1.0 and 2.0 and is generally a function of axial load, confinement, etc.

The earliest formulation of a two-dimensional restoring force model (Nigam, 1967) was a 2-D extension of the bilinear hysteresis (of which the elasto-plastic model is a special case) using the plastic potential theory. Variations of this approach were also investigated by other researchers (Wen and Farhoomand, 1970; Toridis and Khozeimeh, 1971). Available analytical models for biaxial modeling may be classified into three groups:

(i) Yield Surface Models

The simplest model available is the bilinear biaxial model (Fig.1.8). At least three variations of this model can be found in the literature (Tseng and Penzien, 1975; Padilla-Mora and Schnobrich, 1974; and Takizawa and Aoyama, 1976). In this formulation, the column is assumed to be elastic until the moment-combination (specified by the interaction equation) reaches the yield surface. A constant axial force was assumed in all cases. The stiffness beyond yield is controlled by the post-yield stiffness while the yield surface itself translates in moment space without changing shape. Unloading takes place elastically thereby not allowing for any degradation effects. Experimental correlations using bilinear-biaxial models have not been too satisfactory (Lai, 1987).

A significant improvement to the bilinear model came with the formulation of the trilinear degrading model of Takizawa and Aoyama (1976). They used two yield surfaces, an inner cracking surface and an outer yield surface (Fig.1.9b). The size of the surfaces are developed from a uniaxial trilinear curve (Fig.1.9a) which distinguishes cracking and yielding. Here, the elastic stiffness is modified once the cracking surface is reached (Fig.1.9c) beyond which the surface translates without changing shape. Upon reaching the yield surface (Fig.1.9d), both cracking and yielding surfaces are allowed to expand along the direction of yielding (Fig.1.9e). Degradation is achieved by factoring the unloading stiffness by a degradation factor (generally a function of ductility). Comparison with experimental results (Takizawa and Aoyama, 1976; and Lai, 1987) show improved correlation. However, the formulations that define the interaction curves are complex and lengthy.

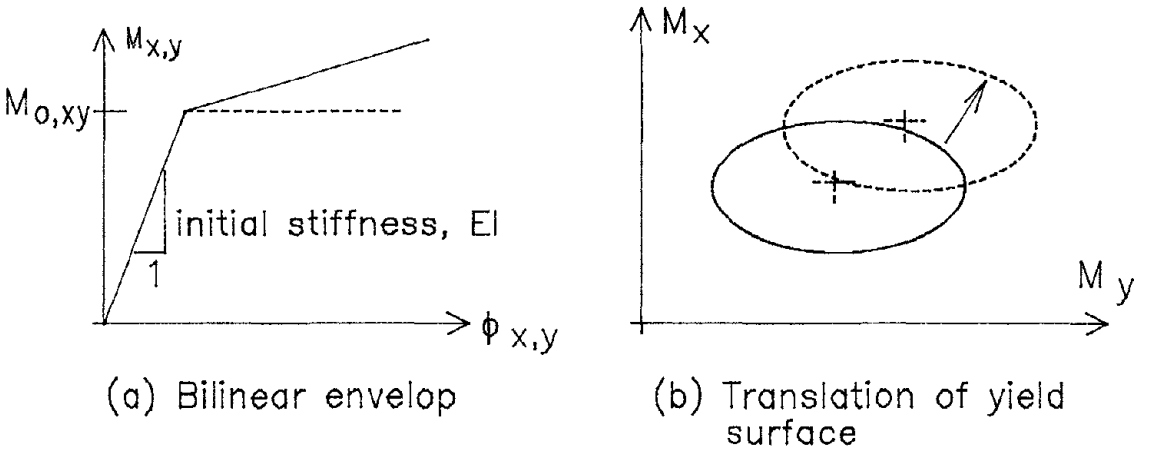

FIGURE 1-8 Bilinear Biaxial Model

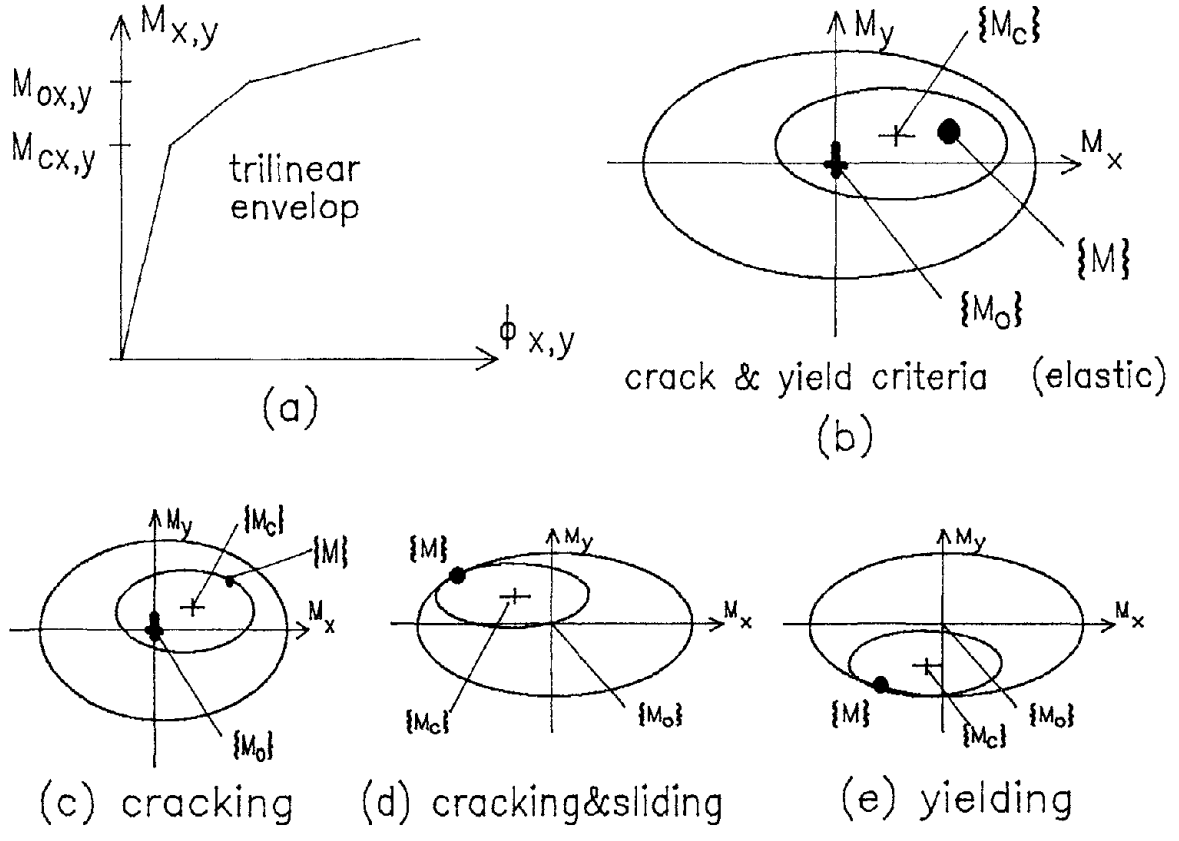

FIGURE 1-9 Trilinear Degrading Biaxial Model

(ii) Filament Models

These models are direct extensions of the filament models used for uniaxial bending. Their greatest advantage lies in the fact that complex hysteresis curves can be generated from fundamental material property curves. Strength deterioration, stiffness degradation and even slipping (during opening and closing of cracks) can be reproduced from a composite combination of steel and concrete. Also, it is possible to include the effects of varying axial force levels. Recently, Mander et al. (1988) demonstrated that strain-rate effects can be incorporated in filament type models though the technique was applied only to uniaxial loading. Reliability of the method depends entirely on the modeling of the stress-strain properties of the constituent materials.

Variations in formulations of this type arises mainly from the modeling of concrete and steel. Aktan and Pecknold (1974), Pecknold (1974) and Suharwardy and Pecknold (1978) suggest various approaches to modeling biaxial bending using the filament model. The greatest disadvantage of the method is the enormous computational time required even for a single cross-section. Consequently, its applicability for analysis of entire structures is limited.

(iii) Multi-Spring Models

The most recent development in biaxial bending formulation was proposed by Lai et al. (1984) whose triaxial-spring model represents a significant advance both in simplicity and accuracy. It does not require the use of a yield surface, instead the region undergoing inelastic yielding is represented by a set of springs representing concrete and reinforcing steel. Inelastic behavior, therefore, is controlled by the description of the stress-strain properties of steel and concrete. To this extent, it may be stated that the drawback of the approach is its total dependence on the prescription of constituent material properties.

Two variations of the triaxial-spring model have been proposed. In its original form, Lai et al. (1984) assumed hysteretic behavior to be concentrated at member ends with each inelastic end element comprising of 4 effective steel spring areas (*As1*-*As4*) and 5 effective concrete spring areas (*Ac1*-*Ac5*) as shown in Figs.1.10a and 1.10c. The force-displacement hysteresis that was used for the steel and concrete springs are shown in Figs.1.10b and 1.10d respectively. The deformations in the springs are related by compatibility equations assuming

plane sections to remain plane after deformation. However, the center of rotation is assumed to be at the centroid of the section leading to coupling of axial force and bending following nonuniform deformation in the springs. This would mean that even pure bending can lead to an accumulation of axial forces.

A refinement to the Lai model was provided by Ghusn and Saiidi (1986) who considered 4 corner composite springs instead of separating them into steel and concrete. Thus the nine-spring model was reduced to a five-spring model. Also, the coupling problem discussed in the previous section was addressed by having the neutral axis translate in response to the stiffness changes in the springs. Good correlations with experimental results have been reported using the above models (Li et al., 1988).

Though multi-spring models seem to capture the essential characteristics of biaxial interaction, they still possess significant drawbacks: extensive loop tracing is necessary for both concrete and steel; the total dependence on modeling of the constituent materials; and the lack of physical meaning on the nature of the interaction.

1.3 Organization and Scope of Report

A number of facts emerge from the review of R/C structural behavior to seismic loads and the state-of-the-art on structural and material modeling of reinforced concrete. In essence, it points to the lack of an integrated computational model that reflects observed behavior patterns of R/C structures in the inelastic range.

The primary goal of this report is to present the details of the development of an enhanced modeling scheme which accounts for essential and critical R/C characteristics. The model is also meant to serve as the basis for future enhancements and for integrating the efforts of experimental research and analytical macromodeling of component behavior. The contents of the report are organized as follows.

Section 2 presents the general 3-D modeling scheme for buildings, in which biaxial bending interaction is considered primarily for column elements. Beams and walls are treated as 3-D elements but the interaction of bending along their two principal axes is not considered. The ability to detect a shear failure in walls is accomplished by separating shear behavior

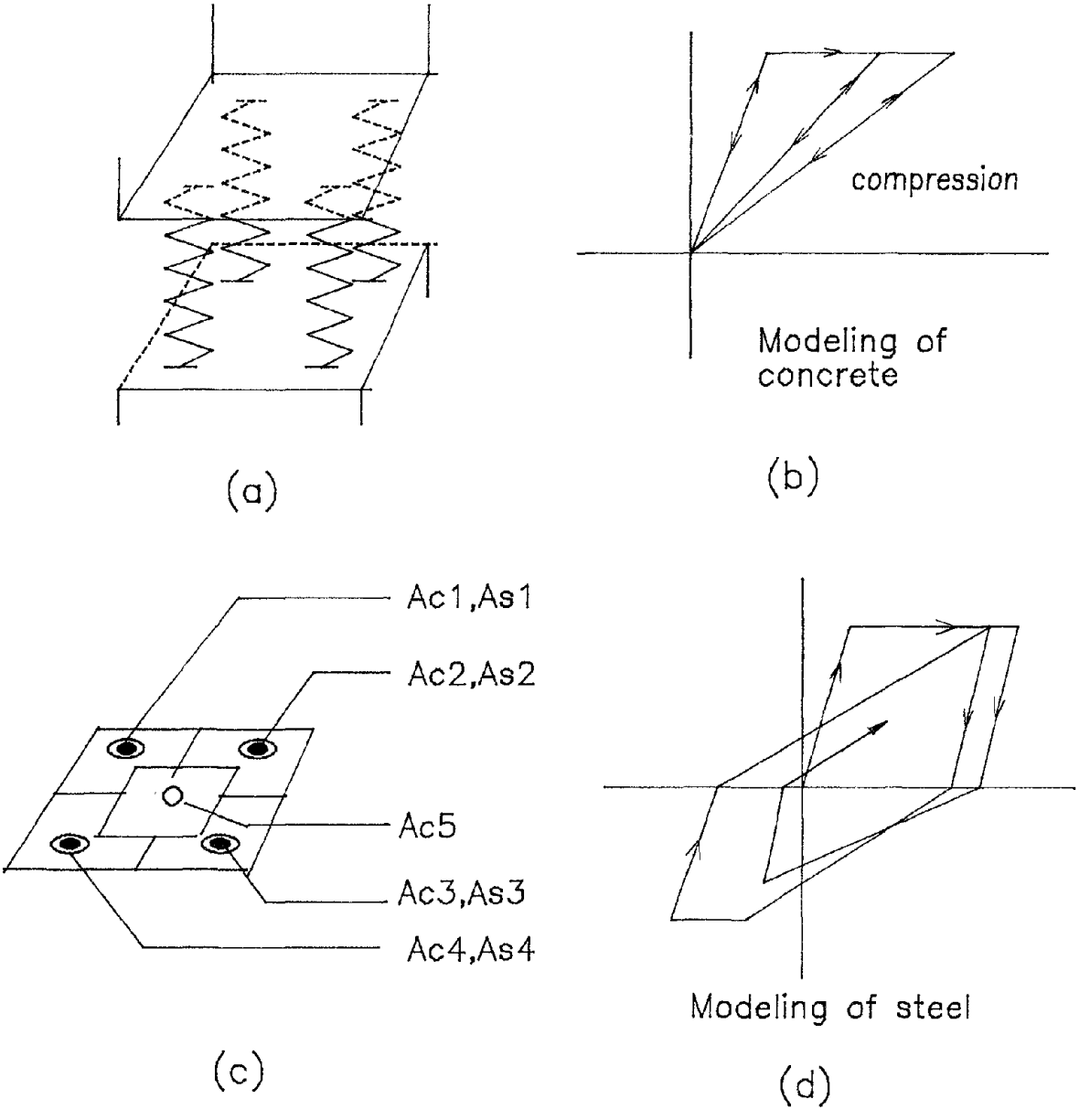

FIGURE 1-10 Triaxial Spring Model

from flexure and modeling each component by different springs. Special considerations of beam-to-wall and wall-to-wall connections is discussed along with some of the limitations of the modeling approach.

The present development also recognizes that inelastic behavior in R/C elements spreads along the member length towards the inflection point, and is not concentrated at the joints, hence concentrated plasticity models are inadequate to capture actual stiffness states. Consequently, a distributed flexibility formulation is developed which permits the modeling of the inflection point within or outside the element. The formulation accounts for two components of bending which allow biaxial modeling of members. The stiffness matrix development includes the finite size of joints.

Sections 3 and 4 deal with the development of behavioral (i.e., force-deformation) models to characterize the component macro-models. The success of macro-modeling depends almost entirely on the representation of the macro-model at the member level and its interaction with other components at the structural level. In the present scheme, rotational springs are used to model flexure and linear springs are used to model shear. The task of building the associated spring characteristics (force-deformation envelope and hysteretic parameters) is the subject of Section 3. Two different models are used: one for biaxial bending in columns, the other for uniaxial deformations in beams and walls. Biaxial modeling of R/C components using yield surface models tend to be cumbersome and complex, especially when stiffness degradation and strength deterioration have to be incorporated into the constitutive laws. Therefore, a unique and efficient scheme is proposed for modeling biaxial bending interaction through the development of a visco-plasticity based force-deformation model which considers both stiffness degradation and strength deterioration. For the uniaxial case, a previously developed 3-parameter model (Park et al., 1987) was used which accounts for the three main behavior patterns in reinforced concrete: stiffness degradation, strength deterioration, and pinching or bond-slip.

Having established both the envelope characteristics and the rules under which loading and reloading occur, it is necessary to describe the process by which these parameters are evaluated. Commonly referred to as structural identification, this feature is totally lacking in

all existing computer programs for R/C analysis. Section 4 presents several approaches to identification. The schemes currently available in IDARC (Park et al.,1987) are outlined, and proposed additions to enhance the method are also discussed.

Section 5 is devoted to the analysis of assembled macro-models. The various solution modules developed for structural analysis are presented, viz., static analysis under initial dead loads; collapse mode analysis under increasing lateral loads; seismic response analysis under vertical and bi-directional excitations; and finally, considerations of P-delta effects due to excessive inter-story drift. Procedures to minimize equilibrium errors due to branch changes, nonlinear transition into post-yield behavior, and stiffness updates during unloading/re-loading, are presented.

The need to express results of the inelastic response analysis in a simple but effective manner so that an engineering interpretation is possible, led to the developments in Section 6 which examines models of seismic damage. A new formulation for damageability assessment is proposed. Correlation studies are presented on a 2-bay, 3-story frame structure for which experimental data was available.

Finally, numerical examples and sample correlation studies using the models developed in this study are presented (Section 7). A review of the models presented, in terms of tasks accomplished and work that remains to be investigated, is described in the concluding part of this report.

All developments have been incorporated into a modular code IDARC-3D. Details of the program and implementation including a user guide will be published as a separate technical manual.

SECTION 2

STRUCTURE MODELING

A macromodeling approach is used to discretize a general 3-D building. The generalized degrees-of-freedom are considered only at the face of joints, however, a distributed flexibility approach is used to construct the stiffness matrix thereby enabling a realistic consideration of the spread of plasticity across the member.

The essence of the overall analytical approach to solving 3-D buildings lies in recognizing two common facts: (1) the response of beams and shear walls in a general 3-D building is predominant within their own planes, therefore, inelastic action need be considered only in the inplane uniaxial direction; (2) and that inelastic biaxial bending interaction is significant only in columns. Hence, the overall inelastic response of the structure can be captured with reasonable accuracy if the interaction of moments in the two principal axes under bi-directional excitation is taken into account. An efficient scheme to include this effect is developed, both at the structural and the material levels. This chapter deals only with the structural component modeling; details of the material hysteretic model are described in Sections 3 and 4.

2.1 Basic Assumptions in System Modeling

In the modeling scheme developed in this study, a 3-D R/C building is idealized by orthogonal elements consisting of columns, walls and beams (Fig.2.1). Each element is modeled using 6 degrees-of-freedom (3 translational and 3 rotational) per node as shown in Fig.2.1. This results in a system which considers inelastic out-of-plane bending of the floor slab system. In-plane bending of beams which form part of the floor system is considered, but its action is restricted to elastic deformations only. To achieve a different modeling scheme, the following sub-sets of the main element types are possible:

(1) Modeling the floor T-beams as horizontal shear wall elements so as to capture inelastic in-plane bending.

(2) Modeling the floor beams as inelastic biaxial column elements so that interaction effects may also be included. This option is useful if torsional modes are significant in the building response.

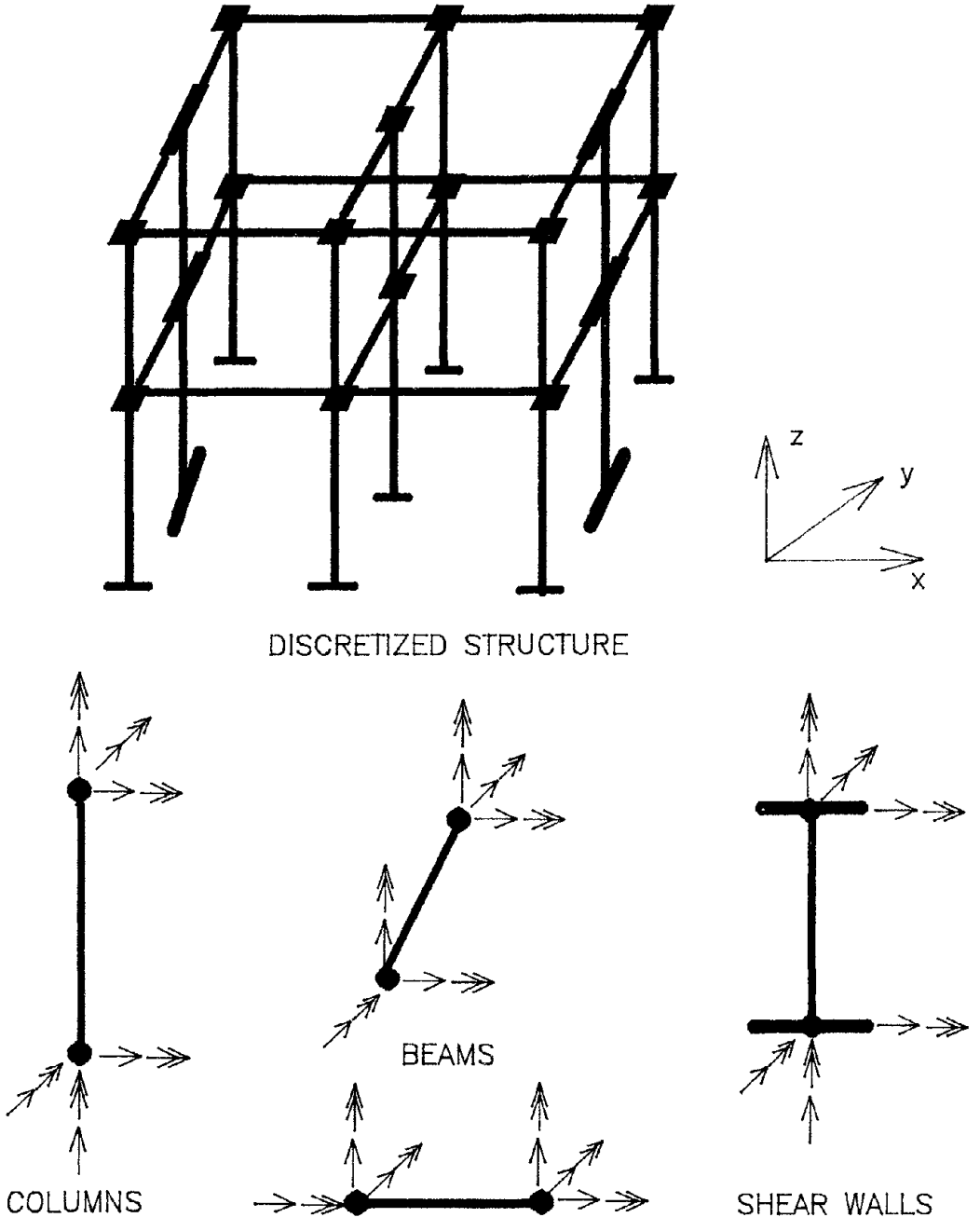

FIGURE 2-1 Modeling of General 3-D Building

The structure is assumed to be fixed at the foundation level. All formulations are based on the assumption that the element cross-sections are prismatic in which the coordinate axes are the local principal axes of the sections. Also, it is assumed that the sections (with the exception of T-Beams) are doubly symmetric so that the shear center coincides with the centroid. Consequently, no stress transformations are required (except T-sections).

In the above formulation, it is assumed that the floor slabs are flexible and that the entire structure is capable of any arbitrary deformation pattern in 3-D space. However, in most structures, it is reasonable to assume that the floor slabs are adequately stiff within their plane resulting in a rigid body motion of the floor. Hence, it is possible to eliminate several local degrees-of-freedom by slaving them to the master floor node, viz., the center of mass. The following section describes this special feature of the 3-D modeling scheme.

Treatment of rigid floor slabs: If the floor slab is assumed to be infinitely rigid in its own plane, it is possible to condense three local degrees-of- freedom per node at each story level. In this formulation, all elements at a story level are assumed to displace an equal amplitude in each coordinate direction in the horizontal plane, and the floor itself is capable of a rotation degree-of-freedom about the center of mass. This gives rise to three independent degrees-of-freedom per floor (Fig.2.2). This modeling scheme is achieved by carrying out a simple linear transformation of the corresponding local degrees-of-freedom to the center of mass of the floor. No static condensation of the remaining degrees-of-freedom is performed since the overall formulation is more efficient by retaining the local element stiffness matrices and recovering directly the local displacement vector for purposes of hysteretic modeling and stiffness updating.

Macro-model representation: The process of macro-model representation for 3-D structures evolves from the inelastic modeling scheme for components, as shown in Fig.2.3. In this scheme, biaxial bending interaction is considered only for column elements. Beam formulations assume uniaxial behavior, though the prescription of the moment-curvature envelope is done in a non-symmetric fashion with different properties in tension and compression. Shear walls are modeled using an idealized representation in which flexure and shear are separated. In the framework of the 3-D formulation, the instantaneous inelastic stiffness matrix considering two components of rotations yields a (4X4) matrix for column elements only. The

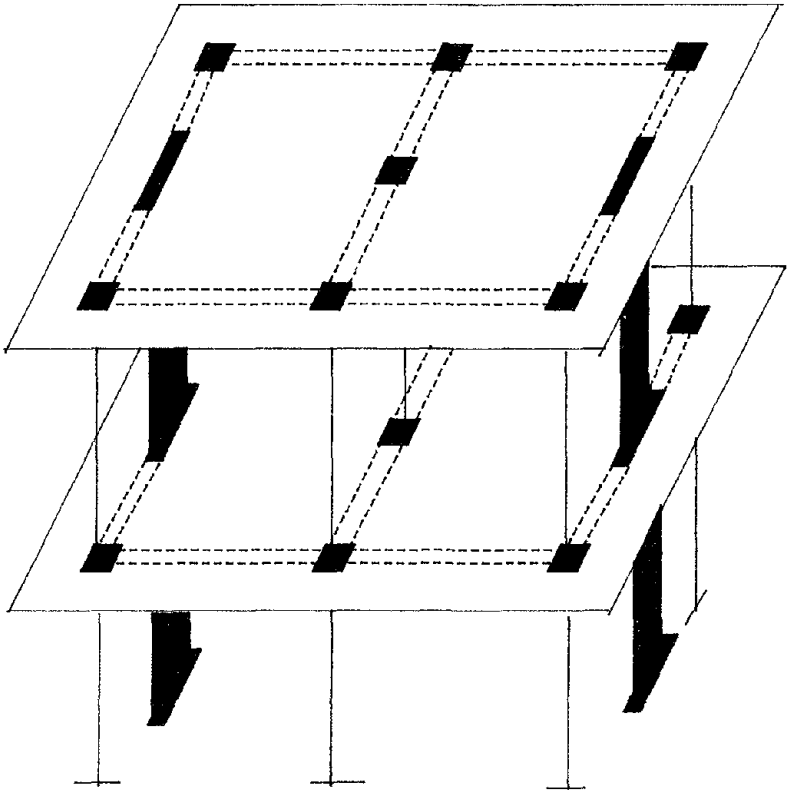

(a) discretized building

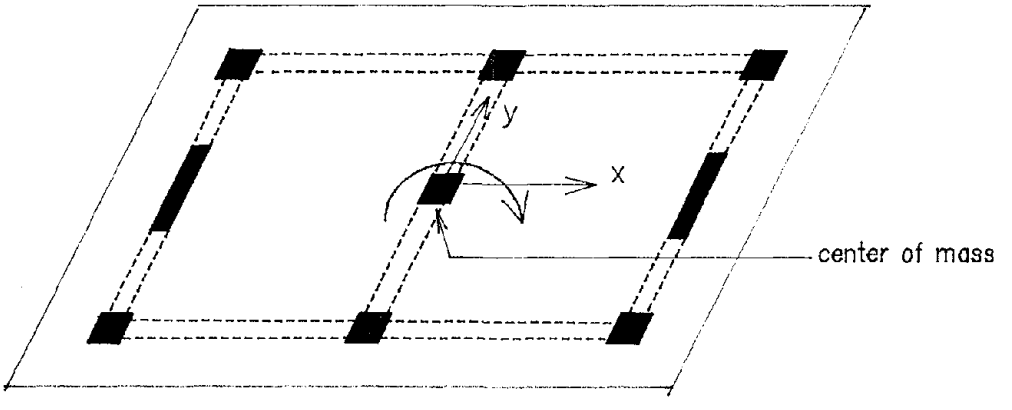

(b) floor degrees-of-freedom

FIGURE 2-2 Modeling of Building with Rigid Floors

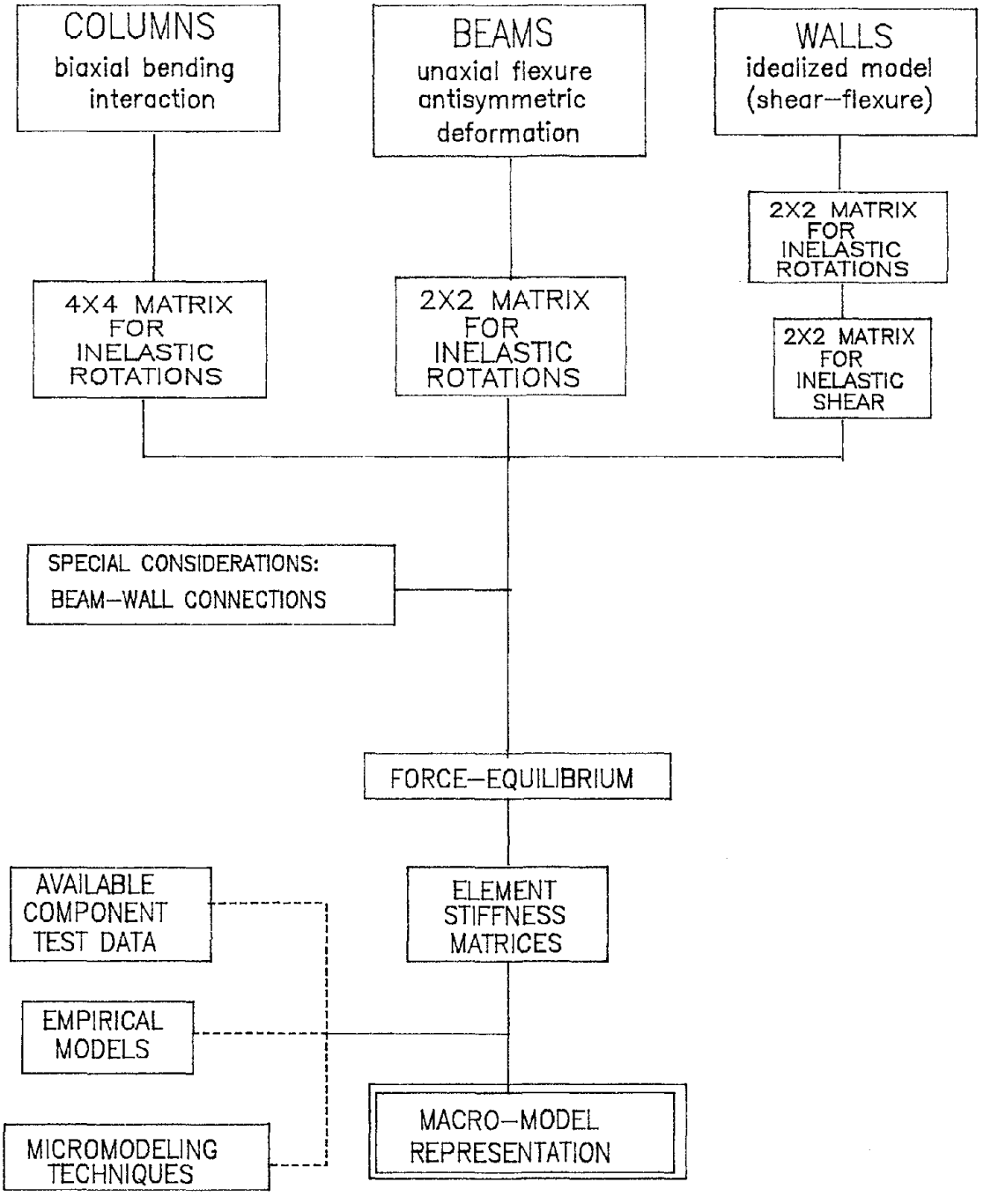

FIGURE 2-3 Inelastic Modeling Scheme for Components

modeling of the remaining elements for inelastic rotations produces a (2X2) matrix. Inelastic shear in walls is considered separately. Special attention is paid to the modeling of beam-wall connections since several corner degrees-of-freedom can be condensed by slaving them to master nodes. The final element stiffness matrices are developed from considerations of component force-equilibrium. Inelastic characteristics of a component is represented by a spring: a rotational spring for flexure and a linear spring for shear. The characteristics of the spring are established in one of three ways: (1) using available component test data; (2) through empirical models (Chapter V); or (3) by micromodeling schemes, typically a fiber model analysis. The integration of the spring characteristics, the inelastic instantaneous stiffness matrices, and the force-equilibrium equations, constitute the overall macro-model representation of a typical R/C component.

Specific details of the each component model are detailed in subsequent sections.

2.2 Modeling of 3-D Structural Systems

The discretization of a 3-D building is achieved using the following four main element groups:

1) Biaxial column elements
2) Uniaxial beam elements
3) Idealized shear wall sections
4) Beam-wall link elements

2.2.1 Column Elements

Column elements form the focus of the inelastic modeling scheme of 3-D building structures as developed in this study.

A typical column element with rigid joint cores is shown in Fig.2.4. Five degrees-of-freedom per node are included. However, inelastic action is restricted to biaxial bending only as shown in the figure. The development of the stiffness matrix for a typical element is described in the Appendix.

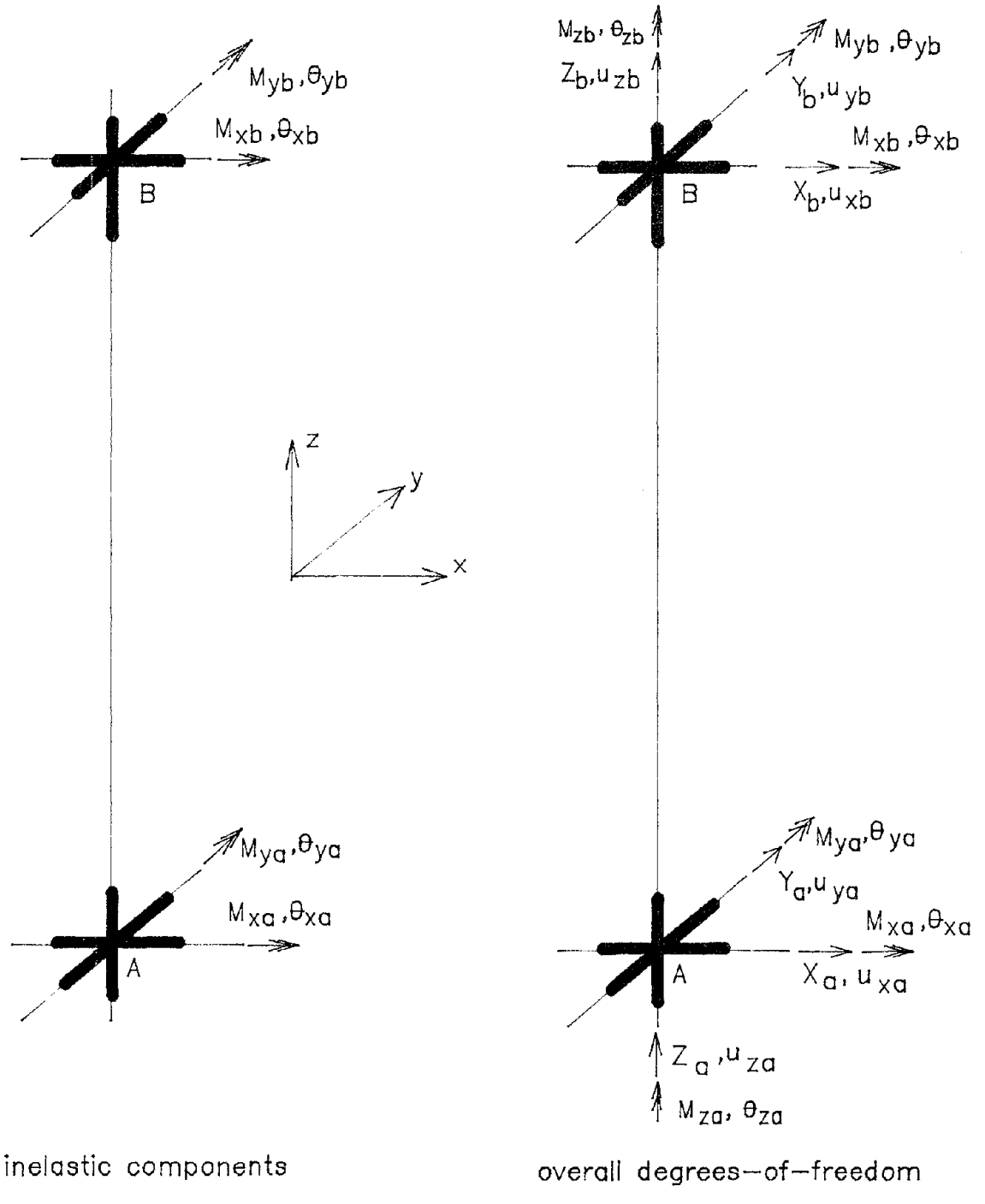

FIGURE 2-4 Component Modeling for Column Elements

The moments and rotations shown in Fig.2.4 correspond to the center of the joint core. A transformation across the rigid zone to the interior faces of the column is accomplished through Eqs.(A.4)-(A.5) (see Appendix):

$$\{F_x\} = [T]\{F_x'\} \tag{2.1}$$

$$\{\theta_x'\} = [T]^T\{\theta_x\} \tag{2.2}$$

where $\{F_x\}, \{F_x'\}, \{0_x\}, \{\theta_x'\}$ are the inelastic force and deformation components at the core and the interior column face respectively. The flexibility relationship of Eq.(A.3) (see Appendix) is expressed in stiffness form by carrying out the inversion of the flexibility matrix. Substitution of the resulting relationship into Eqs.(2.1)-(2.2) gives the inelastic stiffness equation for the column element. To complete the stiffness formulation, the equilibrium of forces for the member (Fig.2.3b) is considered. This gives:

$$\begin{pmatrix} \{F_x\} \\ \{F_e\} \end{pmatrix} = [R]\{F_x\} \tag{2.3}$$

where $\{F_e\}$ are the elastic force components. Eq.(2.3) expresses the relationship between all of the member forces (elastic and inelastic) in terms of the inelastic force components. Next, a similar transformation of the inelastic deformations is carried out. As described in the Appendix, substitution of these transformations into the general force-displacement relationship yields the eventual stiffness equation:

$$\{F\} = [K]\{u\} \tag{2.4}$$

where $[K]$ is a (12 x 12) symmetric stiffness matrix. The original transformations of Eqs.(A.10) produce an (8 x 8) matrix. The final matrix is a consequence of including the axial force and torsion which otherwise do not appear in equilibrium considerations, and consequently in the stiffness matrix of Eq.(2.10).

The description of the hysteretic force-deformation rules which include biaxial bending interaction is presented in the Section 3.

2.2.2 Beam Elements

The exclusion of biaxial bending interaction in beams is a result of two main considerations: (1) first, the secondary bending component is coupled with the floor torsion, and is, therefore, unlikely to play a significant role in the overall structural response; and (2) secondly, there is inadequate test data documenting the interaction of these bending components to enable a reasonable attempt to model such behavior. Any significant deformation in the secondary direction leads to the problem of in-plane diaphragm flexibility and has been presented in an earlier Technical Report (Reinhorn et al.,1988).

The component modeling for beams is shown in Fig.2.5. Inelastic forces and deformations are restricted to uniaxial flexure. The flexibility matrix of Eq.(2.3), therefore, reduces to a (2 x 2) matrix, and the eventual stiffness matrix assumes the following form:

$$\begin{pmatrix} Z_a \\ M_{ya} \\ Z_b \\ M_{yb} \end{pmatrix} = \begin{pmatrix} k_{11} & .. & & \\ k_{21} & k_{22} & .. & SYM \\ k_{31} & k_{32} & k_{33} & \\ k_{41} & k_{42} & k_{43} & k_{44} \end{pmatrix} \begin{pmatrix} u_{za} \\ \theta_{ya} \\ u_{zb} \\ \theta_{yb} \end{pmatrix} \qquad (2.5)$$

The components of the stiffness matrix shown above are obtained using the distributed flexibility model and represent the inelastic force-deformation model. These terms are inserted into the standard finite element beam stiffness matrix to obtain a full (12 X 12) matrix.

2.2.3 Shear Wall Component Modeling

The modeling of shear walls in R/C buildings is generally complex and requires careful consideration of flexure, shear, and axial force interaction. The model described here is based on the original formulation of Kabeyesawa et al.(1985) with the simple modification of excluding the edge axial springs. The removal of the edge springs facilitates the deformation compatibility at the beam-wall joint in the present 3-D formulation. Moreover, the extra edge springs were used in the original model, which was essentially a 2D formulation, to include the effects of wall rocking that was observed in the full-scale psuedo-dynamic tests of a 7-story frame-wall building (Wight, 1985).

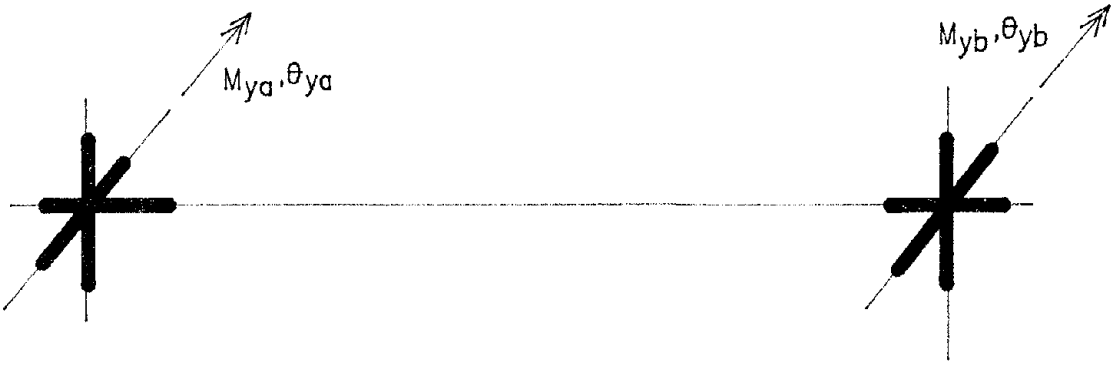

inelastic components of uniaxial flexure

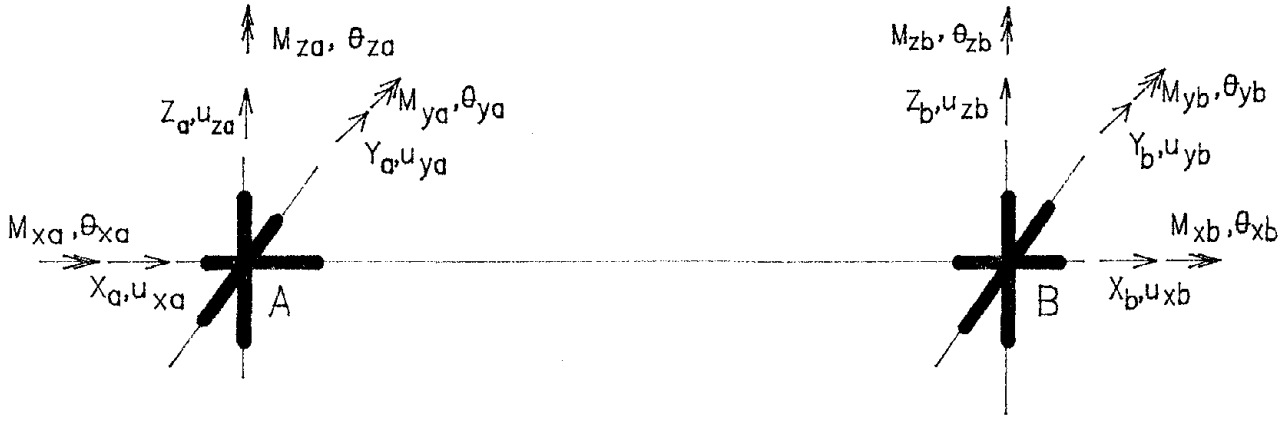

overall degrees–of–freedom

FIGURE 2-5 Beam Component Modeling

The idealized wall model, the overall degrees-of-freedom, and the inelastic springs are shown in Fig.2.6. The stiffness formulation for the wall is identical to the development presented for beams with the exception that the primary shear forces in Eq.(2.6) are X_a, X_b instead of Z_a, Z_b:

$$\begin{pmatrix} X_a \\ M_{ya} \\ X_b \\ M_{yb} \end{pmatrix} = \begin{pmatrix} k_{11} & .. & & \\ k_{21} & k_{22} & .. & SYM \\ k_{31} & k_{32} & k_{33} & \\ k_{41} & k_{42} & k_{43} & k_{44} \end{pmatrix} \begin{pmatrix} u_{xa} \\ \theta_{ya} \\ u_{xb} \\ \theta_{yb} \end{pmatrix} \qquad (2.6)$$

The stiffness equation relating forces and the overall degrees-of-freedom is obtained in a manner similar to that for beam elements. The essential difference in the modeling of shear walls is the inclusion of a shear spring in series with the flexure spring. The characteristics of the shear spring is specified separately. This bifurcation of flexure and shear enables the detection of shear failure mechanisms. This feature is extremely important since shear stiffness decay occurs much more rapidly than flexural stiffness degradation. The ability of the model to capture this phenomenon makes it particularly attractive in damage studies of shear wall buildings.

2.2.4 Special Treatment of Beam - Wall Connections

A fourth class of elements is provided in the modeling scheme of IDARC-3-D for user convenience. It was necessary to include this element type owing to the center-line-style modeling of walls. A beam connected to the end of a wall-section requires a unique formulation of the resulting stiffness matrix due to the rigid link element that connects the beam-end to the wall degrees-of-freedom (Fig.2.7). It is, however, possible to simulate this effect by prescribing a large moment of inertia for the rigid element, but this could lead to problems of numerical instability depending on the relative order of stiffness of the remaining components of the structure. In the present formulation, a linear transformation of the forces and deformations of the wall is carried out to set up the beam stiffness matrix. The following stiffness equation is obtained:

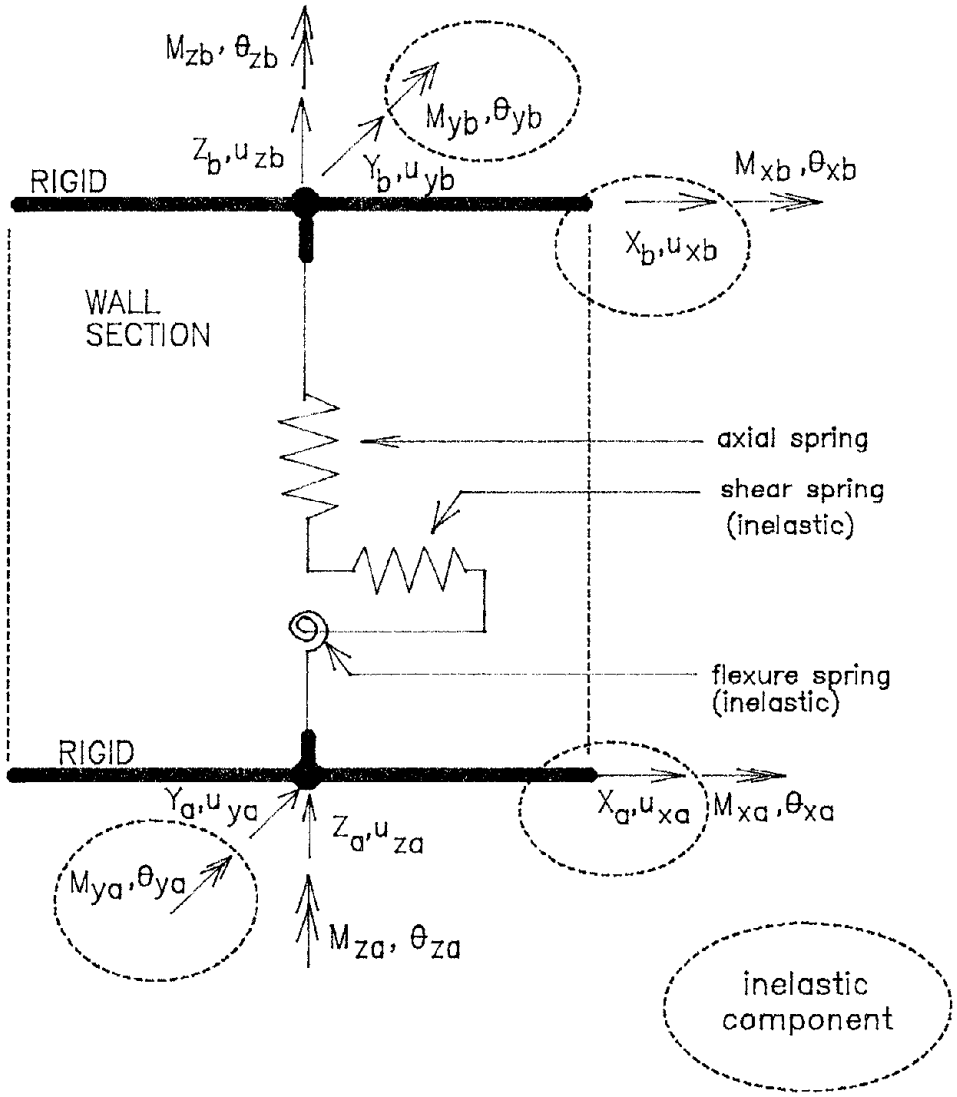

FIGURE 2-6 Idealized Shear Wall Model

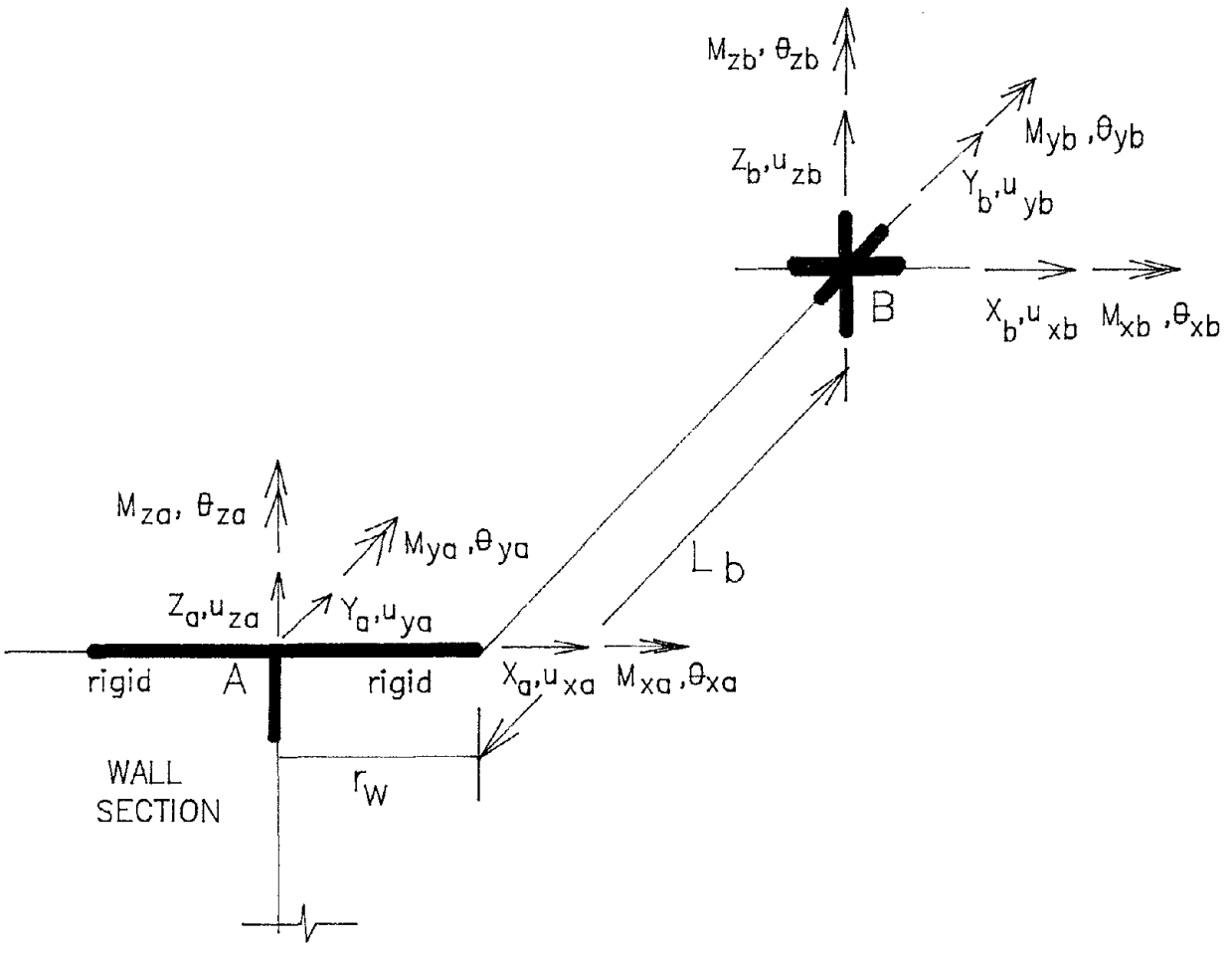

FIGURE 2-7 Modeling of Beam-Wall Connection

$$\{F\} = [K_{BW}]\{u\} \tag{2.7}$$

where:

$$\{F\} = \langle X_a Z_a Y_a M_{xa} M_{za} M_{ya} X_b Z_b Y_b M_{xb} M_{zb} M_{yb} \rangle^T \tag{2.7a}$$

and

$$\{u\} = \langle u_{xa} u_{za} u_{ya} \theta_{xa} \theta_{za} \theta_{ya} u_{xb} u_{zb} u_{yb} \theta_{xb} \theta_{zb} \theta_{yb} \rangle^T \tag{2.7b}$$

where:

$$[K_{BW}] = \begin{pmatrix}
\frac{EA}{L} & .. & .. & .. & .. & & & & & & \\
0 & k_{11} & .. & .. & .. & & & & & & \\
0 & 0 & \frac{12EI_z}{L^3} & .. & .. & SYM & & & & & \\
0 & -k_{x1} & 0 & k_{x2} & & & & & & & \\
0 & 0 & \frac{-6EI_y}{L^2} & 0 & \frac{4EI_y}{L} & & & & & & \\
0 & k_{21} & 0 & 0 & 0 & k_{22} & & & & & \\
-\frac{EA}{L} & 0 & 0 & 0 & 0 & 0 & \frac{EA}{L} & & & & \\
0 & k_{31} & 0 & k_{x1} & 0 & k_{32} & 0 & k_{33} & & & \\
0 & 0 & \frac{-12EI_y}{L^3} & 0 & \frac{6EI_y}{L^2} & 0 & 0 & 0 & \frac{12EI_y}{L^3} & & \\
0 & 0 & 0 & -\frac{GJ}{L} & 0 & 0 & 0 & 0 & 0 & \frac{GJ}{L} & \\
0 & 0 & \frac{-6EI_y}{L^2} & 0 & \frac{2EI_y}{L} & 0 & 0 & 0 & \frac{6EI_y}{L^2} & 0 & \frac{4EI_y}{L} \\
0 & k_{41} & 0 & 0 & 0 & k_{42} & 0 & k_{43} & 0 & 0 & 0 & k_{44}
\end{pmatrix}$$

in which:

$$k_{x1} = k_v r_w \tag{2.8}$$

$$k_{x2} = k_v r_w^2 + k_\theta \tag{2.9}$$

where the sub-matrix k_{ij} is the inelastic matrix of Eq.(2.5), k_θ is the torsional stiffness (GJ/L) , $k_v = 12(EI)_x/L^3$ and r_w is the rigid beam arm, equal to the half width of

the wall section. The above formulation is a function of the orientation of the wall in relation to the beam. An adjacent orientation, for example, will require the modification of the arm length term r_w to a negative quantity.

The four element types discussed above allows for modeling a wide configuration of buildings. There are no inherent limitations to the modeling capabilities other than those specified in Section 2.1. However, it must be noted that an elastic property is given to the torsional degree-of-freedom. *Any torsional yielding in the component will lead to a drastic loss of torsional stiffness and cannot be accounted for in the above formulation.* In regular buildings, such a phenomenon is rare since the lateral responses are generally dominant.

SECTION 3

FORCE-DEFORMATION MODELS

The global modeling of 3-D structural systems using a macro-model representation of the inelastic behavior of R/C components was presented in Section 2. It was further shown that from the inelastic moment-rotation representation, it is possible to construct the element stiffness matrices using force-equilibrium. The primary difference between this approach and the standard finite element representation is that, in the present scheme, no constitutive equations are used. Instead, the spring behavior is described using force-deformation rules which attempt to capture overall member behavior. In theory, it is possible to construct force-deformation curves using constitutive models. However, constitutive laws hold true only for a microscopic point in the material. For an inhomogeneous material such as reinforced concrete, it will take a very fine discretization of the cross section to represent the material behavior in terms of local concrete-steel interaction. As pointed out earlier, even this micro-level analysis cannot guarantee adequate representation of overall member behavior.

Force-deformation relationships, on the other hand, are different in character from the underlying constitutive equations since they reflect member behavior as a whole and also include geometrical effects (Ozdemir, 1976). The basis of development of force-deformation models is experimental testing. From observed member behavior under cyclic loading, it is possible to set up a mathematical model of the spring characteristics. The next two sections deal with the description of two such models: (1) a viscoplasticity-based model for inelastic biaxial column bending; and (2) a generalized trilinear model for uniaxial flexure and shear.

A two-dimensional force-deformation model is developed from the modified Bouc (1967) model (or extended Wen's model) to model the effect of biaxial bending interaction in columns. The primary basis of interaction is introduced by force coupling terms which assumes that there is interaction only in the presence of forces in both directions. Hence, when a force is applied only in one direction, the system responds in the same direction without any interaction effect in the orthogonal direction. The physical validity of the model is established by proving the special case of isotropic material behavior. Details of the development of the model are presented in the next section.

3.1 Biaxial Force-Deformation Model

The need to consider a separate model for columns arises from several facts: (1) The biaxial model developed in this study assumes symmetric properties in compression and tension. This is generally true only for columns and shear walls. (2) The general 3-parameter model (discussed in section 3.2) is capable of reproducing a variety of effects including non-symmetric envelope representation and pinching behavior. However, the tracing of hysteretic loops is a tedious and difficult process. (3) Biaxial modeling using the 3-parameter model is cumbersome because of the complexity of the yield surface representation. Therefore, it was essential to retain the 3-parameter model for modeling special behavior patterns, such as T-beams, shear-pinching effects, etc., and to develop a new efficient model only for biaxial bending of columns.

The review of approaches to biaxial bending interaction in Chapter I clearly indicates that the present stock of models are either too simple to represent actual material behavior (bilinear models), or are too complex for efficient numerical implementation in a general-purpose computer program for inelastic structural analysis. Hence, the main objective here is to develop a model that is not only capable of describing R/C behavior adequately but is also computationally efficient. Three approaches were investigated: (1) yield surface models; (2) equivalent spring models; and (2) viscoplasticity-based models. Of these, it was found that the first class of models leads to extremely complex representations when concrete cracking, reinforcement yielding, and degradation of structural parameters are considered. Equivalent spring models, on the other hand, simplify the process a great extent, but still require extensive book-keeping in completing the model description. It was, therefore, decided to focus the present development on the third class of models which possess great potential in hysteretic modeling of yielding systems. The next section describes the details of the model development, beginning with a brief review of previously used models for hysteretic representation of material behavior.

3.1.1 Review of Viscoplasticity-Based Models for Hysteretic Systems

Viscoplasticity models are rate-dependent models which were developed primarily for characterization of metal behavior. An equation of the following form was first proposed by Malvern (1951):

$$\dot{\epsilon} = \frac{\dot{\sigma}}{E} + g(\sigma, \epsilon) \tag{3.1}$$

where σ, ϵ and E are the stress, strain and elastic modulus respectively. The dot expresses the derivative with respect to time. Using principles based on dislocation theories of solid state physics, Gilman (1969) recommended the following form of g:

$$g(\sigma, \epsilon) = \frac{1}{\tau}\left(\frac{\sigma}{\sigma_o}\right)^n \tag{3.2}$$

where n, τ and σ_o are material constants. It is seen that the above equations reduce to the classical Maxwell model of linear viscoelasticity for $n=1$, and to a viscoplastic model for n greater than unity. A direct extension of Eqs.(3.1)-(3.2) in terms of force and deformation was proposed by Ozdemir (1976) who used the modified viscoplastic model to investigate the hysteretic behavior of energy absorbers. His formulation also included work-hardening using the concept of back-stress, as follows:

$$\frac{\dot{F}}{F_y} = \frac{\dot{\delta}}{\delta_y} - \frac{1}{\tau}\left(\frac{F - s}{F_y}\right)^n \tag{3.3}$$

where F_y, δ_y are the yield force and displacement, and s is the back-stress. It was further demonstrated by Ozdemir that Eq.(3.3) can be expressed in rate-independent form with the following requirement:

$$\tau = \left|\frac{\delta_y}{\dot{\delta}}\right| \tag{3.4}$$

This model is capable of reproducing a variety of nonlinear hysteresis, including the incorporation of stiffness and strength deterioration.

A second versatile scheme which involves the solution of a differential equation is the extended model of Bouc (1967). Used by Wen (1975) for random vibration analysis, the model expresses the restoring force as the linear combination of an elastic force and a plastic force:

$$F = \alpha K u + (1-\alpha) K Z \tag{3.5}$$

where K is the initial stiffness, α is the post-yield stiffness ratio, and Z is the hysteretic parameter given as:

$$\dot{Z} = A\dot{u} - \beta|\dot{u}Z|Z - \gamma\dot{u}Z^2 \tag{3.6}$$

in which A, β, γ are dimensionless quantities which control the shape and magnitude of the hysteresis loops. It has been shown that these equations, under certain conditions, reduce to a form of Ozdemir's viscoplastic model (Constantinou and Adnane, 1987).

Eq.(3.5)-(3.6) were extended by Park et al.(1986) to include biaxial bending interaction. However, they used the model in an equivalent linearization process to study random vibration of hysteretic systems. A variation of all the dimensionless parameters was used to produce the effects of strength loss and stiffness degradation to simulate R/C behavior. This, however, leads to a violation of the basic viscoplastic principles and results in a model without clear physical meaning. An example is the biaxial loading of a purely isotropic material in which the displacement path is a straight line at some fixed angle from the uniaxial directions. By varying all the parameters in Eq.(3.6), the resulting force is not obtained in the direction of the applied displacement. In the present formulation, the viscoplastic nature of the model is retained, while at the same time allowing for stiffness and strength deterioration to be incorporated.

3.1.2 Development of a Viscoplastic Force-Deformation Model for Biaxial Bending

The initial formulation of the biaxial force-deformation model is based on the coupled differential equations for isotropic hysteretic restoring forces suggested by Park et al.(1986):

$$\dot{Z}_x = A\dot{u}_x - \beta|\dot{u}_x Z_x|Z_x - \gamma\dot{u}_x Z_x^2 - \beta|\dot{u}_y Z_y|Z_x - \gamma\dot{u}_y Z_x Z_y \tag{3.7}$$

$$\dot{Z}_y = A\dot{u}_y - \beta|\dot{u}_y Z_y|Z_y - \gamma\dot{u}_y Z_y^2 - \beta|\dot{u}_x Z_x|Z_y - \gamma\dot{u}_x Z_x Z_y \tag{3.8}$$

where u_x, Z_x, u_y, Z_y are the displacement and hysteretic force components in the x and y directions respectively. In the present formulation, Z is represented as a dimensionless parameter, and force and displacement are expressed as moment and curvature.

$$\begin{pmatrix} M_x \\ M_y \end{pmatrix} = \alpha \begin{pmatrix} (EI)_x & 0 \\ 0 & (EI)_y \end{pmatrix} \begin{pmatrix} \phi_x \\ \phi_y \end{pmatrix} + (1-\alpha) \begin{pmatrix} M_x^y & 0 \\ 0 & M_y^y \end{pmatrix} \begin{pmatrix} Z_x \\ Z_y \end{pmatrix} \tag{3.9}$$

where M_x^y, M_y^y are the yield moments in the x and y direction respectively, and the path of the hysteretic components is described by:

$$\begin{pmatrix} \dot{Z}_x \\ \dot{Z}_y \end{pmatrix} = \{A[I] - B[\Omega][\Phi]\} \begin{pmatrix} \dot{\phi}_x \\ \dot{\phi}_y \end{pmatrix} \tag{3.10}$$

where:

$$\Phi = \begin{pmatrix} \dfrac{1}{\phi_x^y} & 0 \\ 0 & \dfrac{1}{\phi_y^y} \end{pmatrix} \tag{3.11}$$

$$\Omega = \begin{pmatrix} Z_x^2\{Sgn(\dot{\phi}_x Z_x)+1\} & Z_x Z_y\{Sgn(\dot{\phi}_y Z_y)+1\} \\ Z_x Z_y\{Sgn(\dot{\phi}_x Z_x)+1\} & Z_y^2\{Sgn(\dot{\phi}_y Z_y)+1\} \end{pmatrix} \tag{3.12}$$

where ϕ_x^y, ϕ_y^y are the yield curvatures in the x and y direction respectively, and

$$Sgn(\dot{\phi}_x Z_x) = 1 \quad \text{if} \quad \dot{\phi}_x Z_x > 0 \tag{3.13a}$$

$$= -1 \quad \text{if} \quad \dot{\phi}_x Z_x < 0 \tag{3.13b}$$

To ensure proper behavior under purely isotropic conditions, it is necessary to impose a constraint on the constants that appear in Eq.(3.10). Consider an arbitrary displacement path given by:

$$\phi_x = \phi\cos\theta; \quad \phi_y = \phi\sin\theta; \tag{3.14}$$

Substitution of these curvatures into Eq.(3.10) and consideration of the maximum magnitudes of Z_x, Z_y by partial differentiation yields the following constraint:

$$A = 2B \tag{3.15}$$

for isotropic material behavior, i.e., $Z_x = Z\cos\theta$ and $Z_y = Z\sin\theta$.

It is worthwhile to note that the interaction matrix of Eq.(3.10) can be expressed in a form similar to the eigenvalue equation suggesting that the two components can be uncoupled by diagonalization. This will lead to the special case of **no** interaction, though this will be true only for some unique instant.

Orthotropic behavior: The relationship given in Eq.(3.10) is for the case of isotropic hysteretic restoring forces. To extend the formulation for orthotropic material behavior, the following transformation is suggested by Park et al.(1986):

$$M_y' = \frac{M_x^y}{M_y^y} M_y \tag{3.16a}$$

$$\phi_y' = \frac{EI_y M_x^y}{EI_x M_y^y} \phi_y \tag{3.16b}$$

The above form of the orthotropic system results in an elliptic yield surface which is now recognized as the likely interaction surface for R/C components (Li et al.,1988).

It will now be shown that stiffness degradation and strength deterioration can be incorporated into the moment-curvature model described by Eq.(3.10), where the constraint equation of the material parameters given by Eq.(3.12) is applied to the governing differential equations.

Stiffness Degradation: Experimental evidence has shown that R/C sections undergo loss of stiffness during repeated cyclic loading as the magnitude of deformation increases. The original Takeda model used an exponential form to express the stiffness decay. Other approaches have also been suggested, though the primary factor governing the stiffness loss

is attributed to the state of deformation. In the present formulation, it was seen that the parameter A controls the unloading and reloading stiffness of the hysteretic component. Hence, the following equation was established to control stiffness degradation:

$$A_k = A_o e^{(-s_1 \mu_k)} \tag{3.17}$$

where:

$$\mu_k = (\mu_{max} + \mu_{k-1})/2 \tag{3.17a}$$

in which s_1 is the control constant which is evaluated using structural identification procedures (Chapter V), and μ_{max} is the maximum ductility level attained during the load history, and μ_{k-1} is the ductility level at the start of the current loading cycle. It will be seen that s_1 controls both the amount and rate of stiffness decay. Numerical examples are presented in Section 3.1.3. It must be mentioned here that any change in A as suggested by Eq.(3.17) will result in a corresponding change in B as given by Eq.(3.15).

Strength Deterioration: There is general agreement that strength loss under cyclic loading can be correlated with the amount of dissipated energy (Gosain et al.(1977), Iwan (1973); Park et al.,1985; Reinhorn et al., 1989). A simple formulation to include this effect is proposed:

$$M^y_{x,y} = M^y_{x,y}\left(1.0 - s_2 \int Z_{x,y} d\phi\right) \tag{3.18}$$

The energy term represented by the integral of the dimensionless hysteretic component and the curvature is normalized by the yield curvature value to give a non-dimensional coefficient. The parameter s_2 controls the amount of strength loss, and like s_1, is determined through system identification techniques.

The effect of s_1, s_2 in prescribing and controlling *stiffness* and *strength* loss respectively is presented in the next section. Also investigated is the effectiveness of the proposed biaxial model to reproduce displacement-controlled experimental tests of R/C specimens under bidirectional loading.

3.1.3 Numerical Testing

The use of the biaxial model, as proposed in this study, requires properties only at the uniaxial level. Hence, it is necessary to first simulate the uniaxial behavior. The properties of the model parameters so determined are then used directly in the biaxial simulation. Therefore, in the numerical study that follows, two series of tests are conducted. The first explores the effect of the stiffness and strength loss parameters as suggested by Eqs.(3.17)-(3.18). The next series of tests examines the validity of the proposed model under actual biaxial loading.

Control Tests: These series of tests investigate the effect of Eqs.(3.17)-(3.18). A simple displacement history (Fig.3.1) with increasing amplitudes is applied to a uniaxial system with the following properties: yield force = 5.0 units; yield displacement = 0.5 units; and post-yield stiffness ratio = 0.05. The resultant response is shown in Fig.3.2 for s1 = s2 = 0.0, indicating that no stiffness or strength loss is imposed.

Fig.3.3 demonstrates the effect the parameter s_1 on the stiffness decay of the system. It can be seen that the stiffness loss increases as the magnitude of deformation. The first simulation uses an s_1 value of 0.15. The effect of increasing this to 0.2 is also shown in the same figure. In both cases no strength deterioration is introduced. The apparent strength loss observed in Fig.3.3b is not due to the s_1 parameter, but a consequence of the mode of transition into the post-yield range. Hence, at large deformation levels, the introduction of some uncontrolled strength loss is unavoidable. However, most of the simulations on actual test data indicate that the probable range of s_1 is between 0.0 and 0.2 (the details are presented in Section 4).

The effect of the strength loss control parameter s_2 is shown in Fig.3.4. It was found that nominal strength loss, typical for well reinforced R/C sections, is achieved with s_2 = 0.001 - 0.005. The first simulation in this parametric study shows a system with significant strength loss per cycle. No stiffness degradation is imposed. Yet, with excessive strength loss, some apparent loss of stiffness is observed.

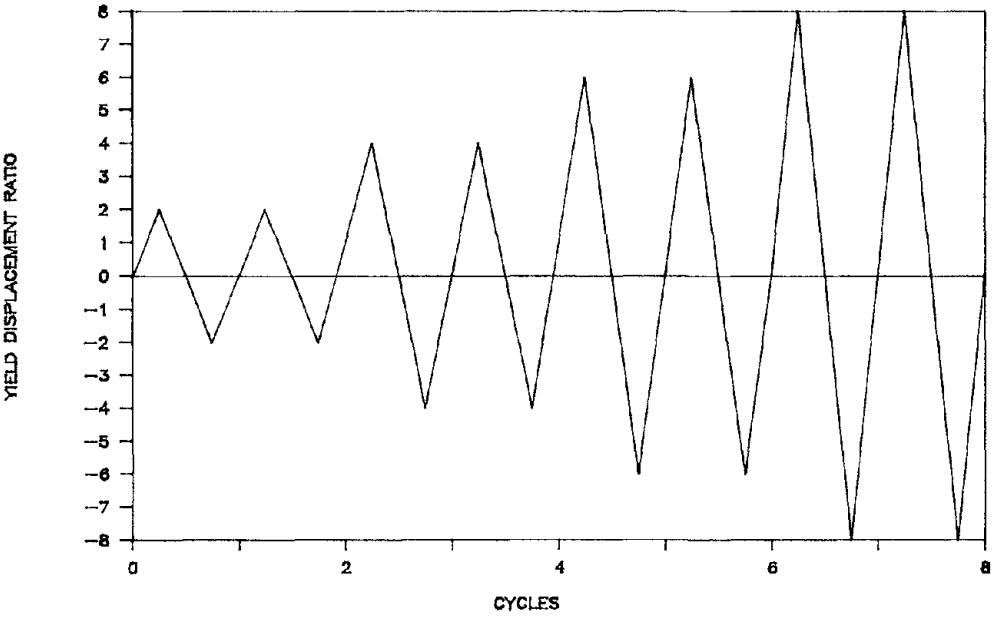

FIGURE 3-1 Displacement History for Model Testing

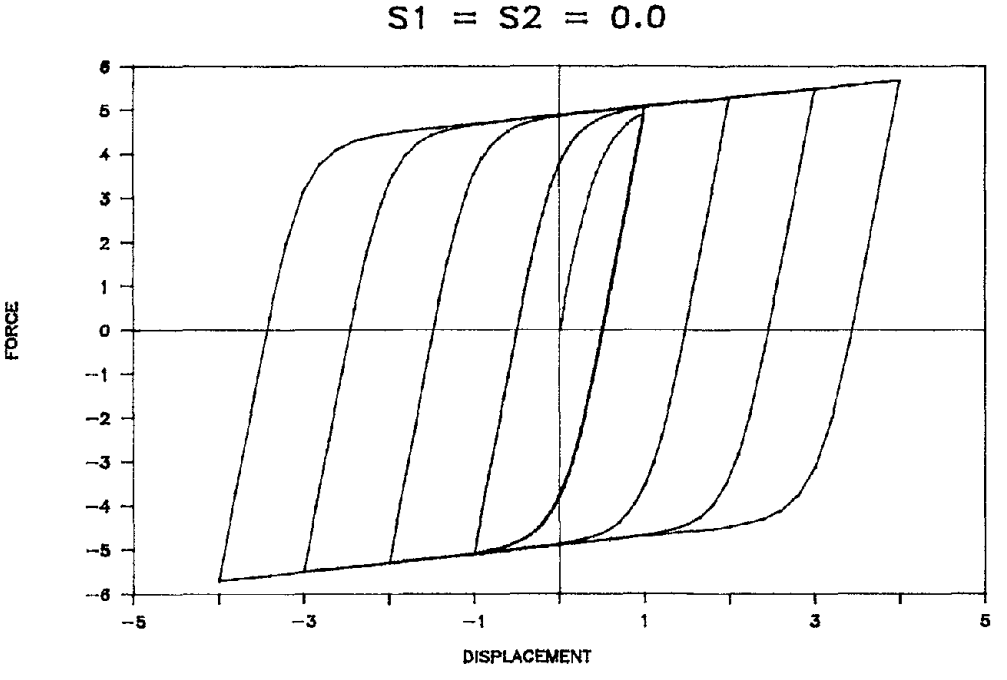

FIGURE 3-2 Hysteretic Response with No Stiffness or Strength Loss

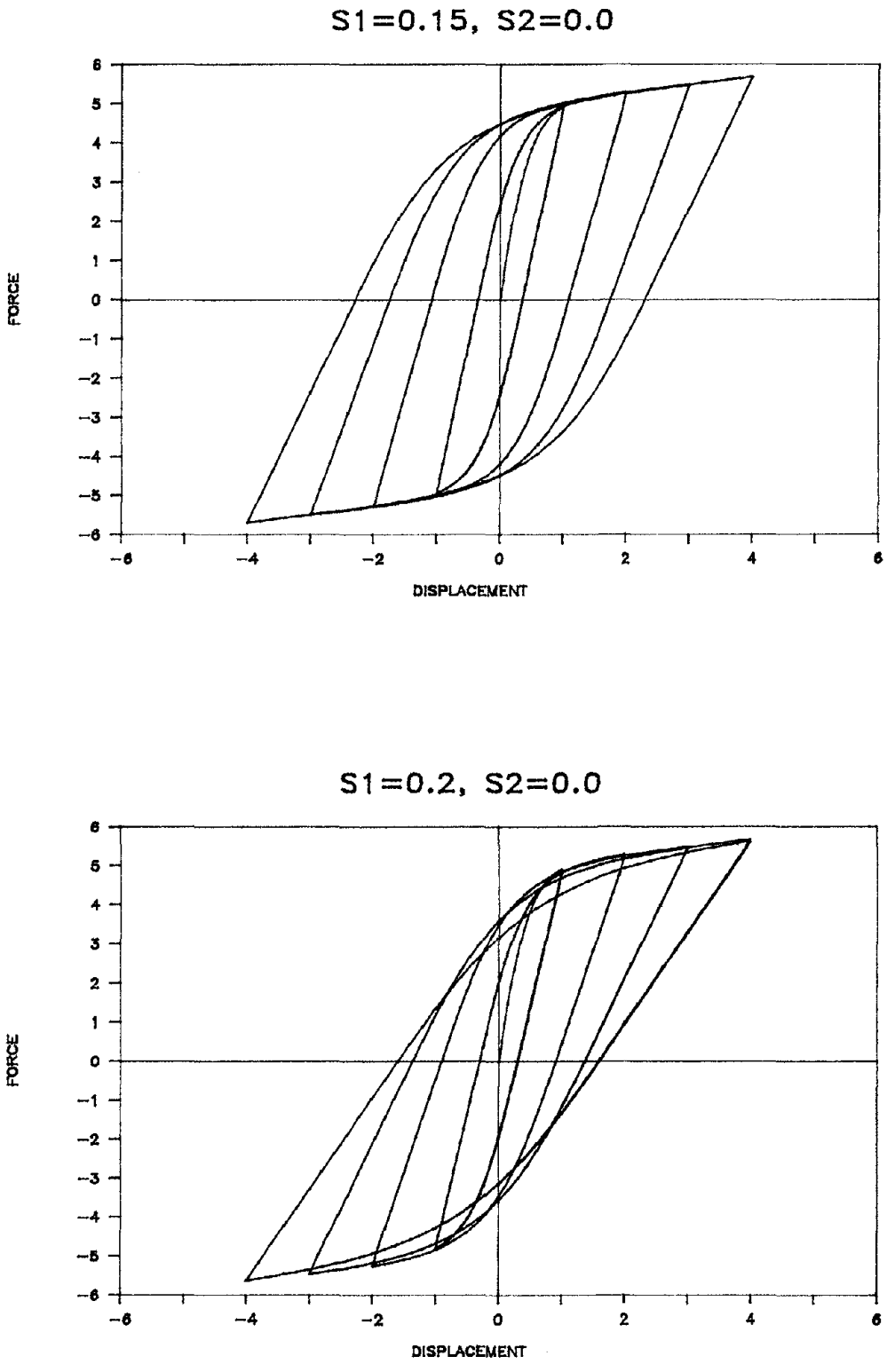

FIGURE 3-3 Effect of Stiffness Decay Parameter on System Response

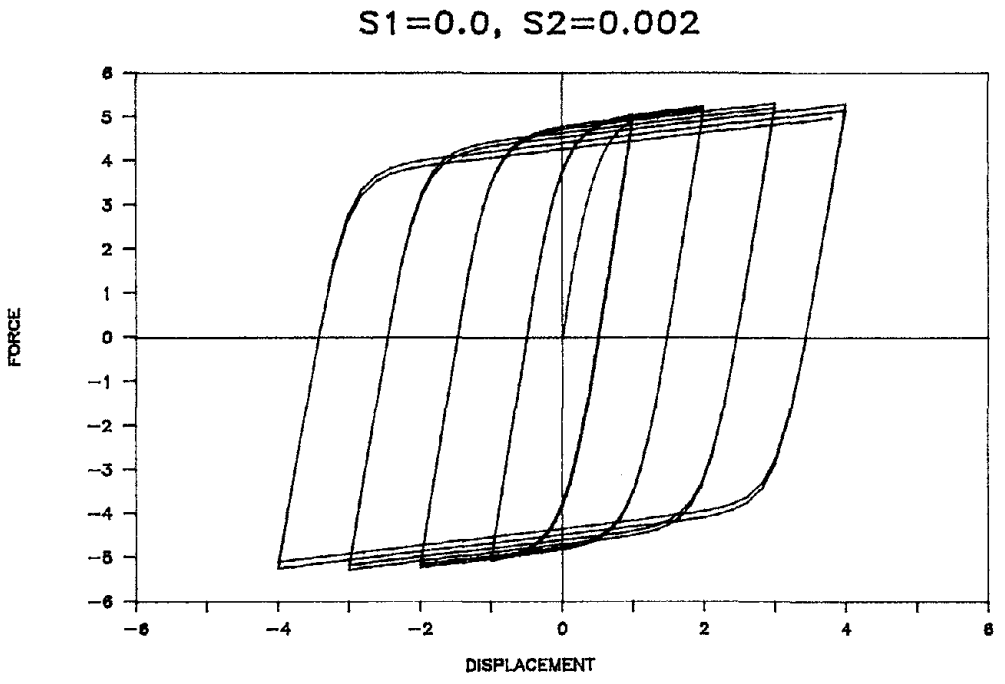

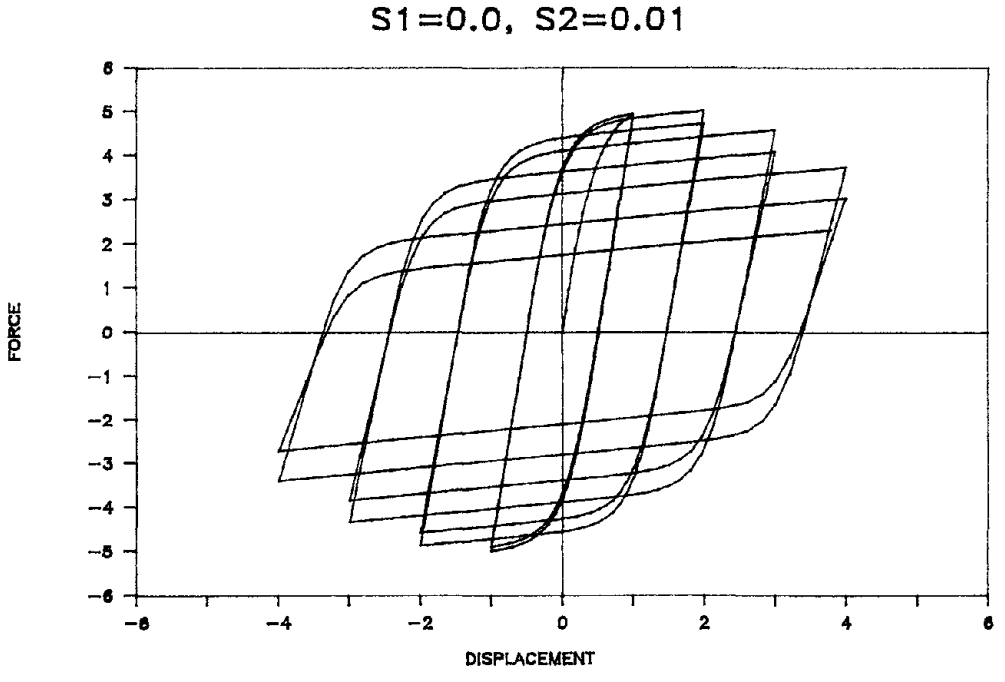

FIGURE 3-4 Effect of Strength Loss Parameter

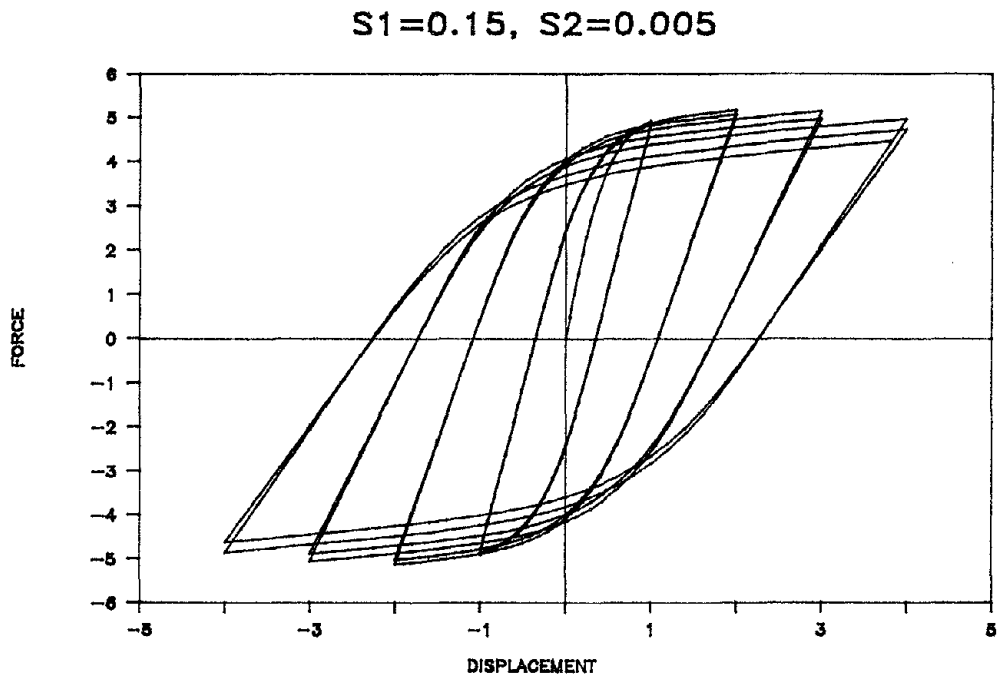

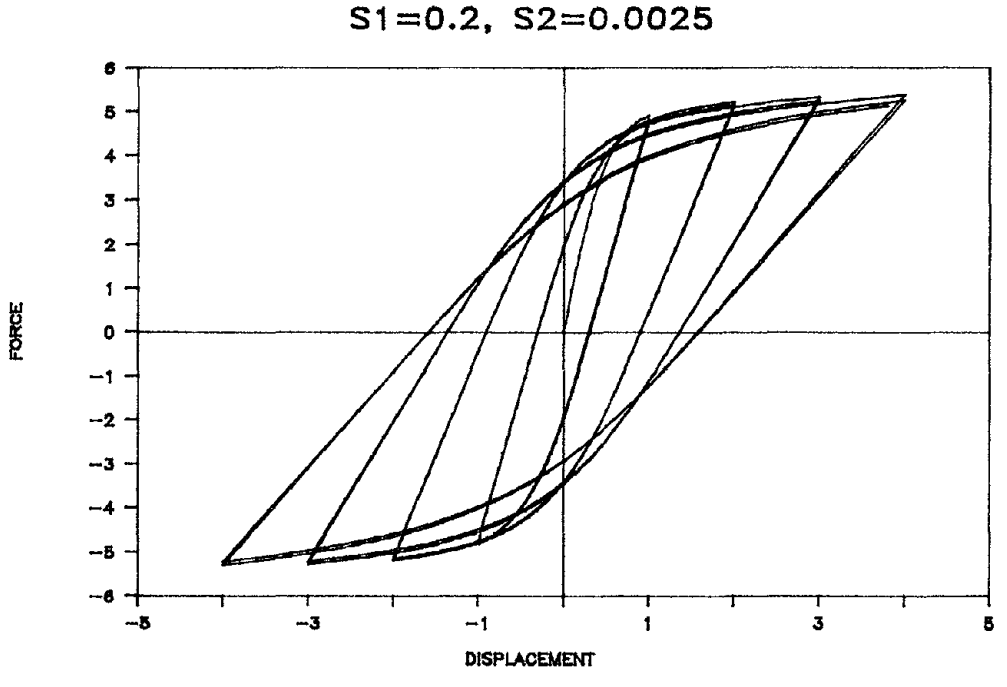

FIGURE 3-5 Combined Effect of Stiffness and Strength Decay Parameters

Again, this is due to the smooth transition mode of the hysteretic component. The magnitude of these discrepancies are negligible and do not affect the nature of the overall member response.

Realistic pattern of R/C behavior involves both stiffness loss and strength deterioration. Two such cases are examined for varying values of s_1 and s_2, as shown in Fig.3.5. The simulations prove the ability of the model to exhibit controlled loop behavior and is proposed as a viable alternative for modeling hysteretic behavior of R/C sections.

Biaxial Model Tests: The tests described in this section are based on data that was acquired from actual biaxial loading of R/C column specimens. The first set of data was obtained from tests conducted by Takizawa and Aoyama (1976) at the University of Tokyo. The test specimen (Fig.3.6) used for all the three simulations presented here consisted of 20.0 cm square columns with a shear span of 3.0 and four 13 mm deformed bars as main longitudinal reinforcement. Fig.3.6 includes a summary of the specimen details. Three displacement paths that were imposed on the specimen are shown in Fig.3.7. The first corresponds to a purely uniaxial displacement path. In the second series, the following displacement path is prescribed:

$$|x_\delta| + |y_\delta| = \text{constant}$$

For the final test, the following displacement path was investigated:

$$|x_\delta| = \text{const}, \quad \text{or} \quad |y_\delta| = \text{constant}$$

In both cases, some deviation from the desired displacement histories was observed, as shown in Fig.3.7.

The comparative results of the experimental and analytical simulations are shown in Figs.3.8-3.10. In Fig.3.8, the results of the uniaxial simulation are presented. It can be seen that the present formulation reproduces the experimental result with greater accuracy than the trilinear degrading model of Takizawa and Aoyama. The remaining simulations are shown in Fig.3.9 and 3.10 along with the corresponding experimental results. In both cases, it is again evident that the model proposed in this study captures the overall behavior with reasonable accuracy.

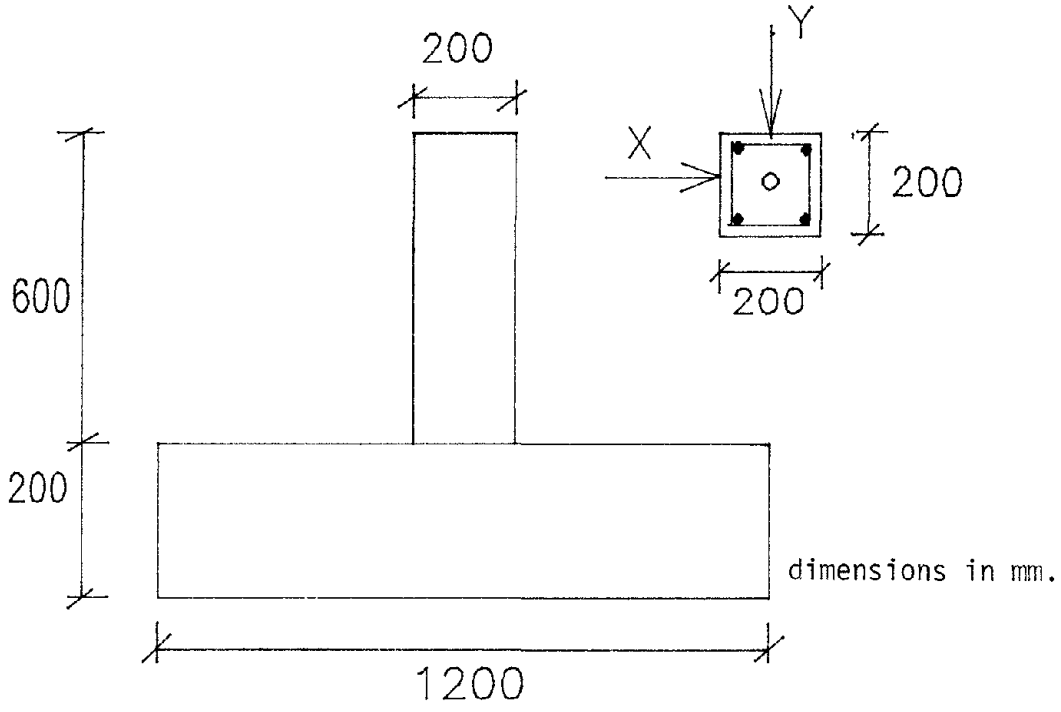

Dimensional details of test specimen

SPECIMEN DETAILS:

longitudinal reinforcement: 4 bars, 13mm dia.
hoop bars: 6 mm dia. @ 50 mm
depth of cover: 25 mm
shear span ratio: 3.0
constant axial force: 16 ton

FIGURE 3-6 Test Specimen for Biaxial Test (Takizawa and Aoyama, 1976)

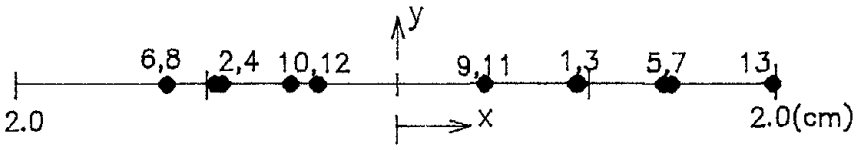

test #1

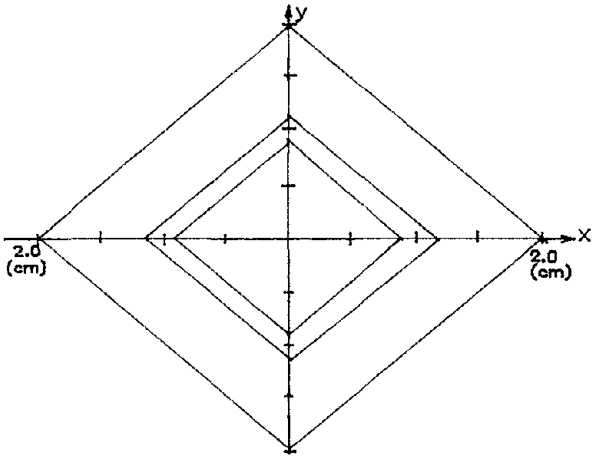

test #2

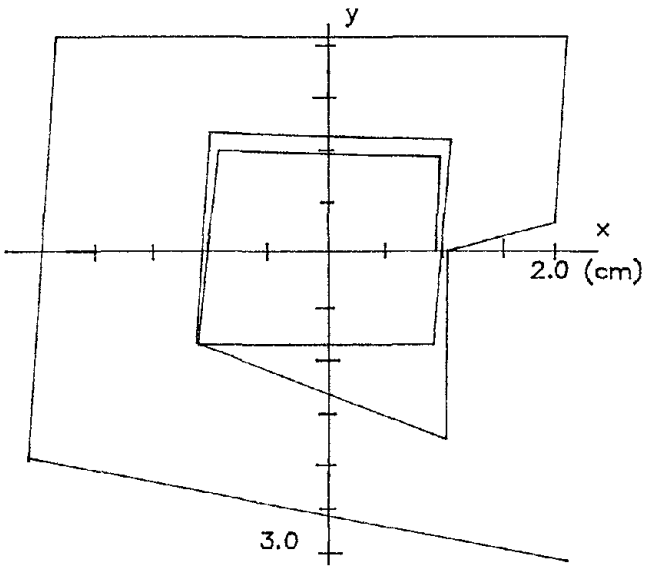

test #3

FIGURE 3-7 Displacement Paths for Biaxial Tests

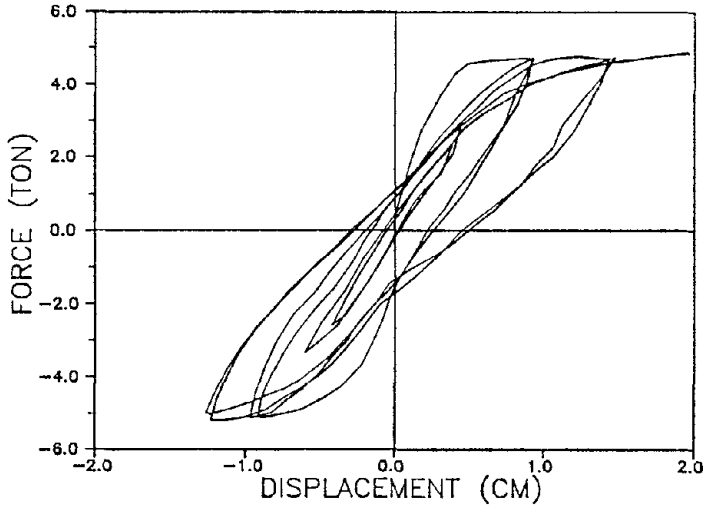

EXPERIMENT

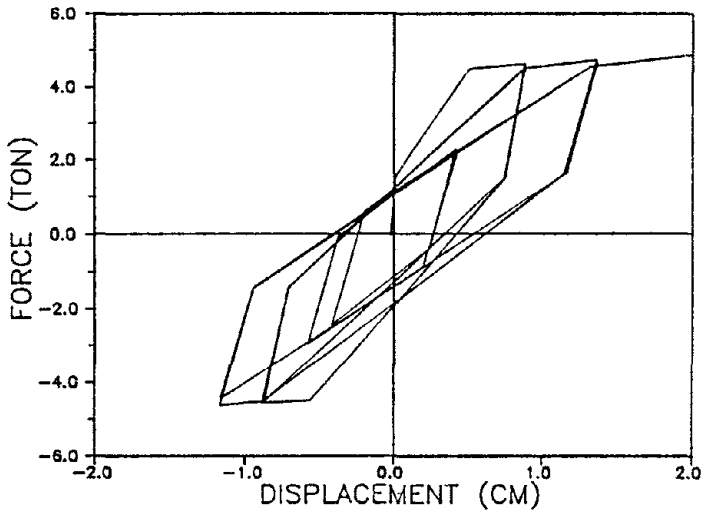

TRILINEAR MODEL
(Takizawa and
Aoyama, 1976)

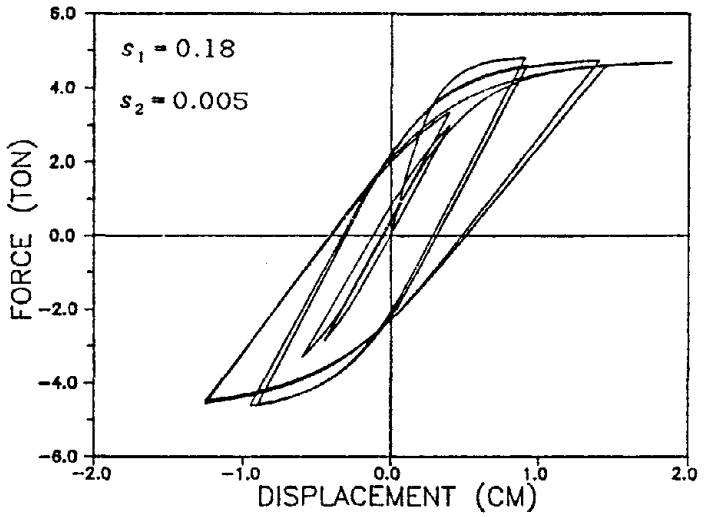

PRESENT
FORMULATION

FIGURE 3-8 Comparative Results for Uniaxial Test

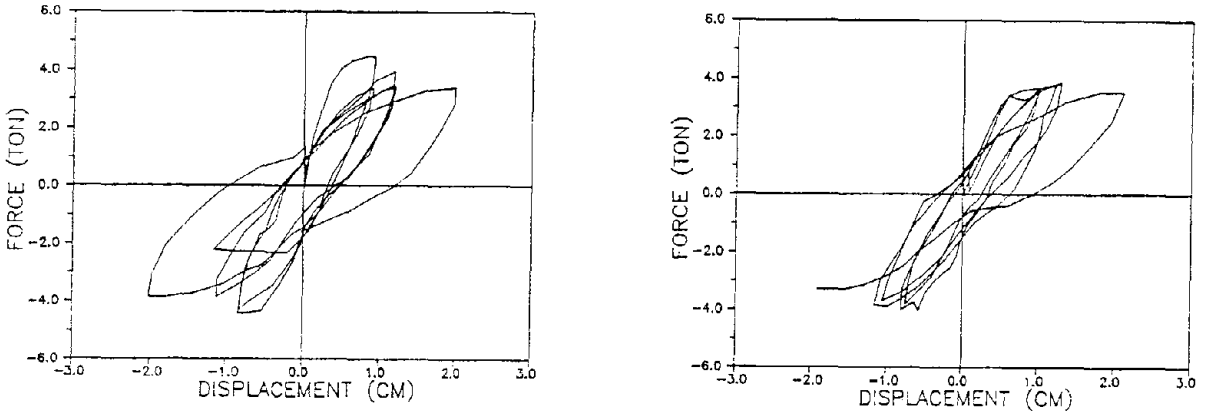

(a) EXPERIMENT

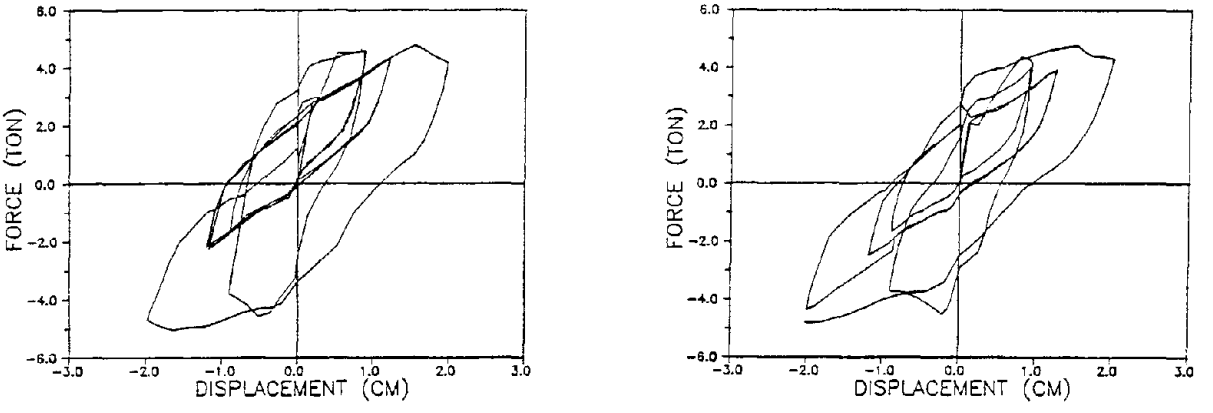

(b) TRILINEAR MODEL (TAKIZAWA AND AOYAMA)

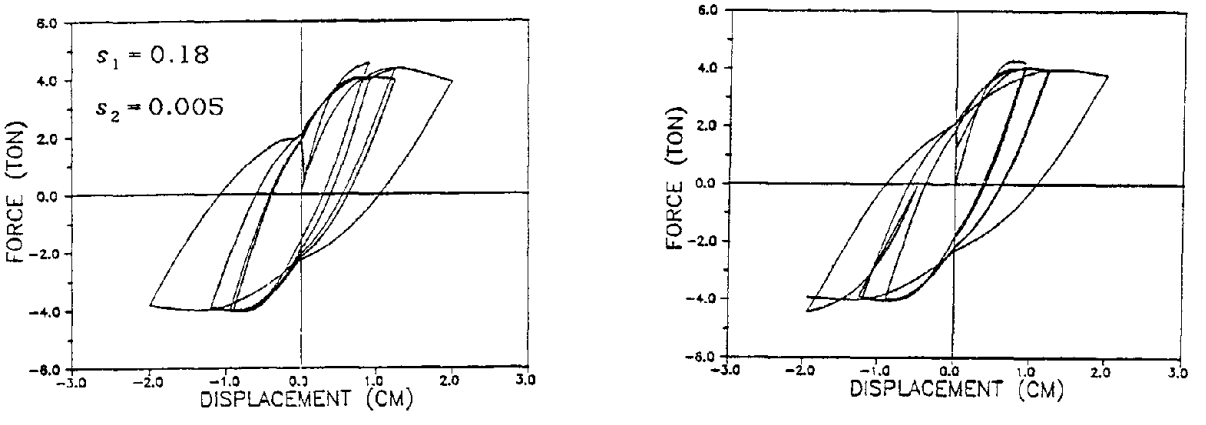

(c) PRESENT FORMULATION

FIGURE 3-9 Comparative Results for Biaxial Test #2

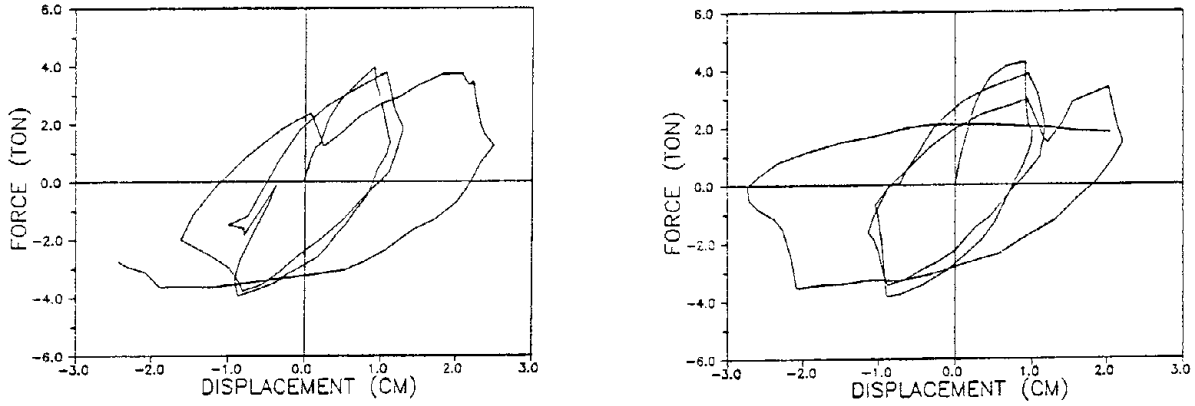

(a) EXPERIMENT

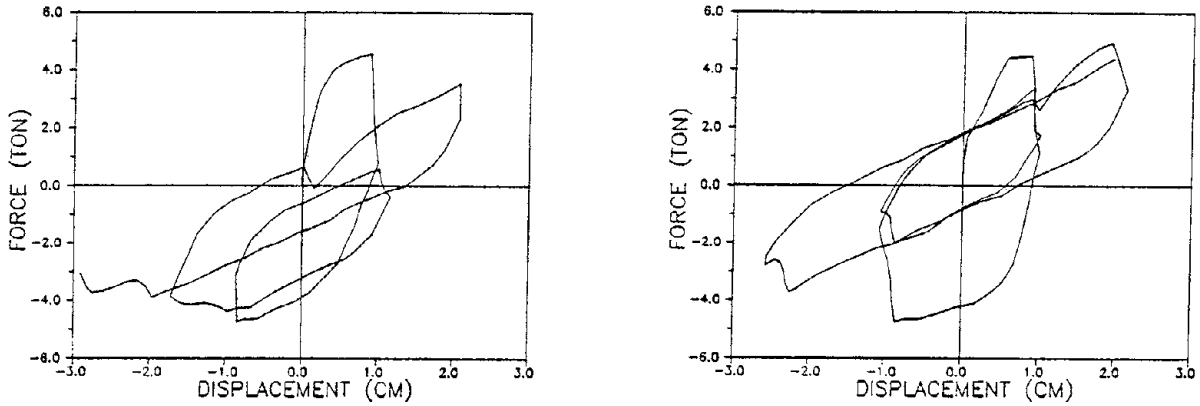

(b) TRILINEAR MODEL (TAKIZAWA AND AOYAMA)

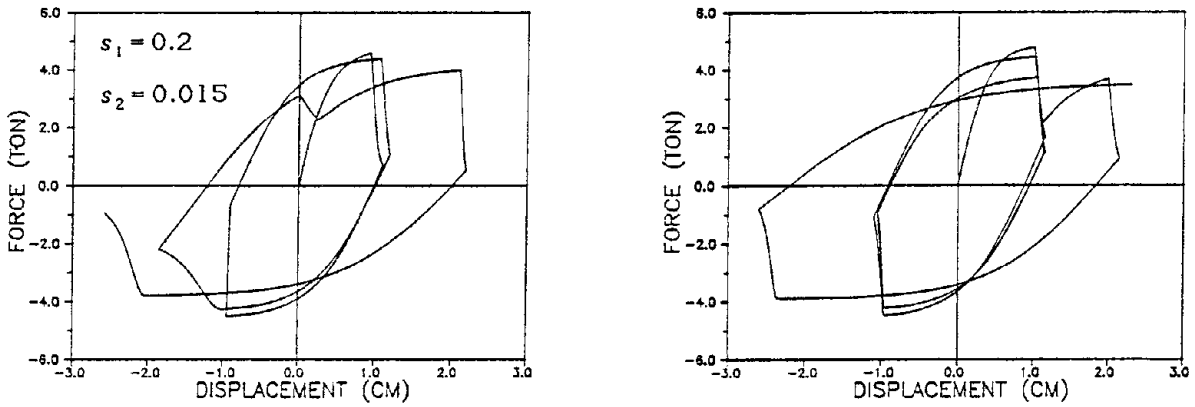

(c) PRESENT FORMULATION

FIGURE 3-10 Comparative Results for Biaxial Test #3

The next simulation was carried out on data taken from Otani et al.(1980). The model specimen details and prescribed loading path are shown in Fig.3.11. The specimen was moved in an approximately square path with amplitudes of the order of half the yield displacement in the south and west directions and almost five times the yield displacement in the north and east directions. The results of other models presented in Fig.3.12 are taken from Lai (1987). With the exception of the bilinear biaxial model, all the other models reproduce the biaxial behavior with adequate accuracy for practical modeling of inelastic R/C response.

The main advantages in using the model proposed in this study are the following: (1) the ability of the model to reproduce a range of hysteretic characteristics by varying the coefficients that appear in Eq.(3.10) and the governing differential equations of (3.9); (2) the implementation of the model requires merely the solution of 2 first-order equations which can be accomplished with ease using a 4th order Runge-Kutte solution; (3) this results in an extremely efficient procedure with high computational efficiency since tracing of the hysteretic loops is not necessary; and (4) very little book-keeping (online storage of essential parameters from previous solution step) is required. These facts make the present formulation versatile and efficient. The results presented here, however, are meant only to reflect the efficiency and applicability of the model for use with fully 3-dimensional analysis of R/C structures in which biaxial bending interaction is considered. The actual nature of the interaction and its sensitivity to material and component parameters is not fully known at this point. A great deal of experimental testing and analytical calibration is necessary before the proposed model is validated for use with reinforced concrete systems.

3.2 One-Dimensional Force-Deformation Model

A separate model is used to characterize the uniaxial behavior of beams, slabs and shear walls. As pointed out earlier, the viscoplastic model developed in the previous section assumes symmetric properties in tension and compression. Also, in its present form, pinching behavior due to bond-slip cannot be reproduced. These limitations make it necessary to retain a conventional unaxial model which can handle (a) T-beams, and (b) the shear spring behavior of walls and slabs.

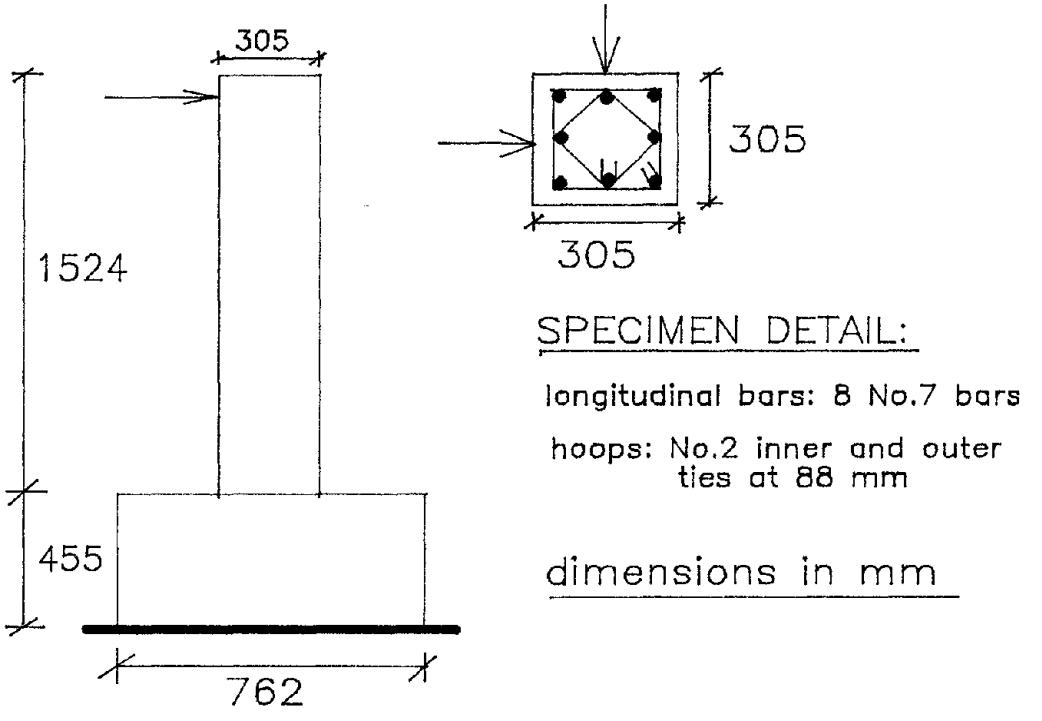

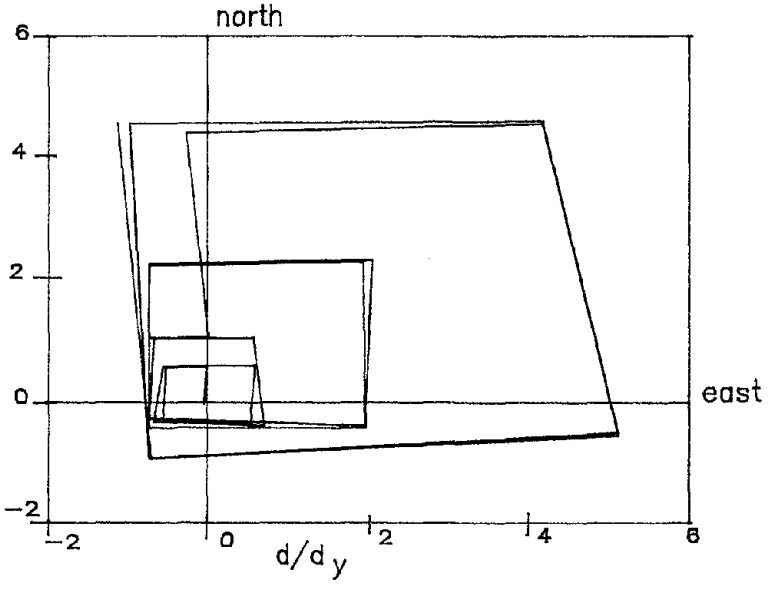

FIGURE 3-11 Specimen Details and Loading Path for Biaxial Test (Lai, 1987)

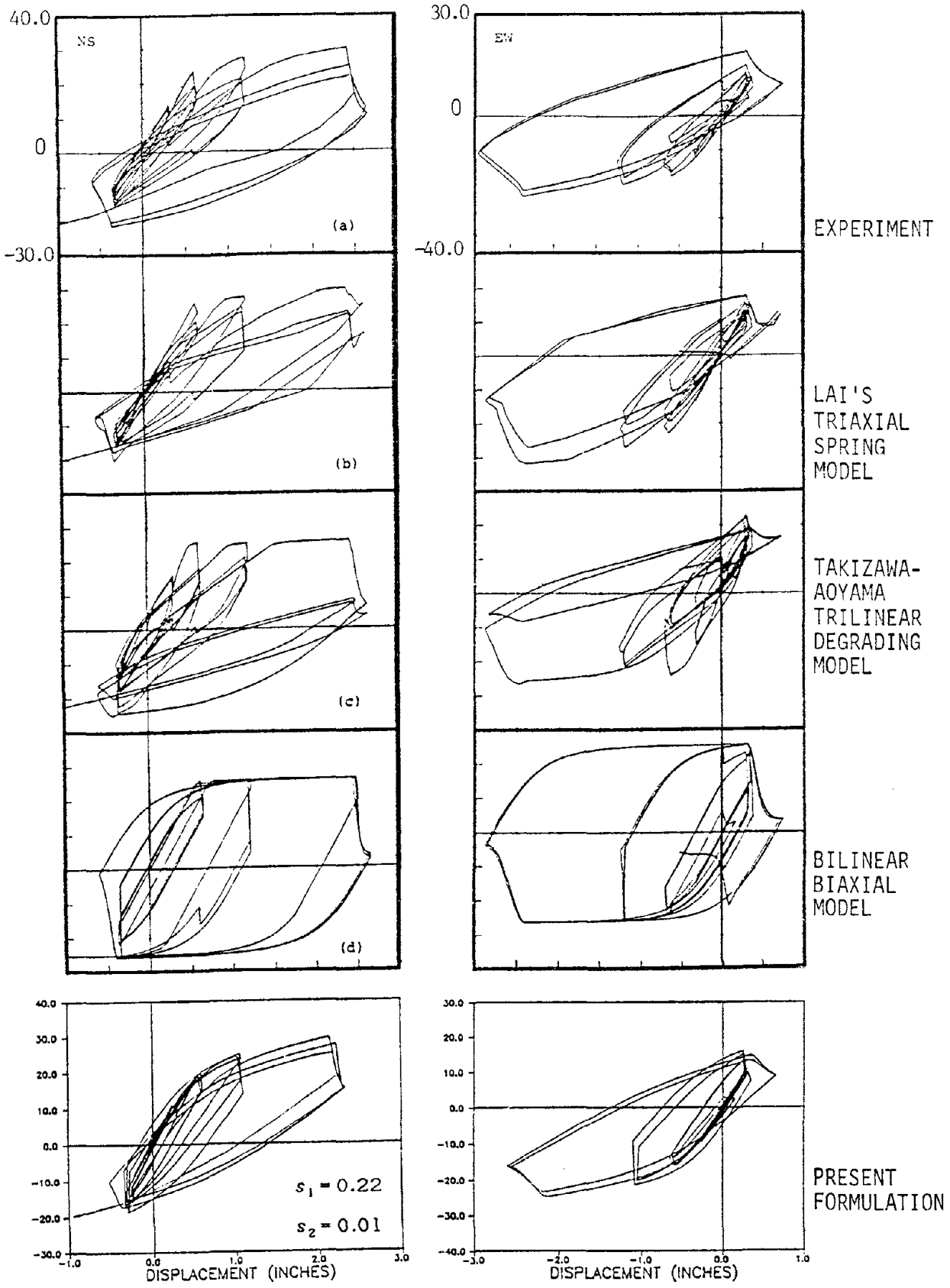

FIGURE 3-12 Comparative Results of Previous Analytical Models and Present Formulation

This model, called the 3-parameter model, was developed earlier in conjunction with an experimental program for substructure testing (Kunnath et al.,1987). Relevant details of the model and specification of hysteretic rules may be found in a separate publication (Park et al.,1987). The 3-parameter model has performed well in the earlier version of IDARC and was shown to simulate a variety of other hysteretic models (Park et al.,1987).

SECTION 4

STRUCTURAL IDENTIFICATION

The idea that a primarily empirical approach is better suited to evaluate the parameters that define hysteretic models is to be found mostly in Japanese literature on R/C modeling. In fact, such a premise forms the focus of a state-of-the-art document prepared by Umemura and Takizawa (1982). The need to resort to such a formulation is almost self-explanatory: reinforced concrete is a complex heterogeneous material whose properties are dependent on innumerable factors ranging from the quantity, quality and arrangement of its constituent components to placement and workmanship of the finished component. The trends dictated by experimental testing is hence bound to be a better indicator of component behavior than analytical predictions based on approximate assumptions. This philosophy forms the basis of the identification module and is central to the overall analytical concepts presented in this study.

The macro-modeling of reinforced concrete components involves the prescription of force-deformation curves and some associated rules for unloading and reloading. The identification task can, therefore, be divided into two parts: the first is to establish the monotonic failure envelopes for each component, and the second is to identify the parameters which define the hysteretic rules related to stiffness degradation, bond-slip, etc. In the present study, a trilinear envelope is used to distinguish cracking and yielding of the component. This envelope is generally non-symmetric in compression and tension for T-beams (or other cross-sections lacking symmetry about the bending axis) but symmetric for columns, walls and slabs.

The modeling of the trilinear envelope for the equivalent inelastic spring of beam and column elements is achieved through empirical relations based on calibrated experimental data. Shear walls are composed of two inelastic springs: flexure and shear. The latter is established through the use of empirical models while the former is determined using an analytical fiber model analysis.

A generalized procedure for the filament (or fiber model) analysis of R/C sections was developed and has been reported in an earlier report (Reinhorn et al.,1988). This enhanced formulation allows for the prescription of varying reinforcement across the cross section, each with different material properties. The developed model is used in this study for the determination of the flexural capacity envelopes of walls. In the case of beams and columns, available empirical models are used, based on statistical analysis of experimental data.

Identification of hysteretic parameters, in this study, is proposed through empirical equations and rational suggestions based on observed experimental data.

Details of the identification procedures is described in subsequent sections which is organized into two main parts: (1) envelope curve determination, and (2) hysteretic parameters identification.

4.1 Trilinear Envelope for Uniaxial Inelastic Deformations

The envelope curve used for all elements is characterized by two turning points: cracking and yielding. All formulations are empirical and based primarily on regression analysis of extensive experimental data. Details of the formulation may be found in an earlier report (Park et al., 1987).

Since two independent springs are used to model the behavior of walls and slabs, the envelope parameters for flexure and shear are developed uniquely. A filament model is used to construct the flexural envelope curve while empirical equations based on the regression analysis of test data is used for the shear parameters. All formulations and equations have been reported in Park et al.(1987).

The empirical models presented above complete the definition of the envelope curve for all components. The next task is to establish the parameters which control the hysteretic behavior. This procedure is detailed in the next section.

4.2 Identification of Hysteretic Parameters

Two sets of parameters need to be identified: (a) hysteretic parameters related to the viscoplastic model, and (b) the data for the three-parameter model. Approximate empirical

equations are suggested for the latter case based on regression analysis of calibrated experimental results. For the viscoplastic model, some preliminary estimates are provided based on observed trends from a sample set of experiments, the details of which discussed in the following section.

4.2.1 Biaxial Viscoplastic Model

The viscoplastic model proposed in this study is meant to serve as the basis of an overall conceptual model for hysteretic systems. Its superiority over other schemes stems from the fact that the force-deformation path is obtained from the solution of differential equations without need for tracing complex hysteretic loops. As explained in Chapter IV, the shape and magnitude of the loops is controlled by two parameters s_1 and s_2. It is necessary to carry out extensive calibration studies to arrive at reasonable empirical values for these parameters. In the present study, a sample set of simulation studies were carried on available test data (Wight and Sozen, 1973). A summary of the simulations is presented in Table 4.1.

This initial parametric study suggests that the value of s_1 lies between 0.08 (for nominal stiffness decay) to about 0.25 for very large degradation of the system stiffness. This was also observed in the analytical simulation of Chapter IV. This parameter is a function of both the axial force level and the amount of transverse steel. Higher axial force levels cause less stiffness decay while lower transverse steel causes larger stiffness loss. Though the concrete strength did not vary much, it was observed that an increase in f'_c reduced the amount of stiffness degradation.

The strength parameter, s_2, showed an exactly opposite behavior pattern for variations of axial force and concrete strength. An increase in the axial force level caused greater strength loss, and lower concrete strengths produced less strength deterioration. However, this may not represent a true correlation since, in these tests, the amount of transverse steel varied more considerably. Hence, it seems that the transverse steel ratio controlled the behavior of the components. As expected, higher ratios of transverse steel produced lower levels of strength loss.

TABLE 4-1 Calibration of Empirical Parameters for Biaxial Model

SPECIMEN	N (%)	ρ_l (%)	ρ_t (%)	f'_c	s_1	s_2
1	17.9	2.4	0.33	5.03	0.08	0.025
2	17.2	2.4	0.33	4.87	0.095	0.01
3	10.7	2.4	0.33	4.88	0.135	0.015
4	0.0	2.4	0.33	4.64	0.25	0.01
5	20.4	2.4	0.48	3.7	0.125	0.005
6	0.0	2.4	0.48	3.75	0.175	0.005
7	17.3	2.4	0.67	4.84	0.10	0.001
8	0.0	2.4	0.67	4.61	0.105	0.001
9	16.5	2.4	0.92	5.15	0.09	0.0005
10	0.0	2.4	1.05	4.85	0.08	0.0005

Notation:

$$N = \frac{P}{0.5A_g[0.85f'_c(1-\rho_l)+f_y\rho_l]}$$

where:

P = axial load

ρ_l = longitudinal reinf ratio

ρ_t = transverse reinf ratio

f'_c = concrete strength

f_y = yield stress of reinforcement

A_g = gross cross-sectional area

(for test setup and additional specimen details, see Wight and Sozen, 1973)

No attempt was made to derive an empirical relation based on the limited correlation studies conducted in this study. However, some of the essential features of the control parameters have been established. It is proposed that more calibration studies be carried out to develop reliable empirical models for the two parameters.

4.2.2 Three-Parameter Model

The uniaxial hysteretic model described in Chapter IV is characterized by three parameters: α, β and γ which represent stiffness degradation, strength deterioration and pinching respectively. The following general scheme works well for typical sections:

an origin-oriented model for the shear spring in shear walls, achieved by setting $\alpha = 0$

nominal degradation for moderate to heavily reinforced elements is achieved by setting $\alpha = 2 \rightarrow 3$

no slip is suggested for beams and columns (though the biased loop behavior in T-Beams is automatically simulated).

The identification of these parameters is straightforward if cyclic testing is carried out on typical components. A procedure has been developed at SUNY/Buffalo (Yeh, 1988) using nonlinear search algorithms and optimization techniques to identify the three parameters when test data is readily available. Analytical simulations were carried out on a large set of available experimental data of cyclic testing. The following initial estimates are proposed based on the regression analysis of the simulated data:

$$\alpha = 2.38 N^{-0.07} \rho_l^{-1.06} f_c'^{-0.23} \tag{4.1}$$

$$\gamma = 0.45 \rho_l^{-11.7} \rho_t^{0.03} f_c'^{1.3} \tag{4.2}$$

where:
$$N = \frac{P}{0.5 A_g [0.85 f_c' (1 - \rho_l) + f_y \rho_l]} \tag{4.3}$$

in which:

P = axial load

ρ_l = longitudinal reinf ratio

ρ_t = transverse reinf ratio

f_c' = concrete strength

f_y = yield stress of reinforcement

A_g = gross cross-sectional area

The coefficients of variation for the two parameters was 0.39 and 0.11 respectively. The transverse reinforcement ratio was not used in equation for the stiffness degradation parameter because the regression analysis indicated very poor correlation. The strength deterioration parameter has been empirically formulated from regression analysis of a large set (261) of beam and column cyclic test data (Park et al.,1987):

$$\beta = [0.37 n_o + 0.36(k_p - 0.2)^2]0.9 p^w \qquad (4.4)$$

where:

n_o = *normalized axial stress*

k_p = *normalized steel ratio* $\left(\frac{p_t f_y}{0.85 f_c'}\right)$

f_y = *yield stress of reinforcement*

p_w = *confinement ratio* $\geq 0.4\%$

The equation shows a negative correlation between the deterioration parameter and the confinement ratio and weak positive correlations between all the other parameters. Considerable scatter was observed between calculated and experimental values (with a coefficient of variation of 60%).

The various models proposed in the above sections for inelastic property identification is incorporated into the overall modeling scheme of the present study. Since the results of the statistical analysis are by no means conclusive, the definition of these parameters in the

computer model is open-ended with options for the user to over-ride program generated values. More calibration studies are proposed for improving the reliability of the identification task.

SECTION 5

RESPONSE ANALYSIS OF ASSEMBLED MACRO-MODELS

The element stiffness matrices are assembled onto the global structural stiffness matrix after combining the common degrees-of-freedom. The inelastic response analysis is carried out on the assembled element stiffness matrix in conjunction with the force-deformation models formulated in Chapter 3 and the identified inelastic properties presented in Chapter 4. The analysis of the assembled macro-models involves the following sequence of operations:

(a) Computation of initial stress states in components under dead and live loads.

(b) Failure/collapse mode analysis under monotonic lateral loading. Lateral loading is applied in both lateral directions. This operation is extremely useful to detect primary failure modes, estimate the building strength, and make necessary design changes prior to a full dynamic analysis.

(c) Incremental response analysis under either (a) bi-directional and vertical seismic excitations using the Newmark's beta algorithm, or (b) cyclic loads with force or deformation control.

(d) Finally, a seismic damage evaluation of the building is performed using a new conceptual model of damage. Complete details of the damage model are presented in Section 6.

For a fully 3-D analysis, all six degrees-of-freedom per node are considered, producing an overall stiffness matrix whose order is six times the number of free nodes in the system. If a rigid floor option is used, the three degrees-of-freedom corresponding to the floor degrees-of-freedom (see Section 2) are transformed to the center of mass, thereby resulting in a system with fewer degrees of freedom. No static condensation of the remaining nodal degrees-of-freedom are performed. In all cases, the final equilibrium equation to be solved assumes the following form:

$$[K]\{u\} = \{F\} \tag{5.1}$$

where [K] is the overall stiffness matrix, {u} is the vector of unknown nodal displacements,

and {F} is the vector of applied equivalent forces on the system. Since the stiffness matrix is symmetric and banded, a compact scheme is used to store the resultant matrix (Fig.5.1) in which the main diagonal is offset to the first column and only the remaining half band width is saved.

The basic solution procedure used in the inelastic analysis is shown in Fig.5.2. Stiffness matrices are stored at the element level. These matrices are then assembled onto the global stiffness matrix. The load vector corresponding to the right-hand side of Eq.(5.1) is established, depending upon the type of analysis being performed (static, monotonic, cyclic, or dynamic). Following the solution of the equilibrium equation, the inelastic moments at the ends of each element are computed from the recovered member nodal displacements. Since the formulation of the element stiffness matrix, as detailed in Chapter II, enables the creation of inelastic rotation sub matrices, they can be used directly in the computation of inelastic end moments at the face of the element across the rigid panel zone. The updating of stiffness matrices is carried out only in the event of a stiffness change.

In the framework of the overall modeling scheme, several unique features were developed in this study to facilitate a rational and reliable inelastic response analysis. A single step force-equilibrium correction procedure was incorporated into the cyclic and seismic analysis routines. A stiffness updating procedure was developed to minimize errors during unloading and reloading in post-yield regions. Finally, a simple equivalent force method was devised to account for P-delta effects due to inter-story drift. Details of these procedures and the general features of the analyses modules are presented in the following sections.

5.1 Static Analysis Under Initial Loads

The analysis phase begins with the evaluation of the initial stress states of members under equivalent dead and live loads that exist in the structure prior to application of cyclic or earthquake loads. The same initial state is assumed prior to the failure mode analysis under monotonically increasing lateral load. For the static analysis option, loads can be specified in two ways: (a) uniformly distributed loads; and (b) nodal forces and/or moments. If a uniform load is specified, equivalent nodal values with fixed-end forces are computed.

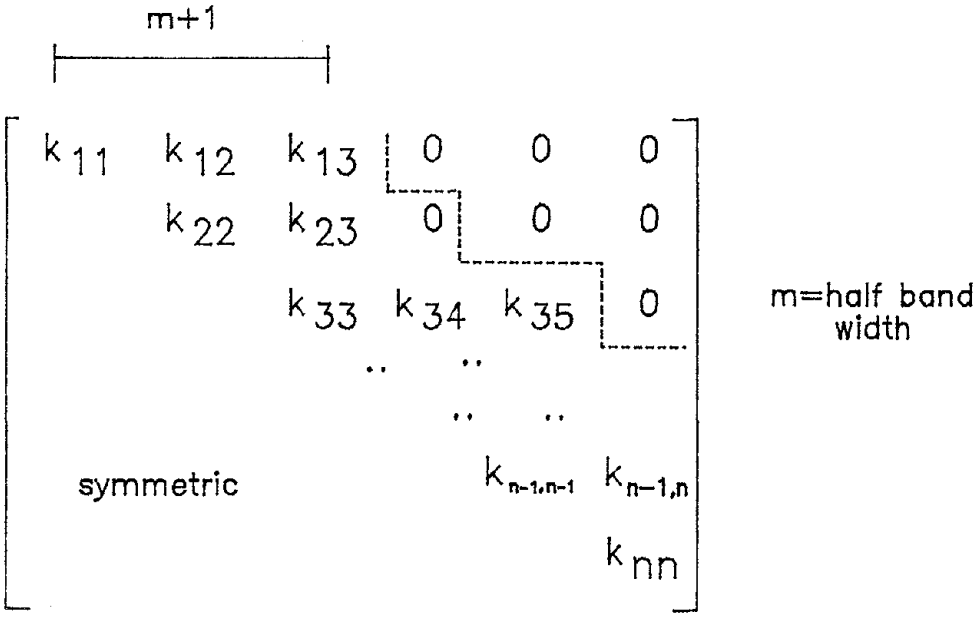

Actual stiffness matrix

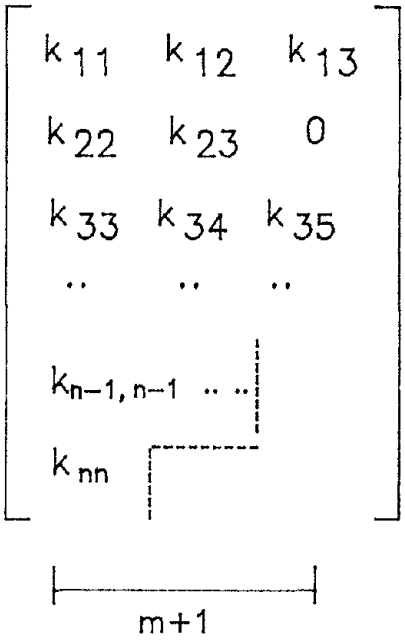

Compact storage scheme

FIGURE 5-1 Storage Scheme for Global Stiffness Matrix

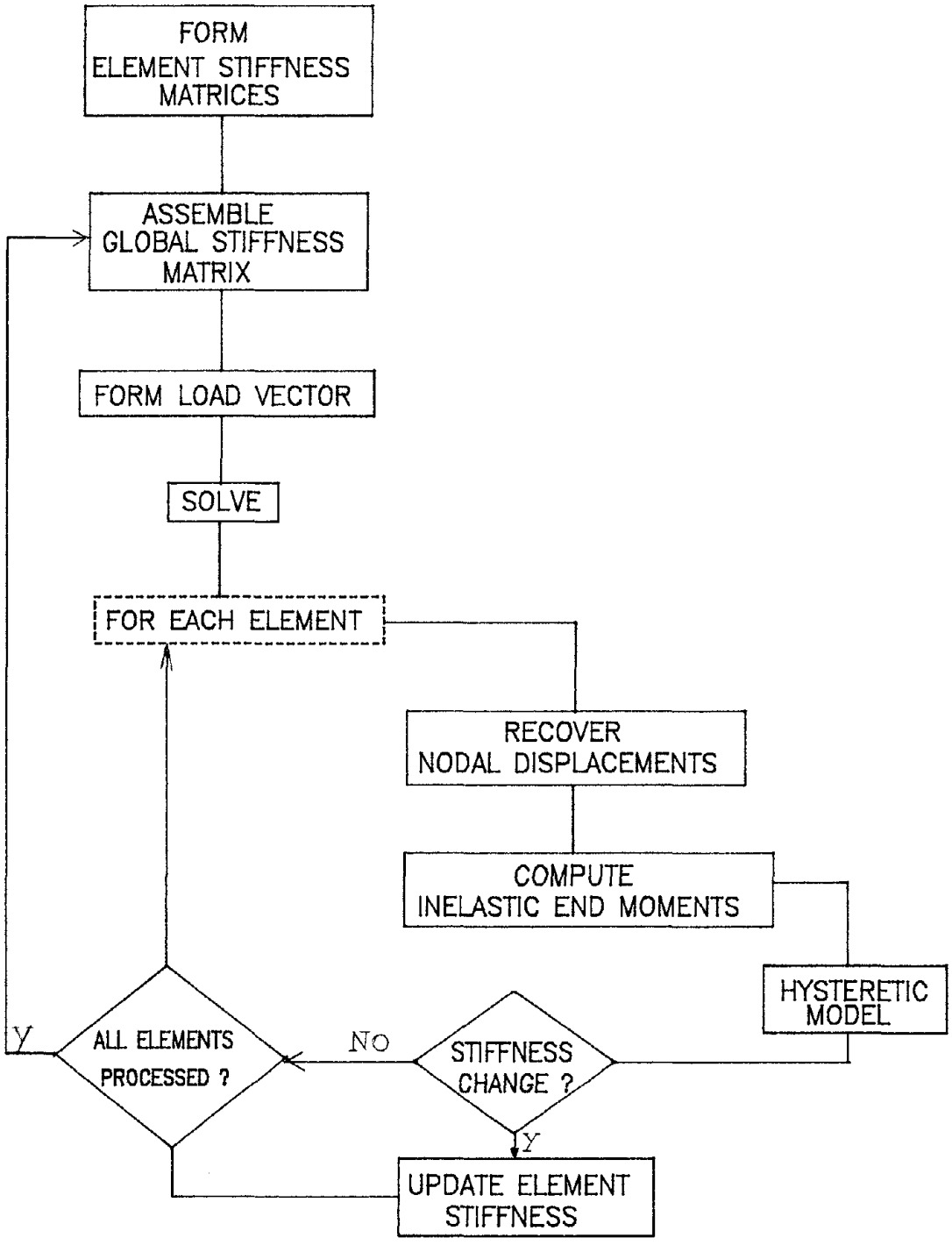

FIGURE 5-2 Basic Solution Procedure for Inelastic Analysis

Alternatively, the initial stresses may be input by the user from actual measurements prior to testing, and input as direct initial forces in the members. Due to the assumed linear moment distribution in the flexibility matrix, stress levels in the members due to initial loads must be relatively small so that the assumed moment distribution pattern is not seriously violated. Also, since no equilibrium check is performed at this stage, the stresses in all elements must be below the cracking strength of the respective components.

5.2 Monotonic Analysis for Failure Mode

A collapse mode analysis is a simple and efficient technique to predict seismic response behavior prior to a full dynamic analysis. The method provides a means to assess design requirements and consequently change appropriate parameters to achieve a desired sequence of component yielding. The monotonic analysis involves an incremental solution procedure whereby the structure is loaded laterally in the two principal horizontal directions. Two types of loading patterns may be applied: (a) uniform load, or (b) inverse triangular form.

Buildings with rigid floors: The force vector corresponding to the lateral degree-of-freedom/floor in one direction is computed as follows:

for uniform load distribution:

$$f(i) = \frac{\Sigma w_i}{N} \tag{5.2}$$

where w_i is the weight of story i, and N is the total number of stories.

for inverse triangular distribution:

$$f(i) = \bar{w}_b \frac{\Sigma w(i)}{\Sigma w(i)h(i)} w(i)h(i) \tag{5.3}$$

where w, h and $\bar{w}_b$ are the weight, height and factored base shear estimate and the subscript i refers to the story level under consideration.

General 3-D buildings: In this case, the above equations can still be used by dividing the building into frames and determining the floor weights for each frame. Equations (5.2) and

(5.3) can then be applied to the respective frames. The computed equivalent lateral load per floor for each frame is divided propotionally among all the lateral degrees of freedom on that floor.

The lateral load distribution, as computed from one of the above procedures, is then applied to the structure in small increments, as a function of building weight. The stress state of each member is evaluated at the end of each step of load application. Stresses are determined at critical sections only, viz., the end sections, except for floor slabs and walls where shear failure is also monitored. Analysis proceeds till the deflection of the top of the structure exceeds 2% of the total building height. The analysis is carried out for both lateral directions of the building.

5.3 Incremental Dynamic Analysis under Earthquake Loads

The incremental solution of the assembled system of equations involves the following dynamic equation of equilibrium:

$$[M]\{\Delta\ddot{u}\} + [C]\{\Delta\dot{u}\} + \{R(u_t)\} = \{F(t)\} \qquad (5.4)$$

in which:

$[M]$ is the lumped mass matrix

$[C]$ is the viscous damping matrix

$\{R(u_t)\}$ is the restoring force vector at the start of the time step

u is the relative displacment

$\{F(t)\}$ is the effective load vector

The solution of Eq.(5.4) is accomplished by a direct step-by-step integration procedure using the Newmark method (Bathe, 1982). The following assumption is an extension of the linear acceleration method:

$$\{\dot{u}\}_{t+\Delta t} = \{\dot{u}\}_t + \Delta t[(1-\delta)\{\ddot{u}\}_t + \delta\{\ddot{u}\}_{t+\Delta t}] \qquad (5.5)$$

$$\{u\}_{t+\Delta t} = \{u\}_t + \Delta t\{\dot{u}\}_t + (\Delta t)^2[(1/2-\beta)\{\ddot{u}\}_t + \beta\{\ddot{u}\}_{t+\Delta t}] \qquad (5.6)$$

Newmark proposed an unconditionally stable algorithm with $\delta = 1/2$ and $\beta = 1/4$ which reduces the above scheme to a constant-average-acceleration method. Substitution of these coefficients and rearranging of Eqs.(5.4)-(5.5) yield the following expressions for incremental velocity and acceleration:

$$\{\Delta \dot{u}\}_{t+\Delta t} = \frac{\Delta t}{2}\{\ddot{u}\}_t + \frac{2}{\Delta t}\{\Delta u\}_{t+\Delta t} - 2\{\dot{u}\}_t - \Delta t\{\ddot{u}\}_t \tag{5.7}$$

$$\{\Delta \ddot{u}\}_{t+\Delta t} = \frac{4}{(\Delta t)^2}\{\Delta u\}_{t+\Delta t} - \frac{4}{\Delta t}\{\dot{u}\}_t - 2\{\ddot{u}\}_t \tag{5.8}$$

Substituting the above expressions into the dynamic equation of equilibrium (Eq.5.4), it is possible to solve for the incremental displacements at the current time step:

$$\{\Delta u\}_{t+\Delta t} = [K^*]\{\Delta F^*\}_{t+\Delta t} \tag{5.9}$$

where K^* and ΔF^* are the equivalent dynamic stiffness and load vector given by:

$$[K^*] = \frac{4}{\Delta t^2}[M] + \frac{2}{\Delta t}[C] + [K] \tag{5.10a}$$

$$\{\Delta F^*\} = \{\Delta F\}_{t+\Delta t} + (4/\Delta t[M] + 2[C])\{\dot{u}\}_t + (2[M] + \Delta t/2)\{\ddot{u}\}_t \tag{5.10b}$$

Once the displacement at time $t + \Delta t$ is known, it is possible to compute the corresponding velocities and accelerations by direct substitution in Eqs.(5.6)-(5.7).

The effects of rotational inertia are included in constructing the diagonal mass matrix.

Equilibrium correction: The solution is performed incrementally, assuming that the properties of the structure do not change during the time step of analysis. However, since the stiffness of some element is likely to change (i.e., elastic to cracking or cracked to post-yield) during some calculation steps, the new configuration may not satisfy equilibrium. A compensation procedure is adopted to minimize this error by applying a one-step unbalanced force correction.

At the end of some given time step, t_i, assume that the right hand side of Eq.(5.2) yields a vector of total system forces $\{F\}_i$ which is not in equilibrium with the applied force in the previous step giving an unbalanced force vector $\{\Delta F\}$ as follows:

$$\{\Delta F\} = \{F\}_i - \{F\}_{i-1} \tag{5.11}$$

This corrective force is allowed to act for the next time step of analysis and then removed in the subsequent analysis step since allowing the corrective force to continue to act will produce cumulative error leading to a modification of the applied force history. Such a procedure was first adopted in DRAIN2D [Kannan and Powell, 1973] since the cost of performing an iterative nonlinear analysis would become prohibitive especially for large building systems.

Stiffness Updating during Unloading/Reloading: Besides the unbalanced equilibrium error discussed in the previous section, there arises another important consideration when updating stiffness terms during an unloading or reloading. Generally, unloading or reloading in the inelastic range implies an abrupt change in stiffness, hence the assumption of a constant stiffness between one load step and the next can lead to a major deviation from the force-displacement path. A unique formulation is developed whereby the step-by-step solution procedure is intercepted with a stiffness-updating module to account for such changes. The schematic diagram of the proposed procedure is shown in Figs.5.3a and 5.3b. It involves monitoring the velocity of all rotational degrees of freedom. When the velocity changes sign during the analysis, the program is routed to a stiffness updating module. The idea is to reduce the loading rate near a region of unloading or reloading. The details of the implementation are as follows:

After a solution step, check to see if any sign change occurs in the velocity of the inelastic rotational degrees of freedom.

If a sign change is detected, the program retreats one time step backwards and scans for all elements that experience a change of state. Since a constant acceleration scheme is used, the variation of velocity is linear, thus enabling the detection of the approximate zero-crossing. The element that unloads the earliest is thus determined.

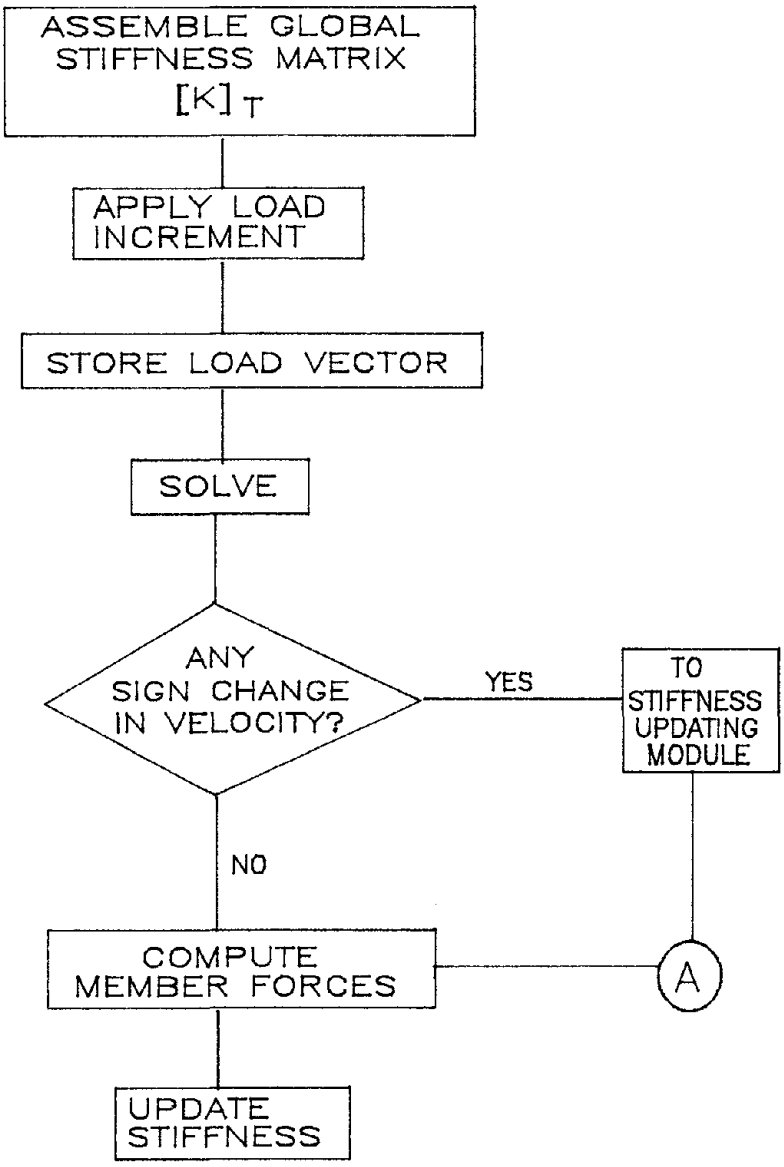

FIGURE 5-3a Stiffness Updating During Unloading/Reloading

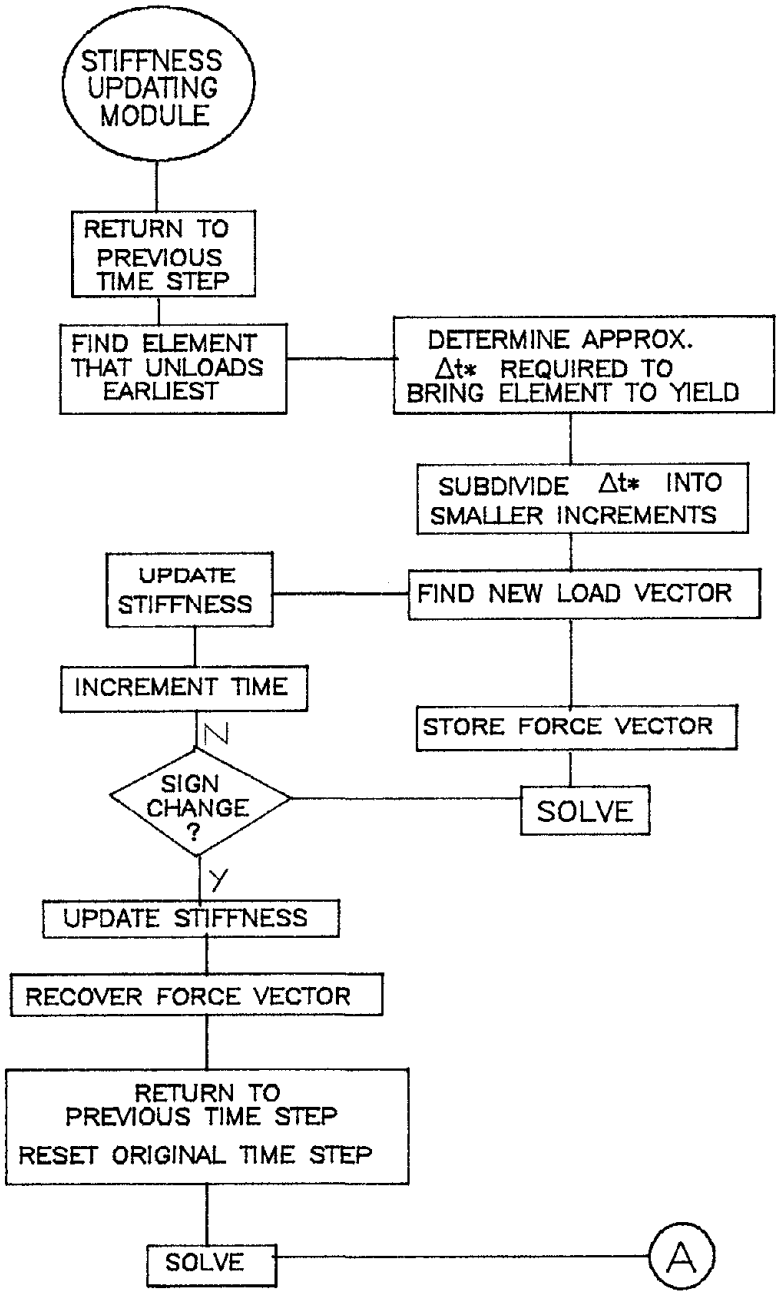

FIGURE 5-3b Stiffness Updating Procedure (continued)

Using the linear variation of velocity, the time increment required to bring that particular element to yield is computed. This computed time increment is further sub-divided into smaller increments so that the transition from loading to unloading or vice-versa is smooth and not abrupt.

The analysis is now carried out using the smaller time increment. The sign of the velocities continues to be monitored. If no sign change is detected, the analysis is continued in the usual manner with stiffness updating and assembling. However, when the velocity changes sign again, it is necessary to retreat backwards once more, update the element to the new stiffness, recover the force vector and perform the solution again.

The original time step of analysis is recovered, and the solution proceeds as before, until a new element begins to change state. This procedure ensures a smooth transition between loading and unloading states.

It must be pointed out that the stiffness updating procedure is used only when the element is unloading or reloading in the inelastic range. Further, it is possible to set up a threshold stiffness above which it is not necessary to check for stiffness updating since the error during transition is not expected to be significant. Such a procedure works extremely well, especially for systems in which the first mode dominates the response, and is more efficient than a fully iterative nonlinear procedure.

Natural Period and Damping: The fundamental period of the structure is determined using the Rayleigh method. This period is used primarily to assign a constant viscous damping factor during the response analysis. Viscous damping at the structural level is not an important quantity and its contribution as a resisting force is not well understood. Hence no attempt was made to perform a sophisticated eigenvalue analysis. Instead, a simple approximation to the fundamental structural frequency is obtained, and a constant damping factor is used based on this frequency.

The general form of the Rayleigh quotient is obtained by equating the maximum potential and kinetic energies of the system:

$$\omega^2 = \frac{\{\psi^T\}[K]\{\psi\}}{\{\psi^T\}[M]\{\psi\}} \tag{5.12}$$

where [K] and [M] are the stiffness and mass matrix of the system, respectively, ω is the fundamental frequency, and $\{\psi\}$ is the *shape* vector of fundamental mode of vibration of the system. In the present analysis, the deflected shape of the structure using an inverted triangular load pattern is assumed to be similar to the first mode shape.

The actual mechanism of damping in a structure subjected to inelastic loading reversals in not clearly established. But it can be stated that the contributions of viscous damping is clearly negligible when compared to the energy that will be dissipated through hysteretic action.

5.4 Analysis of P-Delta Effects

The additional overturning moments generated by relative inter-story drift are generally referred to as P-delta effects. It arises essentially due to gravity loads and is usually taken into consideration by evaluating axial forces in the vertical elements and computing a geometric stiffness matrix which is added to the element stiffness matrix. Though gravity effects on medium rise buildings are known to be not significant, a study by Padilla-Mora and Schnobrich (1974) indicated that the inclusion of P-delta drifts is important when the biaxial response of systems is considered. Hence, it was decided to include considerations of gravity effects in the present modeling scheme.

In the present study, P-delta effects are represented by equivalent lateral forces, equal in magnitude to the overturning moment caused by eccentric gravity forces due to inter-story drift. Consider a typical vertical element between two story levels shown in Fig.5.4. Taking moment about the x-axis at the lower story level, the following equilibrium equation is obtained:

$$M_{x,i-1} + M_{x,i} - Y_i h_i + Z_i \Delta y_i = 0.0 \tag{5.13}$$

Therefore:

$$Y_i = Y_i' + Y_i^* \tag{5.14}$$

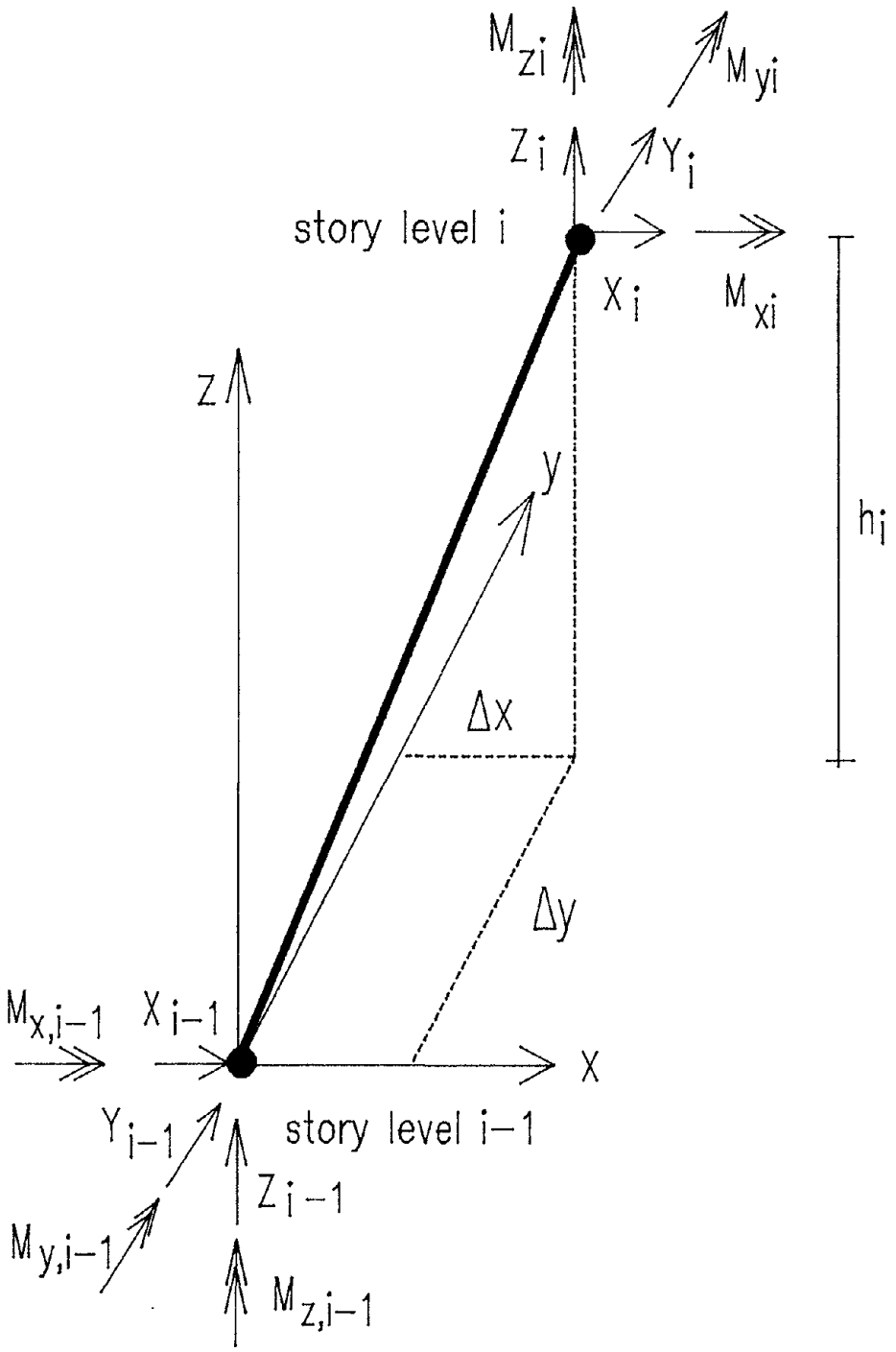

FIGURE 5-4 Equivalent Force Computation for P-Delta Effects

where: $Y_i' = (M_{x,i} + M_{x,i-1})/h_i$ is the normal shear force in the y-direction, and $Z_i \Delta y_i / h_i$ is the additional shear due to gravity effect. For each vertical element, two components of the extra shear term will be produced:

$$\begin{pmatrix} F_{\xi}^{*} \\ F_{yi}^{*} \end{pmatrix} = \begin{pmatrix} \frac{Z_i}{h_i} & -\frac{Z_{i+1}}{h_i} & 0 & 0 \\ 0 & 0 & \frac{Z_i}{h_i} & -\frac{Z_{i+1}}{h_i} \end{pmatrix} \begin{pmatrix} \Delta x_i \\ \Delta x_{i+1} \\ \Delta y_i \\ \Delta y_{i+1} \end{pmatrix} \tag{5.15}$$

The above equations can be written in the following form for each component:

$$\{F^{*}\} = [K]_G \{\Delta u\} \tag{5.16}$$

where $[K]_G$ is similar to the geometric stiffness matrix in finite elements. This matrix is added to the overall stiffness matrix prior to the start of a new analysis step.

The procedures described in this Section have been numerically tested using single components and exhibit stable performance with good results. Some analytical simulations of experimental testing on actual structures using the developed models are presented in Section 7.

SECTION 6

DAMAGE MODELING

Current practice in earthquake-resistant design of reinforced concrete structures allows for energy dissipation of components through inelastic cyclic deformation. Consequently, the design of R/C structures calls for adequate analytical tools that can evaluate the inelastic response of the system. Since inelastic deformations imply some degree of damage (cracks, spalling, etc.), it must be possible, following the nonlinear analysis, to express the response quantities in terms of the damage sustained not only by the components but also by the overall structure. It must also be possible to ascertain the degree of damage as a function of reserve capacity thereby permitting an assessment of structural vulnerability in the event of a future earthquake.

A conceptual model of structural damage has been developed in the present study (a summary of the formulation and the results presented in this chapter are described in Reinhorn et al., 1989). Based on the fundamental idea of demand and capacity, it combines two recognized sources of damage: permanent deformation and strength deterioration. An implementation of the model to bilinear hysteresis is presented as an initial application though further experimental testing is necessary to establish the parameters that quantify the damage levels for more general hysteresis. Before setting forth the details of the damage model, a review and appraisal of existing damage indexing techniques is presented.

6.1 Review of Damage Models

The earliest references related to damage are ductility based. Newmark and Rosenblueth (1974) who proposed the idea of ductility ratio as a quantitative measure of damage established the simplest notion of structural integrity. Despite the inability of such a ratio to handle damage caused by cyclic fatigue, it has been recognized as one of the important parameters that contribute to damage and has, therefore, found a role (directly or in alternative forms) in numerous major models of damage indexing as will be seen below.

A second source of damage definition finds its roots in steel models of low cycle fatigue. Though it is improbable that a damage model developed for steel can be used for reinforced

concrete, it is quite likely that the principles or criteria on which it was based can be extended with suitable modifications for R/C members. A case in point is the recent model of Stephens and Yao (1987) who attempted to extend to reinforced concrete, the hypothesis of Yao and Munse (1962) developed essentially for metals. They expressed the total damage index *(D.I.)* As a function of accumulated plastic deformation after N cycles:

$$D.I. = \sum_{i=1}^{N} D_i \tag{6.1}$$

where the damage index for cycle i is given by:

$$D_i = \left(\frac{\Delta \delta_{pt}}{\Delta \delta_{pf}} \right)^{\alpha} \tag{6.2}$$

in which $\Delta \delta_{pt}$ and $\Delta \delta_{pf}$ correspond to a positive change in plastic deformation for the *i'th* cycle and the maximum change in plastic deformation to cause failure. The power term α is further expressed as a function of the ratio of the negative and positive change in plastic deformation for that cycle thereby taking into account the antisymmetric nature of R/C section behavior. The main problem with this definition is the improbability in ascertaining the fixed parameters of the model.

Energy-based indices for damage prediction began to appear after Gosain et al (1977). They proposed a normalized energy index called the work index (I_w) as follows:

$$I_w = \sum_{i=1}^{N} \frac{p_i \Delta_i}{p_i \Delta_y} \tag{6.3}$$

where N corresponds to the number of cycles in which the load exceeds atleast 75% of the yield strength, and p and Δ refer to load and displacement. It has been suggested that $p_i = p_y$ if it assumed that the load generally varies from $0.75 p_y$ to $1.25 p_y$. This simplifying assumption reduces Eq.(6.3) to a normalized cumulative deformation index and also suggests the possible correlation between energy and deformation based indices.

Energy dissipation mechanisms in reinforced concrete are complex and depend upon several parameters ranging from the composition and properties of the constituent materials to the fluctuations in axial force, the magnitude of critical shear span ratios, and the nature of loading. Hence, energy-based indices tend to be less reliable. In fact, Gosain et al. (1977) added a modification factor to Eq.(6.3) to possibly account for such effects. A couple of variations to this approach appeared later: the first by Hwang and Scriber (1984) and the other by Darwin et al. (1986). The former introduced stiffness degradation to factor the work index of Eq.(6.3) while the latter proposed a new energy index arrived at by investigating various parameters that were known to control energy dissipation.

Another approach to damage prediction is based on the degradation of a certain structural parameter. Lybas and Sozen (1977) used overall stiffness degradation as a measure of damage. A more refined form of this technique was later adapted by Roufaiel and Meyer (1985) who proposed a modified flexural damage ratio which related damage to the maximum stiffness reduction normalized by the available stiffness reduction. However, no attention is paid either to cumulative damage or the effect of load history. Such indices may produce some information on the state of the component after loading but cannot account for the distinction between capacity, consumption and reserve.

Inherent in all approaches to modeling damage is the idea of demand and capacity. This concept formed the literal basis of the cumulative damage model developed by Bertero and Bresler (1977) who were among the first to extend the local damage index to the overall structure:

$$D.I. = \frac{1}{\sum_{i=1}^{M} \omega_i} \sum_{i=1}^{N} \frac{\omega_i \eta_i s_i}{\gamma_i r_i} \qquad (6.4)$$

where s_i and r_i are the demand and capacity of the i'th element, the ω_i's are the weights based on relative importance factors and η_i, γ_i are service factors. Since demand and capacity were expressed as deformation levels, the index reduced to a ductility-based model. However, an important contribution was made: local component indices need to be calibrated to arrive at global structural damage and the calibration had to made on the basis of importance factors.

It is obvious from the drawbacks of the models listed above that a next step towards an improved representation should encompass all of the essential characteristics of a valid damage model: the concepts of demand and capacity, the contributions from deformation-based damage, and the role of energy dissipation. The synthesis was provided by Park et al. (1985) who investigated the physical implication of deformation demand. They came to the conclusion that the deformation capacity of an element is reduced as a consequence of dissipated hysteretic energy caused by cyclic load reversals. A further significant observation was the possible relationship between dissipated energy and strength loss. Thus, they postulated:

$$D.I. = \frac{\delta_m}{\delta_u} + \frac{\beta}{P_y \delta_u} \int dE \qquad (6.5)$$

where δ_m is the maximum deformation under the earthquake load, δ_u is the ultimate deformation capacity under monotonic load, β represents a strength deterioration parameter, P_y is the yield strength of the component, and dE corresponds to the incremental absorbed energy. This damage index is the only calibrated index based on observed damage data of nine reinforced concrete buildings that were moderately or severely damaged during the 1971 San Fernando earthquake and the 1968 Miyagi-ken-Oki earthquake in Japan. However, the calibration yielded building failure with damage indices in the region of 0.4 suggesting either that the linear combination of Eq.(5.5) is inappropriate or the calibration itself was inadequate. This model has also been used to evaluate damage of overall buildings using an energy weighting scheme (Park et al., 1987).

Numerous variations of the models listed above may be found in the literature. Comprehensive reviews (Chung et al., 1987; Powell and Allahabadi, 1988) of damage indexing techniques have also appeared. Chung et al. also define a new accelerated damage index, an extension of Miner's modified hypothesis. They introduce an interesting concept of an available strength deterioration at a given deformation level. However, instead of developing a rational index based on concepts such as demand and capacity, they proceed to set up a complex definition of damage. The use of a parameter such as *number of cycles* is not realistic since a system subject to random earthquakes do not undergo complete inelastic cycling

reversals. Due to the large number of parameters that need to be monitored, it is unlikely that such a model will lend itself to adaptation in an analysis program where a 3-dimensional structure with a large number of components has to be analyzed.

In summary, it may stated that the models listed above are not able to relate physically the quantitative measure of the model and the actual damaged state of the structure. Nor are these models capable of expressing a measure of strength or energy reserve in the structure following seismic action.

6.2 Development of a Conceptual Model of Seismic Damage

A conceptual model of damage is developed herein which utilizes the concepts of *consumption* and available *damage potential*. Damage potential is defined as the total capacity of the component to sustain damage. Damage consumption is that portion of the available capacity that is lost or dissipated during the course of the applied load history. These terms will be further detailed in a physical sense.

A component that is failed by purely monotonic loading represents an *upper bound* phenomenon since it is unlikely that any alternative load path will cross the bounds of the monotonic envelope. At the other extreme of this loading scenario is cyclic fatigue which constitutes repeated cycling at a given deformation level. If an envelope were to be drawn joining all failure points of inelastic fatigue testing at different deformation levels, a new curve would result, representing a *lower bound* phenomenon. Fig.6.1 attempts to capture these upper and lower bound envelopes in a conceptual sense. Two important facts emerge from such a construction of the bounding curves: (1) For any given deformation level, there is an available capacity for strength loss. (2) The available strength loss at lower deformation levels is greater than strength-loss capacity at larger deformations. This fact can be drawn both from a physical understanding of the inelastic cyclic deformation process and from observed experimental testing. The shape of the inelastic failure envelope is thus justified.

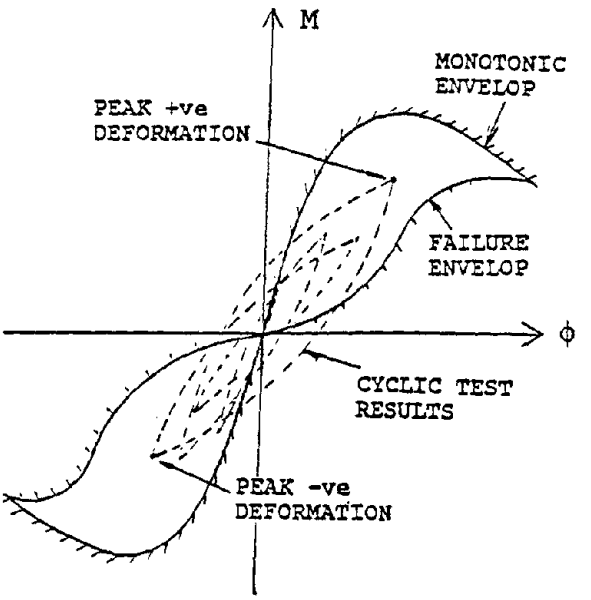

(a) Mmnotonic and failure envelopes

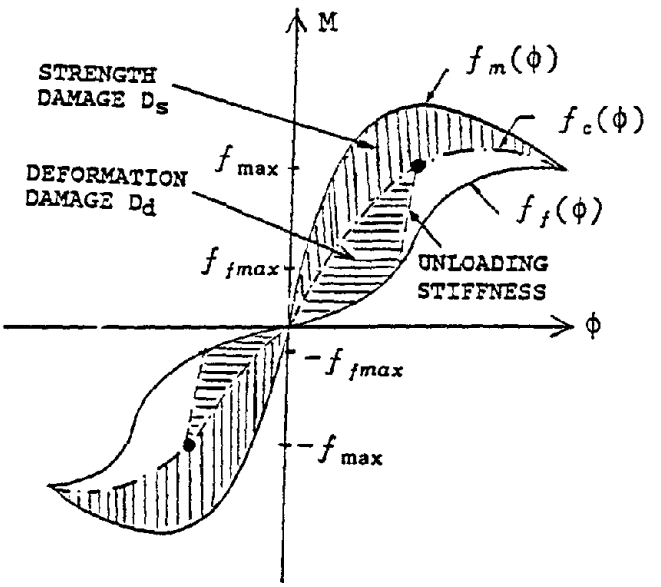

(b) components of damage

FIGURE 6-1 Conceptual Model of Damage

The damage potential D_p of an R/C structural component is hereby defined as the total area enclosed by the monotonic and inelastic failure envelopes. Assuming, for numerical purposes, that the monotonic envelope is specified by some function $f_m(\phi)$ and the failure envelope is defined by another function $f_f(\phi)$, then the damage potential is determined from:

$$D_p = \int_{-\phi_u}^{+\phi_u} \{f_b(\phi) - f_f(\phi)\} d\phi \qquad (6.6)$$

where ϕ is the curvature and ϕ_u is the ultimate curvature.

To arrive at an expression for damage based on this concept of a damage potential, consider an R/C component for which the results of a random cyclic test is available. Fig.6.1a shows such a sample test superimposed on the bounding envelopes. Of significance here is the establishment of the positive and negative peak deformations. A new curve needs to be defined representing the current damage level of the component. This is done by defining $f_c(\phi)$ which assumes an intermediate path between the upper and lower bound curves. This function represents a dynamic upper-bound envelope that is constantly dropping as a consequence of inelastic cyclic deformation. It further implies that this dynamic bounding curve cannot be exceeded in any future traversals of the load-deformation path. To complete the modeling scheme, two lines, representing the positive and negative unloading stiffness paths are drawn to intersect the deformation axis.

Two components of damage are isolated (see Fig.6.1b): the first corresponding to strength-loss and the second arising from deformation related damage. *Strength damage* is defined as the loss of damage potential due to strength deterioration and hysteretic dissipated energy. This accounts for the lowering of the monotonic or upper-bound curve. Strength damage D_s is determined as:

$$D_s = \int_{-\phi_u}^{+\phi_u} \{f_m(\phi) - f_c(\phi)\} d\phi \qquad (6.7)$$

Deformation damage, on the other hand, accounts for the remainder of the loss of the damage potential. It corresponds to irrecoverable permanent deformations and is evaluated from the

area bounded by the current damage level curve and the inelastic failure curve upto the current maximum deformation levels:

$$D_d = \int_{-\phi_a}^{+\phi_a} \{f_c(\phi) - f_f(\phi)\} d\phi \qquad (6.8)$$

where ϕ_a represents the line joining f_{max} and f_{fmax} (Fig.6.1b). The cumulative effect of strength damage and deformation damage is termed as *damage consumption.* A structural *damage index (D.I.)* is, therefore, established as the ratio of damage consumption to damage potential:

$$D.I. = \frac{D_c}{D_p} \qquad (6.9)$$

where damage consumption $D_c = D_s + D_d$

The developed conceptual model of structural damage will now be applied to a simple bilinear hysteretic model to demonstrate the applicability of the scheme to practical analysis of reinforced concrete structural systems.

6.2.1 Application of the Model to Bilinear Hysteresis

The application of the conceptual model developed above depends upon the hysteretic model used in the analysis of the structural system. The following section presents an approach to the modeling of bilinear hysteretic systems.

Consider a component whose force-deformation history at member ends is known following a regular response analysis. A prerequisite to evaluating its damage index is knowledge about the force and deformation at yield and ultimate levels for monotonic loading. This is established either through the use of empirical equations or some micro-modeling scheme. Details on identification techniques to evaluate fixed structural parameters were presented in Chapter V. For bilinear modeling, information related to the yield and ultimate levels is adequate to construct the upper-bound envelope.

The next step is both crucial and complex. It involves the setting up of the inelastic failure envelope. Strictly speaking, such an envelope should come directly form experimental testing. However, the task of building experimental envelopes as a function of component parameters may be too time-consuming and expensive. Consequently, only theoretical possibilities based on observed patterns of fatigue failure for metals (and some limited data on concrete) can be postulated. Two possible variations are shown in Figs.6.2a and 6.2b. The first assumes a transposed form of the bilinear envelope itself. This produces a constant available deterioration for most of the deformation range indicating perhaps that the damage evaluated using this approximation may be underestimated. The other possibility is a simple straight line (Fig.6.2b). It is quite likely that the actual curve may lie somewhere between the two. The interesting aspect of these envelopes, however, is the suggestion that they could represent an upper and lower bound of the failure envelope. An analysis using each of the failure criteria could, therefore, yield a range of damage values: the boundaries representing the least and maximum probable damage.

The formulation of the damage index requires merely the evaluation of Eqs.(6.6)-(6.8). For the case of the transposed failure envelope, the following expressions are derived:

$$D_s = (m_2^+ - m_1^+)\phi_2^+ \sin\alpha^+ + (m_2^- - m_1^-)\phi_2^- \sin\alpha^- \qquad (6.10)$$

$$D_d = (m_1^+)\phi_1^+ \sin\alpha^+ + (m_1^-)\phi_1^- \sin\alpha^- \qquad (6.11)$$

$$D_p = (m_2^+)\phi_2^+ \sin\alpha^+ + (m_2^-)\phi_2^- \sin\alpha^- \qquad (6.12)$$

(for notation, see Fig.6.2)

Generally, the initial and post-yielding stiffness in tension is assumed to be the same in compression. Hence, $\alpha^+ = \alpha^-$. In addition, if the envelope characteristics are assumed to be the same in compression and tension, as in the case of typical columns, the following simplified expression results:

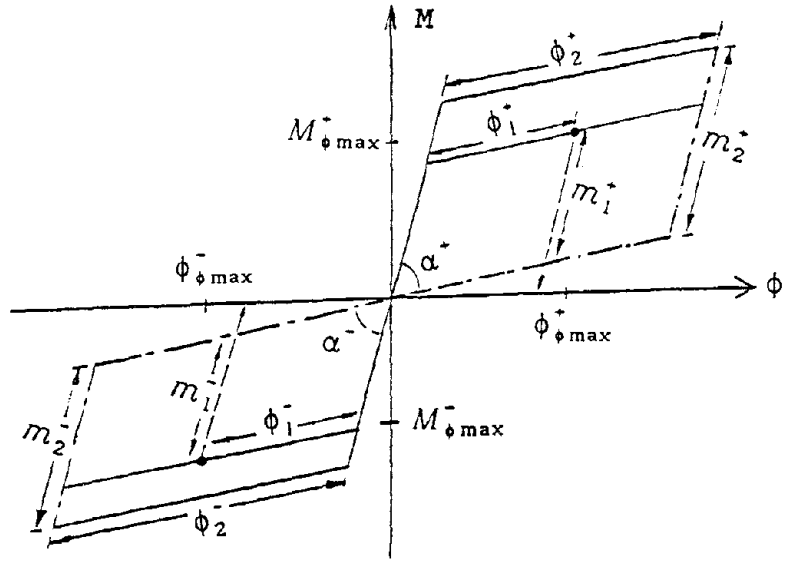

(a) Lower bound estimate of failure envelope

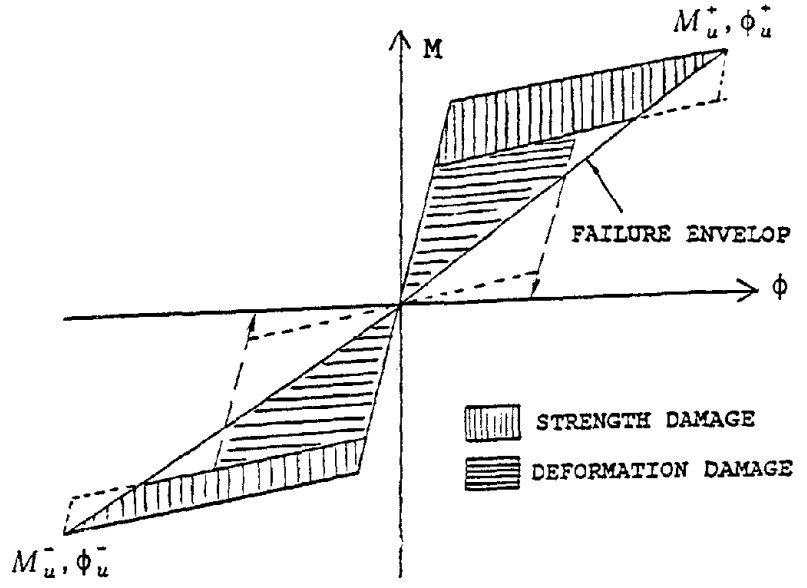

(b) Upper bound failure envelope

FIGURE 6-2 Damage Model Implementation for Bilinear Hysteresis

$$D.I. = D_1 + D_2 - D_1 D_2 \tag{6.13}$$

where $D_1 = \phi_1 / \phi_2$ and $D_2 = m_2 - m_1 / m_2$.

In the case of option 2, the above formulations still remain valid with the change that the excess areas shown in dotted lines (Fig.6.2b) must be neglected. This can be achieved with ease if the slope of the failure line is established.

The formulations presented above are based on a certain degree of approximation in constructing the inelastic fatigue failure curve. However, there is always the possibility of numerically simulating fatigue failure at different deformation levels using some failure criteria (peak concrete strain, steel fracture, etc.) as the threshold. It will be necessary to calibrate some of the simulations with actual experimental testing.

6.2.2 Member-Level and Overall Structure Damage

Eq.(6.8) corresponds to the damage at a member end (in one principal direction) where inelastic rotations are being monitored. The next task is to formulate a simple weighting scheme that can be used to extend the indexing procedure first for the complete member and subsequently for story levels and the entire structure. Two basic approaches are suggested, and a final damage prediction scheme is proposed.

Self-Weight Procedure: The simplest technique in combining local indices is to use a weighting procedure. The weighting scheme can be extended from the member level to the overall structure. The fundamental expression for the procedure is:

$$(D.I.)_{total} = \frac{\sum_{i=1}^{N} w_i (D.I.)_i}{\sum_{i=1}^{N} w_i} \tag{6.14}$$

where w_i is the weight assigned to each local index. If the local index corresponds to a member end section in one principal direction, the summation is carried over all principal directions to arrive at the section joint index. The weighting procedure is then performed at the member

level across the 2 joints of the component. From component level indices, it is possible to determine a total index for any substructure, story-level or the entire structure using the same weighted indexing method.

The choice of a weighting factor is critical since it should convey, quantitatively, the physical measure of damage. A convenient approach is using self-weights, that is, the local damage index itself:

$$(D.I.)_{total} = \frac{\sum_{i=1}^{N} (D.I.)_i^m}{\sum_{i=1}^{N} (D.I.)_i^{(m-1)}} \qquad (6.15)$$

where m is a desired power to enhance the importance of the most severely damaged element.

Peak Damage Limit: This approach is based on the idea that any procedure to combine local indices is bound to lead to erroneous conclusions. Physical evidence shows that a member can fail as a consequence of severe plastic deformation at one end alone, irrespective of the condition of the other end. By combining indices, therefore, there is a likelihood that the overall damage index is scaled down!

The concept of a peak damage limit requires that a member damage index be limited to the extreme of the two local end indices:

$$(D.I.)_{total} = \max \{(D.I.)_i, (D.I.)_j\} \qquad (6.16)$$

where i and j refer to the member ends. This procedure can also be extended to the story and structure level. At the story level, however, some additional weighting parameter needs to be introduced to distinguish column failure against beam failure. A story level index should be made to reflect panel mechanisms caused primarily by yielding of columns.

The difficulty with extending the procedure beyond the member level is a consequence of subjective judgement and the need to define levels of importance so that peak indices actually reflect the true nature of the damage sustained by the structure.

Importance Factors: The idea of assigning importance factors to members and to story levels is vital in assessing the quality of damage. Importance factors may be tied in with weighting factors directly. It is conceivable, therefore, that column elements are assigned higher importance factors than beams, likewise lower story levels must be considered more important than upper levels.

Proposed procedure for combining indices: The task of building importance factors and generalized weighting schemes into an analysis program that performs damage analysis can be complex and tedious since all possible failure modes must be considered before incorporating a damage indexing procedure. In the context of the overall modeling schemes proposed in the present study, the following approach is suggested:

(1) Compute the local damage index using the model developed in Section 6.2.

(2) At the member level, use the peak limit procedure, which assigns to the component the maximum of the two local end indices.

(3) Use the self-weight procedure to weight indices beyond the member level.

(4) Allow the user to assign importance factors to components and to story levels. Importance levels start at 1.0 indicating nominal or basic importance. These factors are multiplied by the weighting parameters to arrive at quality weights for each component and for each story.

The process of seismic damage assessment is eventually subjective and entails a certain degree of uncertainty. By its very nature, damage is a random process that does not lend itself easily to deterministic procedures. Hence, the emphasis must be on simulation and not prediction. Damageability must be expressed as a range and not a quantity. The range should delineate the least and worst scenarios wherein the maximum probable damage is further substantiated with assumptions and initial conditions.

In the present study, damageability assessment is looked upon as a post-processing task, whereby the results of a comprehensive inelastic seismic analysis are presented with an engineering flavor. Peak deformations and stresses are expressed both as numbers and as qualitative indicators of capacity, demand and reserve.

6.3 Numerical Testing

The damage model developed is applied in evaluation studies of a 2-bay, 3-story R/C frame structure that was tested to failure (Yunfei et al.,1986). The test structure and the load history are shown in Fig.6.3. Loading comprised of three preliminary cycles upto yield after which the structure was subjected to three cycles each at consecutive ductility levels. The structure was analyzed under the prescribed displacement history using IDARC-3-D, the computer model developed in this study. The results indicate excellent agreement between analytical simulation and experimental testing (Fig.6.4). The discrepancy on the negative side was caused by the fact that most of the beams in the test structure had varying reinforcement at the ends while the version of IDARC-3-D used in this study used only constant properties along the member.

The response statistics of the structure and its components were used to implement the model of damage developed in this Chapter. The hysteresis of the left joint of beam #4 (Fig.6.3) is shown in Fig.6.5. The damage evaluation of this component using options #1 and #2 (lower and upper bounds) are displayed in Figs.6.6 and 6.6. The three lines on each of the graphs correspond to deformation, strength and total damage as outlined in development of the damage model. Deformation damage controls the overall index. This is in agreement with the concept of ductility damage. However, near failure, the index is strongly influenced by strength damage. Fig.6.8 shows the total damage index for beam #4 using the lower bound failure envelope (option #1) and the upper bound failure envelope (option #2) wherein the member index was obtained from the local joint indices using the peak-limit combination procedure discussed earlier.

The progressive damage of the structure is examined in Fig.6.9 Both component damage and overall structure damage at different levels of yielding are shown. A close observation of the damage states show good agreement with the experimental test results: (1) the significant yielding in beams at the second story level, particularly near failure; (2) the general pattern of damage to columns with most of the yielding concentrated at the bottom level, and in particular the lower left column.

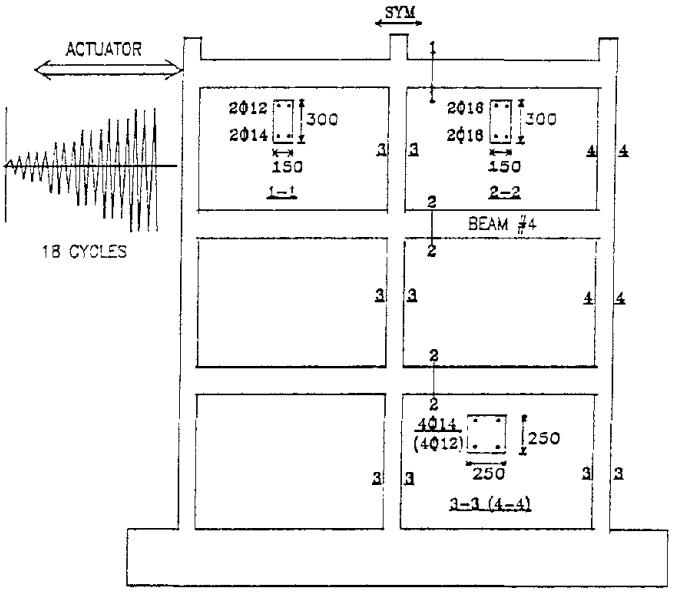

FIGURE 6-3 Details of Test Frame

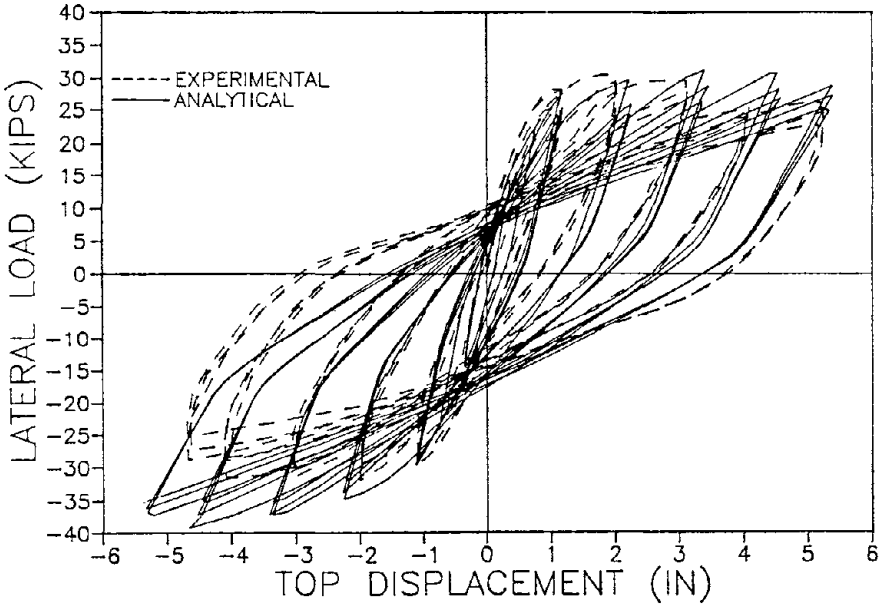

FIGURE 6-4 Analytical Simulation of Experimental Results

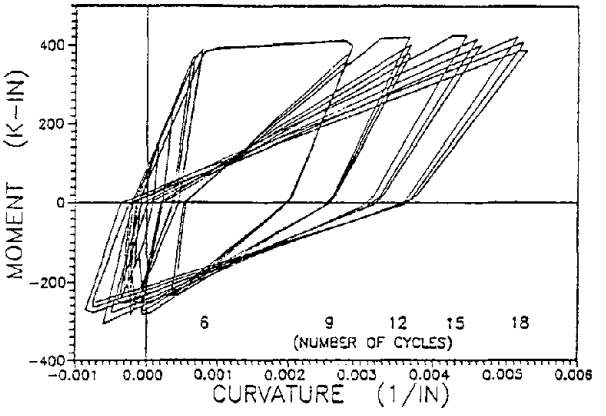

FIGURE 6-5 Hysteresis for Left Joint, Beam #4

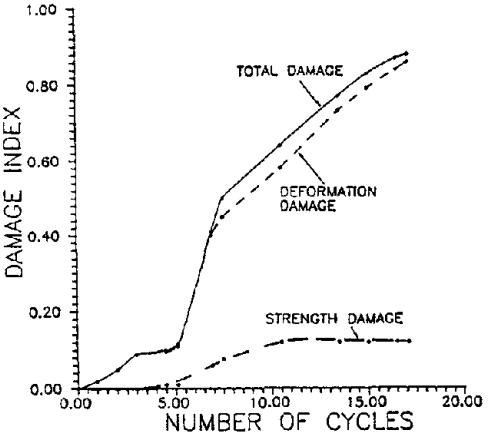

FIGURE 6-6 Beam Damage (lower bound)

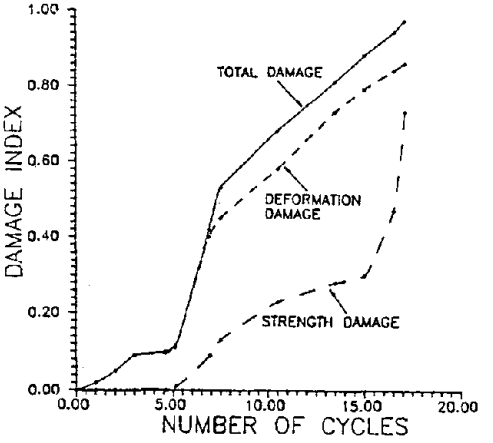

FIGURE 6-7 Beam Damage (upper bound)

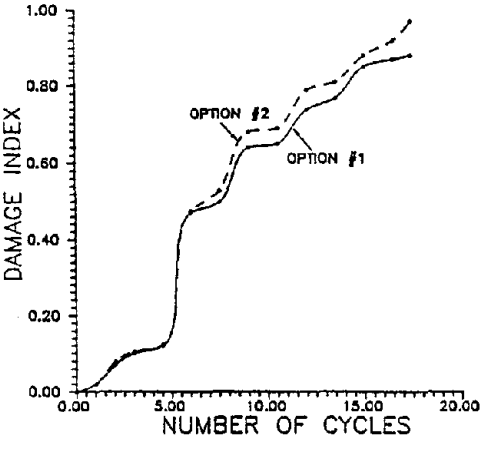

FIGURE 6-8 Overall Beam Damage (upper and lower bound)

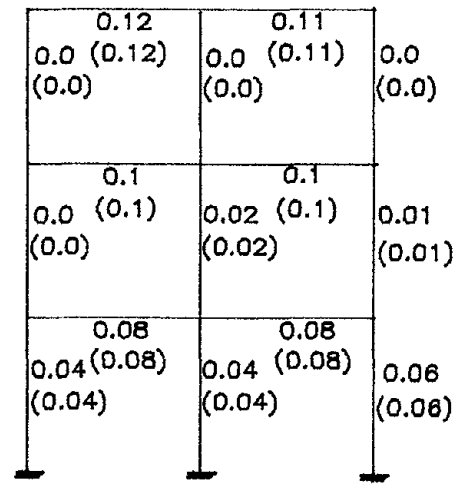

OVERALL DAMAGE INDEX = 0.07 (0.07)

(a) ductility level = 1

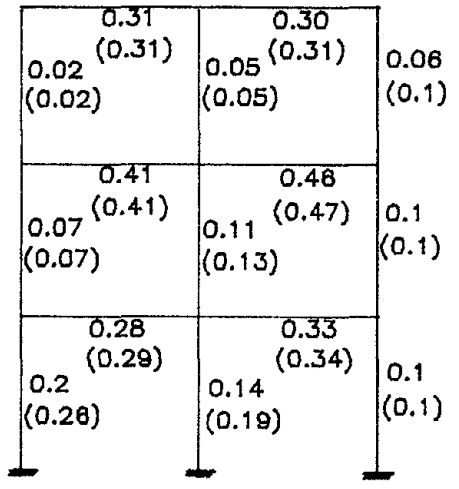

OVERALL DAMAGE INDEX = 0.295 (0.3)

(b) ductility level = 2

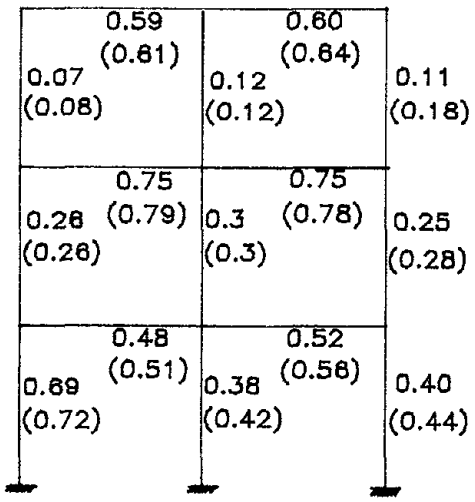

OVERALL DAMAGE INDEX = 0.52 (0.56)

(c) ductility level = 3

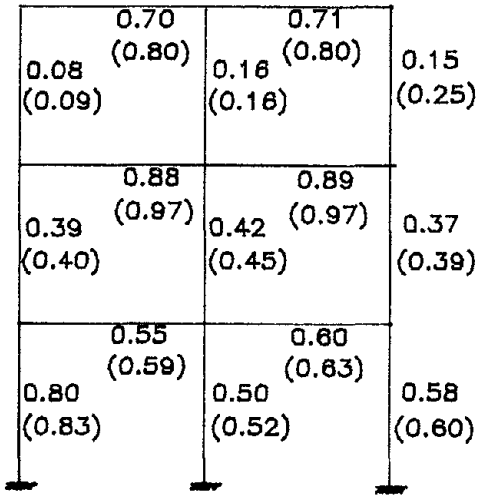

OVERALL DAMAGE INDEX = 0.69 (0.77)

(d) frame failure

FIGURE 6-9 Progressive Damage of Frame Under Cyclic Loading

The quantification of damage using the proposed model, therefore, shows very good correlation with observed and measured damage. The normalization to unity (meaning collapse) is an adequate measure for quantification of damage for components and subassemblages. For the overall structure, the same index needs further calibration, or refinement of combination techniques, in order to produce an adequate normalized quantity. Usability of a damaged structure can then be assessed quantitatively.

In the present study, damageability assessment is looked upon as a post-processing task, whereby the results of a comprehensive inelastic seismic analysis are presented with an engineering flavor. Peak deformations and stresses are expressed both as numbers and as qualitative indicators of capacity, demand and reserve.

SECTION 7

NUMERICAL TESTING

The analytical and computational models developed in this study are used in preliminary numerical studies to demonstrate the effectiveness and suitability of the modeling schemes to practical analysis of building systems. The following illustrative examples are presented:

A comparative study of the response of a 2-story, single bay frame is carried out using another available inelastic program, DRAIN2D.

The simulation of experimental results of a 2-bay, 3-story frame structure which was cycled at increasing ductility levels to failure.

A comparative numerical study of the uniaxial and biaxial response of a column element under bi-directional earthquake excitations.

The details of the numerical testing program, with respect to both modeling and input data, are presented in the following sections.

7.1 Comparative Study of Inelastic Response of 2-Story R/C Frame

The frame structure used for the initial calibration study is taken from the revised version of the DRAIN2D Manual (Powell, 1973). The primary purpose of this analysis is to validate IDARC-3-D. To achieve the simulation, the input parameters to IDARC-3-D had to be modified so as reproduce a bilinear hysteresis as used in DRAIN2D. The input details of the frame are shown in Fig.7.1. A 5% strain hardening ratio was assumed for the post-yield range. A constant viscous damping at 5% of critical at the fundamental period of 0.4 secs was used. The Takeda model was used in the DRAIN2D analysis for all elements. The 3-parameter model was used in the IDARC simulation with inelastic properties similar to the Takeda model. The frame was subjected to the Taft 1952 N69W component accelerogram with a scaled peak value of 0.44g. The comparative response of both the first and second story level are shown in Fig.7.2. It is observed that the DRAIN2D results overestimate the response in comparison with IDARC.

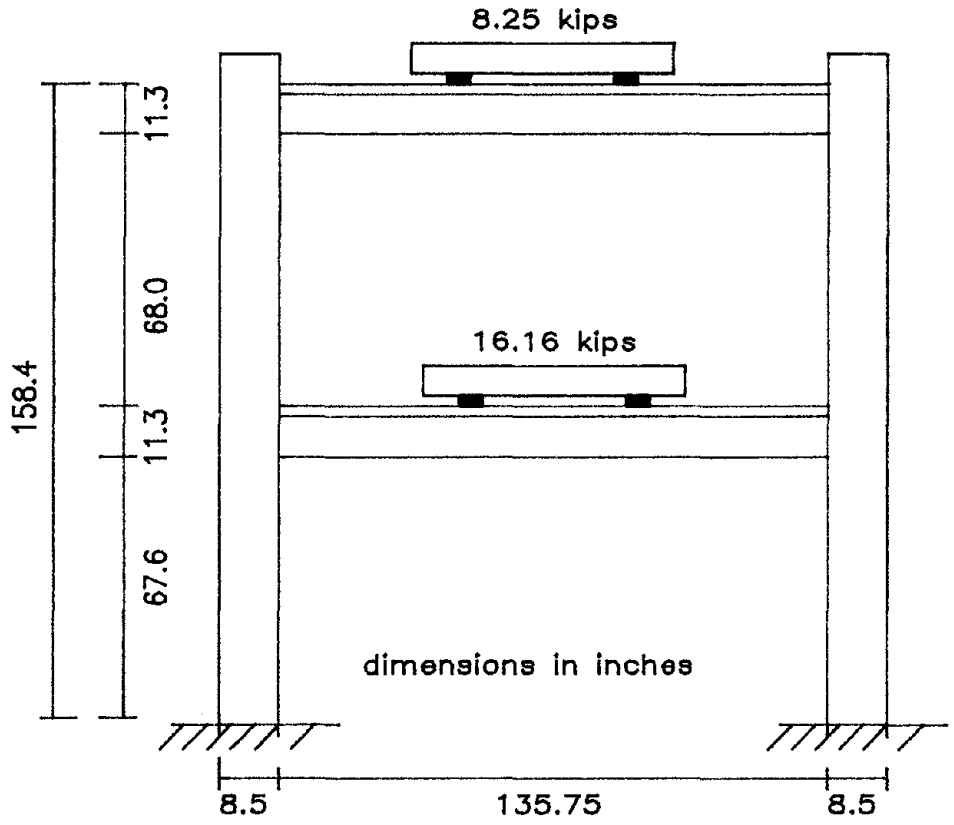

STIFFNESS/STRENGTH PROPERTIES

STORY	MEMBER	(EI)	(EA)	My+	My−
1	COLUMN	146,700	54,260	150.0	−150.0
	GIRDER	580,000	−	237.3	−303.4
2	COLUMN	223,100	54,260	150.0	−150.0
	GIRDER	688,200	−	182.9	−209.9

FIGURE 7-1 Details of Test Frame Used in Comparative Study

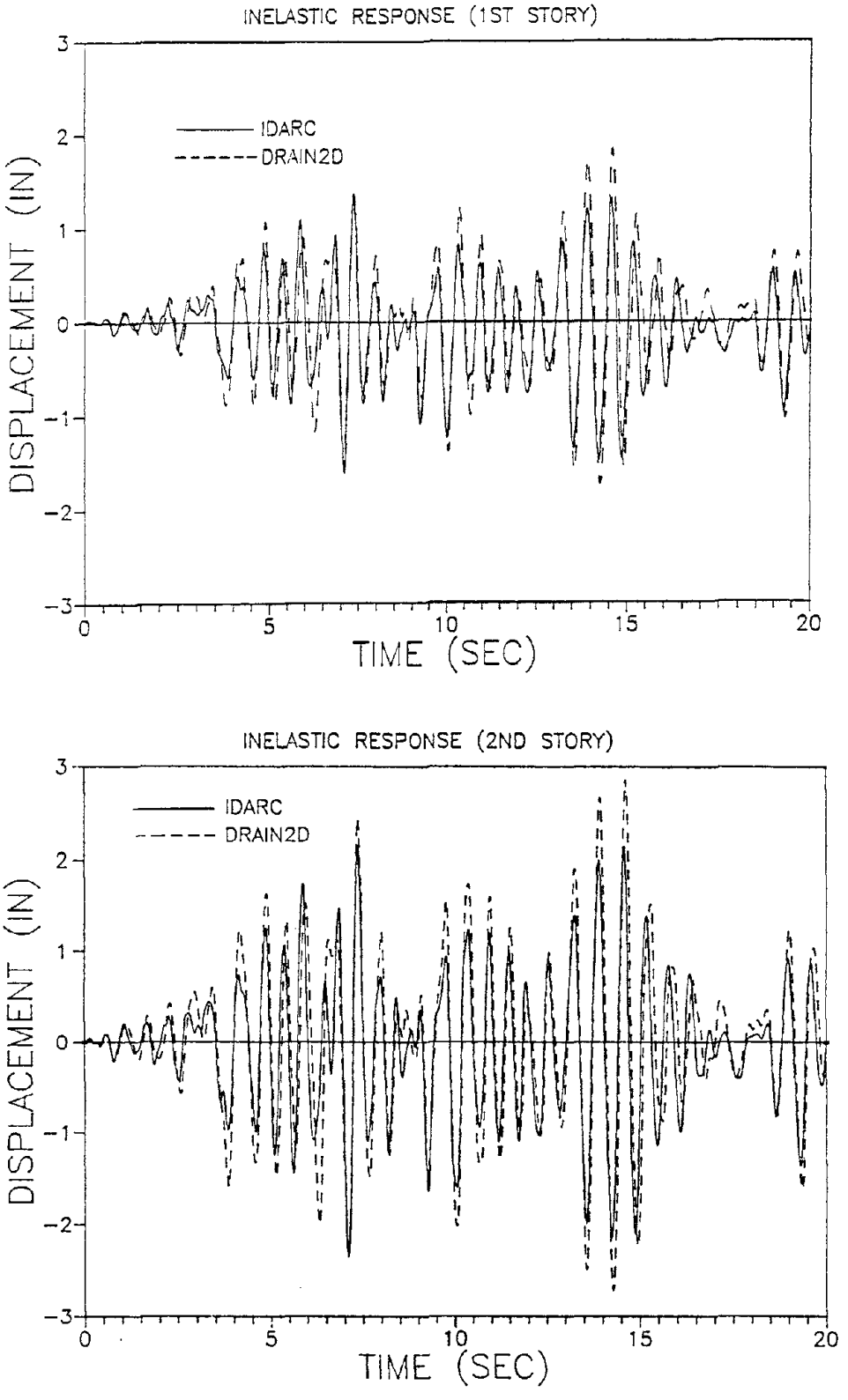

FIGURE 7-2 Comparative Response of Story Level Displacements

This is an expected consequence since DRAIN uses a concentrated hinge model which produces more rotation at the hinges while IDARC uses a distributed flexibility approach which accounts for the spread of the plastic zone. The general response pattern is otherwise similar.

7.2 Cyclic Testing of 2-Bay, 3-Story Frame Structure

The versatility of the modeling schemes proposed in this study is further validated by simulating the experimental response of an actual test structure that was cycled inelastically at increasing deformation levels to eventual failure. The structure consisted of a 2-bay, 3-story frame (Fig.7.3) which was subjected to a deformation controlled loading. The first three cycles of loading caused cracking and first yield of the system. The structure was then subjected to three cycles at consecutively increasing ductility levels. An eventual ductility of approximately 5.0 was obtained before failure. The results of the experimental and analytical response for the top story level of the structure is shown in Fig.7.4. The sequence of hinge formation is shown in Fig.7.5 which compares the actual observed results with the analytical prediction.

The results show extremely good correlation. The slight difference in the deformation levels attained in each cycle, especially in the negative direction, is because the IDARC simulation assumed equal cycles in both directions, while the experiment used the actual yield values, which turned out to be slightly different in the two directions. The sequential hinge pattern also correlates very well with the observed strong-column weak-beam phenomenon. In fact, the structure was designed to produce primary yielding in beams, thereby verifying the recommended design standards in China for R/C structures in earthquake-prone regions.

7.3 Column Testing Under Bi-directional Earthquake Excitation

The final numerical simulation study conducted was based on the bi-directional earthquake testing of an R/C column specimen (Takizawa and Aoyama, 1976). The following uniaxial properties were used in analytical model of Takizawa and Aoyama:

elastic period:	0.3 secs
cracking strength:	0.1 ton

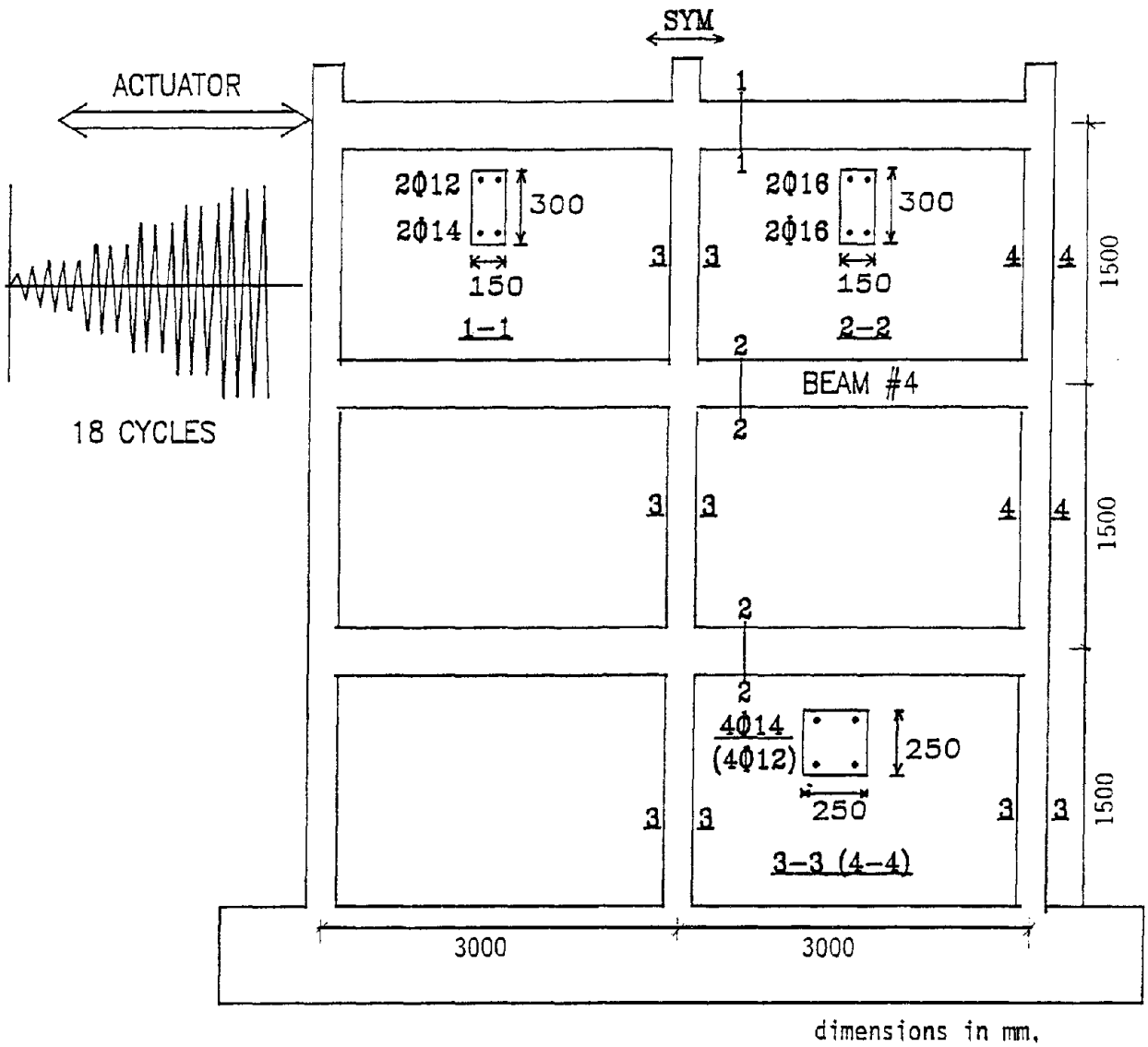

FIGURE 7-3 Details of Test Frame Used for Cyclic Load Analysis

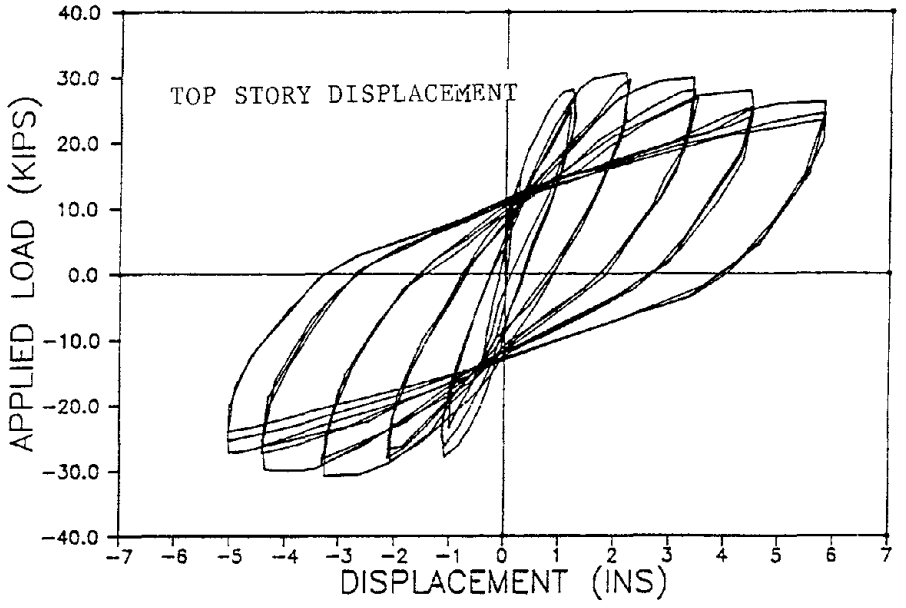

(a) EXPERIMENT

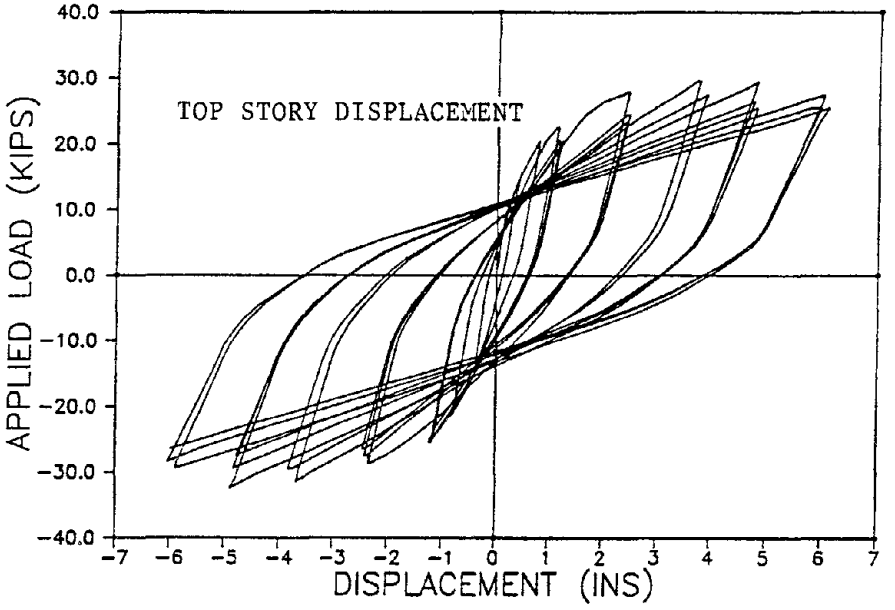

(b) ANALYSIS

FIGURE 7-4 Analytical Simulation of Experimental Results

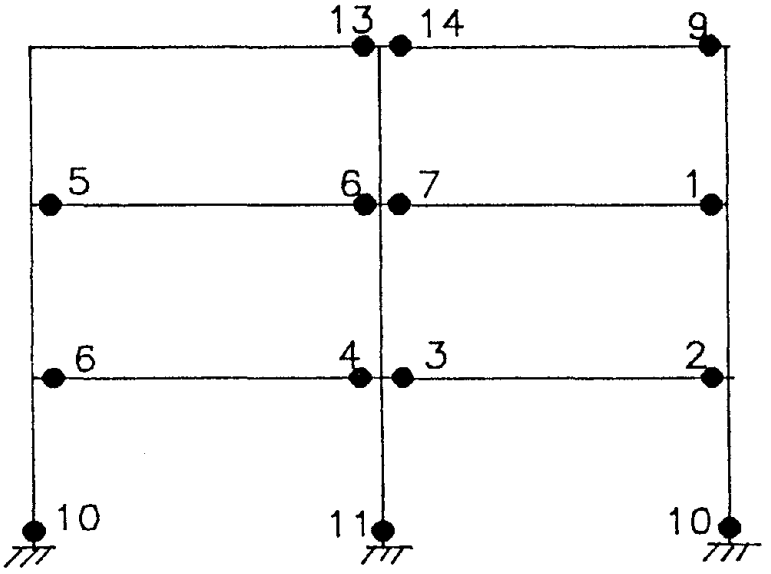

EXPERIMENT

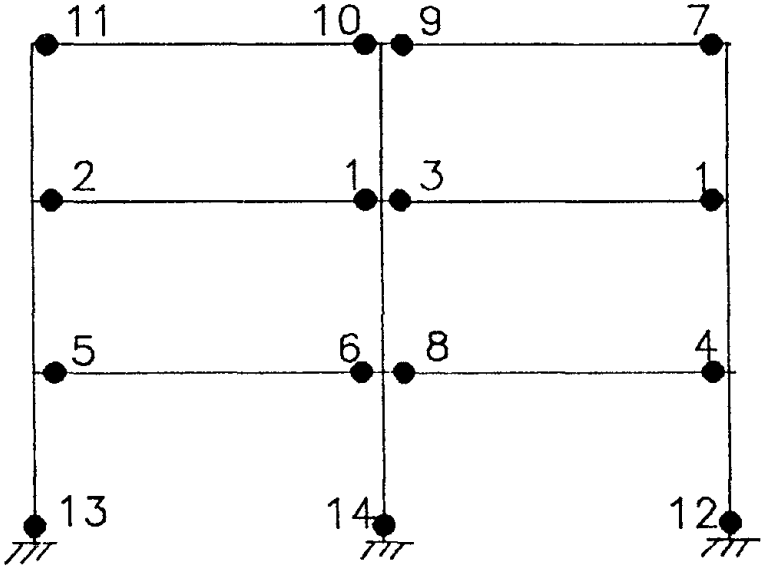

ANALYTICAL

FIGURE 7-5 Sequence of Formation of Plastic Hinges

yield strength:	0.3 ton
crack displacement:	0.223 cm
yield displacement:	3.35 cm

The input acceleration consisted of the NS and EW components of the 1940 Imperial Valley earthquake at El Centro (Fig.7.6). A secant stiffness reduction ratio of 0.2 was used by Takizawa at the yield point to induce stiffness degradation. No direct correlation between this and the s_1 parameter described in Section 3 exists. However, for the present study, a value of $s_1 = 0.1$ was used since the behavior of the Takizawa model indicated only nominal degradation. The results of the uniaxial response using Takizawa's reported simulation and the present analysis is shown in Fig.7.7 for the NS direction only. The comparative bi-directional response is shown in Fig.7.8. The difference in the response magnitude between the uniaxial and biaxial modeling schemes is presented in Fig.7.9.

A qualitative assessment of the results show that the overall magnitude of the response using the biaxial model is greater than that for the uniaxial model. It was noted by Takizawa and Aoyama, in further simulations, that the biaxial response altered significantly the behavior of the system only in the limited ductility range of 2.0-3.0. The interaction effect was not as important for larger ductilities. At this point, however, it is premature to make any conclusions on the significance of biaxial bending interaction from a design point of view. Several simulations, analytical and experimental, on structures of realistic size must be carried out to arrive at more meaningful conclusions.

The numerical examples presented in this Section are only representative of the capability and versatility of the modeling schemes developed in this study. Additional examples will be presented in Part II of the Report along with the program User Guide. It has been shown that the response results using the present developments are in agreement with either experimental or other analytical models. However, the scope of the modeling techniques extend far beyond the limited examples presented in this Section, with definitive applications in inelastic response analysis, seismic simulation studies, laboratory testing of components and structures, monotonically, cyclically, and on shaking tables, damageability evaluation, and a host of related applications.

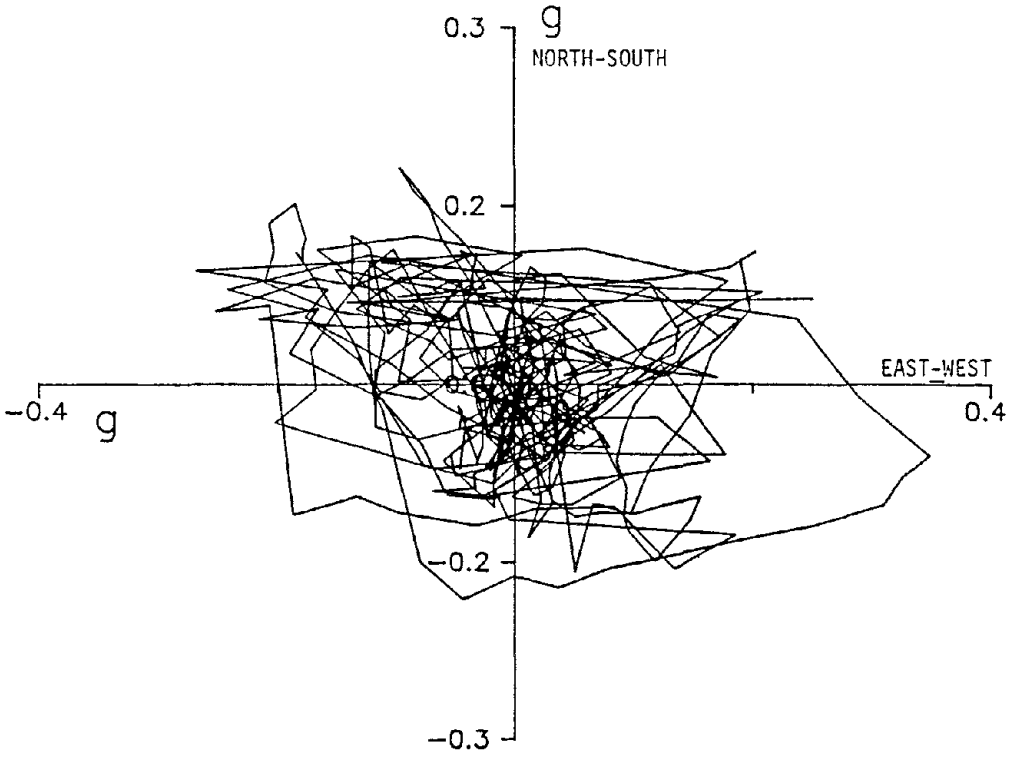

FIGURE 7-6 Bidirectional Input of El Centro Accelerogram

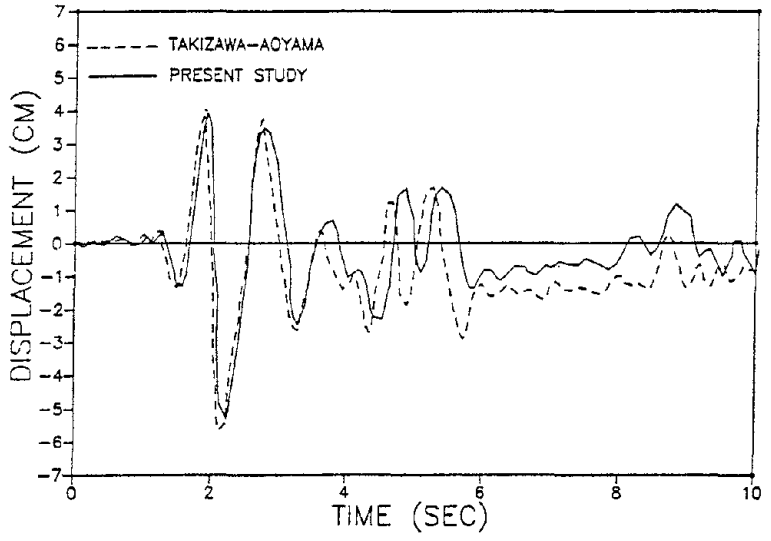

FIGURE 7-7 Comparative Study of Uniaxial Response

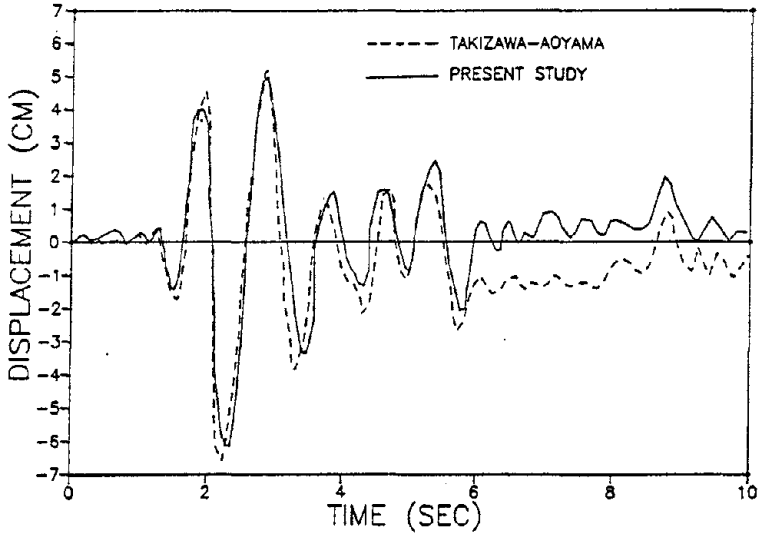

FIGURE 7-8 Comparative Study of Biaxial Response

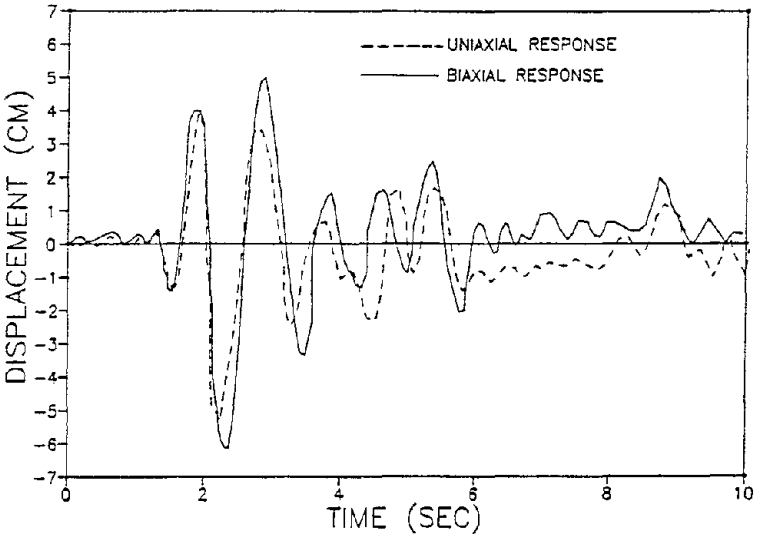

FIGURE 7-9 Comparison of Uniaxial vs. Biaxial Response

SECTION 8

CONCLUSION

The main focus of this report has been the development of a comprehensive modeling scheme for general *3-dimensional analysis* of reinforced concrete buildings subjected to inelastic action under *monotonic, cyclic and/or seismic loads*. The modeling tasks were undertaken both at the material and structural levels. The resulting response quantities were expressed in an engineering sense using a conceptual model of damage, where capacity and demand find explicit representation. Several new modeling techniques were presented, many existing procedures were generalized and integrated into the proposed modeling scheme. A summary of these procedures, the expected advantages of the proposed methods, and a brief list of enhancements and extensions that still need to be investigated, are presented in this concluding section.

The study commenced by exploring the relative merits of *macro-modeling* as opposed to *micro-modeling* schemes for R/C structural analysis. It is established that micro-modeling techniques are suitable only for analysis of single components since their implementation at the structural level would be too time-consuming, computational demanding, and expensive. Moreover, since the complex interaction of steel and concrete cannot be modeled accurately, the efforts of refined micro-modeling do not offer any compensating improvement in reliability of response results. It was decided, therefore, that the present study would adhere to a macro-modeling approach, which offers an attractive alternative both in the economy of computation and in the flexibility of modeling.

An efficient and versatile macro-model to represent an R/C structural element was used (the details are summarized in the Appendix). The model uses a *distributed flexibility* approach which recognizes that inelastic action in R/C sections do not concentrate at joints

but spreads along the length of the member. A 3-dimensional element stiffness matrix was formulated in which the components of *inelastic biaxial bending* were derived from the distributed flexibility model. The finite size of joint panel zones were included in the stiffness matrix development.

The 3-dimensional element model is applied to global modeling of entire 3-D building systems. Buildings with both flexible and rigid floors are considered. The general 3-dimensional formulation decomposes a structure into columns, beams, and shear walls. The overall modeling scheme was developed from the premise that biaxial bending interaction is significant only for column elements. Beams and shear walls were also modeled with 6 degrees-of-freedom per node, but inelastic behavior is considered only in one principal direction.

The modeling of inelastic biaxial bending interaction was achieved through the development of an efficient *viscoplasticity-based force-deformation model.* The model incorporates both stiffness and strength decay thereby making it suitable for use with R/C systems. The hysteresis loops are generated through the solution of coupled differential equations without need for extensive book-keeping or actual tracing of force-deformation curves. The incorporation of this model into the overall scheme of building analysis constitutes a significant improvement over existing methods for R/C structural analysis.

A *system identification* module is proposed for establishing the inelastic properties of the macro-models. Micromodel (filament model) analysis and available empirical models obtained from statistical analysis of experimental data are recommended for setting up the envelope curves and hysteretic parameters.

Procedures are established for the analysis of assembled macro-models under static, monotonic, cyclic, or dynamic loads. For the inelastic response analysis, two distinct schemes

are used to control loss of equilibrium due to stiffness changes. A single step *force correction* is used to minimize errors due to equilibrium loss, and a unique formulation is developed to update element stiffnesses during unloading and reloading. An approximate procedure to account for *P-delta effects* is developed, based on incremental shears that accumulate due to inter-story drift.

A conceptual model of *seismic damage* is formulated to enable the engineering interpretation of an inelastic response analysis. The model uses the concept of energy capacity and energy demand. A new normalized damage index is derived, and a procedure is presented to evaluate component, story level, and overall structural damage.

The proposed modeling schemes have been incorporated into a modular computer program, **IDARC-3-D**, which is capable of performing static, monotonic, cyclic, or seismic response analysis of 3-D building structures. To facilitate analytical development of experimental research programs, procedures were proposed for sequential testing of components and structures and for macro-model calibration.

Another major objective was to consolidate the basis of a new interactive computer model with graphic visualization and interactive capabilities for data preparation, model analysis, damage evaluation, and automated redesign of R/C buildings. The foundation for this ambitious effort has begun through the development of a *graphical preprocessing module* for definition of R/C sections and prescription of seismic loads. The developments have been incorporated into Cornell University's 3-D graphics preprocessor, CU-PREPF. This module is expected to serve as the base program for all future enhancements.

Complete details of the program development and implementation including a User Guide is being prepared as a separate Technical Manual.

The modeling capabilities formulated in this study are general, versatile, and efficient. The three-dimensional component macro-model can be used for modeling of all types of elements: beams, columns, slabs, and walls. The use of a distributed flexibility approach combines the essence of micro-modeling schemes with the efficiency of single component models. The development of the viscoplastic biaxial hysteretic model has resulted in a procedure which is error-free at the material level and extremely simple to implement at the structural level. The correction techniques used to restore force equilibrium during the inelastic response analysis, though approximate, have proven to be more efficient than fully iterative procedures. The damage model provides a physical interpretation of the state of a structure following inelastic action. Finally, the concept of a system identification procedure provides for a flexible modeling scheme in which the reliability of the system response can be monitored.

However, in the context of the developments presented in this report, there still remain a number of aspects which need to be investigated. The conceptual damage model needs to be calibrated in terms of the overall (or story level) damage index and the actual physical condition of the structure. The calibration must relate to terms such as *mild* or *moderate* damage, *severe* or *irreparable damage*, and structural *failure* or *collapse*. It should also be capable of assessing the quality of structural design thereby becoming a tool for seismic evaluation of building designs. The biaxial model needs to be studied in greater detail, beginning with the calibration of the stiffness and strength decay parameters. To gain a better understanding of the nature of biaxial bending interaction, an extensive experimental program is necessary.

The simulation of inelastic response using the comprehensive schemes developed in this study can also provide a better understanding of 3-D structural behavior, thereby leading to the development of simplified procedures for analysis of R/C buildings.

Extensive simulations using probabilities models must be carried out using the developed computer model to study the sensitivity of material and component parameters. This can lead to the formulation of simple design guidelines for use by practicing engineers.

Reinforced concrete is, after all, a complex material. In order to gain a clear insight into the mechanics of its behavior, it is necessary to be guided by the trends dictated by experimental testing in which the variation of section and material parameters is explicitly considered. The incorporation of macro-behavioral models based on these trends into analytical modeling schemes for structural analysis, as set forth in this study, offers a concise and rational approach to inelastic modeling of reinforced concrete structures.

SECTION 9

REFERENCES

Aktan, A.E. and Pecknold, D.A., "Response of a Reinforced Concrete Section to Two-Dimensional Curvature Histories", ACI Journal, Vol.71, No.5, 1974.

Atalay, M.B. and Penzien, J., "The Seismic Behavior of Critical Regions of Reinforced Concrete Components Influenced by Moment, Shear and Axial Force", Report No.UCB/EERC/75/19, University of California, Berkeley, 1975.

Aoyama, H. and Sugano, T., "A Generalized Inelastic Analysis of Reinforced Concrete Structures Based on Tests of Members", Recent Researches of Structural Mechanics - Contributions in Honor of the 60th Birthday of Prof. Y. Tsuboi, Tokyo, 1968.

Baber, T.T. and Wen, Y.K., "Random Vibration of Hysteretic, Degrading Systems", J. of Engrg. Mech., ASCE, 107, EM6, 1981.

Berg, G.V. and DaDeppo, D.A., "Dynamic Analysis of Elasto-Plastic Structures", Journal of the Engineering Mechanics Division, ASCE, Vol.86, EM2, 1960, pp.35-58.

Bertero, V.V. and Bresler, B., "Design and Engineering Decision: Failure Criteria (Limit States), Developing Methodologies for Evaluating the Earthquake Safety of Existing Buildings", EERC Report No.77/06, University of California, Berkeley, 1977.

Bertero, V.V. and Popov, E.P., "Seismic Behavior of Moment-Resisting R/C Frames", ACI Special Publication No.53, 1977.

Bresler, B., "Design Criteria for Reinforced Concrete Columns Under Axial Load and Biaxial Bending", ACI Journal, Vol.57, No.5, 1960.

Bouc, R., "Forced Vibration of Mechanical System with Hysteresis", Proc., 4th Conf. on Nonlinear Oscillation, Prague, 1967.

Celebi, M. and Penzien, J., "Experimental Investigation into the Seismic Behavior of Critical Region of R/C Components as Influenced by Moment and Shear", Report No. EERC 73-4, University of Californai, Berkeley, 1973.

Charney, F.A. and Bertero, V.V., "An Evaluation of the Design and Analytical Seismic Response of a Seven-Story Reinforced Concrete Frame-Wall Structure", EERC Report No.82/08, University of California, Berkeley, 1982.

Chung, Y.S., Meyer, C. and Shinozuka, M., "Seismic Damage Assessment of Reinforced Concrete Members", Technical Report NCEER-87-0022, State University of New York at Buffalo, October 1987.

Clough, R.W., Benuska, K.L. and Wilson, E.L., "Inelastic Earthquake Response of Tall Buildings", Proceedings of the 3rd WCEE, New Zealand, Vol.II, 1965, pp.68-89.

Clough, R.W. and Johnston, S.B., "Effect of Stiffness Degradation in Earthquake Ductility Requirements", Proceedings of the Japan Earthquake Engineering Conference, Tokyo, 1966.

Constantinou, M.C. and Adnane, M.A., "Dynamics of Soil-Base-Isolated-Structure Systems: Evaluation of Two Models for Yielding Systems", Report to NSF, Department of Civil Engineering, Drexel University, September 1987.

Darwin, D. and Nmai, C.K., "Energy Dissipation in RC Beams under Cyclic Load", Journal of Structural Engineering, ASCE, Vol.112, No.8. 1986.

Ewing, R.D., Kariotis, J.C. and El-Mustapha, A., "LPM/I: A Computer Program for the Nonlinear Dynamic Analysis of Lumped Parameter Models", Report No.2.3-1, EKEH, California, 1987.

Ghusn, G.E. and Saiidi, M., "A Simple Hysteretic Element for Biaxial Bending of R/C Columns and Implementation in NEABS-86", Report No. CCEER-86-1, University of Nevada Reno, July 1986.

Giberson, M.F., "Two Nonlinear Beams with Definitions of Ductility", Journal of the Structural Division, ASCE, Vol.95, ST2, 1969, 137-157.

Gilman, J.J., "Micromechanics of Flow in Solids", McGraw-Hill, New York, 1969.

Gosain, N.K., Brown, R.H. and Jirsa, J.O., "Shear Requirement for Load Reversals on RC Members", Journal of Structural Division, ASCE, Vol.103, ST7, 1977.

Heidebrecht, A.C., Fleming, J.F. and Lee, S.L., "Dynamic Analysis of Inelastic Multi-Degree Systems", Journal of the Engineering Mechanics Division, ASCE, Vol.89, EM6, 1963, pp.193-215.

Hwang, T.H. and Scribner, C.F., "RC Member Cyclic Response During Various Loadings", Journal of Structural Engineering, ASCE, 110, 3, 1984.

Iwan, W.D., "A Model for the Dynamic Analysis of Deteriorating Structures", Proceedings of the 5th WCEE, Rome, 1973.

Kabeyasawa, T., Shiohara, H., Otani, S. and Aoyama, H., "Analysis of the Full-Scale Seven-Story Reinforced Concrete Test Structure", Journal of the Faculty of Engineering, University of Tokyo, Vol.XXXVII, No.2, 1983.

Kanaan, A.E. and Powell, G.H., "DRAIN-2D - A General Purpose Computer Program for Dynamic Analysis of Inelastic Plane Structures", Report No.UCB/EERC/73/06 and 73/22, University of California, Berkeley, 1973.

Keshavarzian, M. and Schnobrich, W.C., "Analytical Models for Nonlinear Seismic Analysis of Reinforced Concrete Structures", ACI Convention, Los Angeles, March 1983. (also Engineering Structures, Vol.7, April 1985, pp.131-142)

Kunnath, S.K., Park, Y.J. and Reinhorn, A.M., "Substructuring Technique for Shaking Table Testing", 6th ASCE Engineering Mechanics Specialty Conference, State University of New York, Buffalo, 1987.

Kustu, O. and Bouwkamp, J.G., "Behavior of Reinforced Concrete Deep Beam-Column Subassemblages Under Cyclic Loads", Report No.UCB/EERC/73/08, University of California, Berkeley, 1973.

Lai, S.S., "Post-Yield Hysteretic Biaxial Models for Reinforced Concrete Members", ACI Structural Journal, May-June 1987.

Lai, S.S., Will, G.T. and Otani, S., "Model for Inelastic Biaxial Bending of Concrete Members", Journal of Structural Engineering, ASCE, Vol.110, No.11, 1984.

Li, K-N., Aoyama, H. and Otani, S., "Reinforced Concrete Columns Under Varying Axial Load and Bi-Directional Lateral Load Reversals", 9th World Conference on Earthquake Engineering, Tokyo, August 1988.

Lybas, J. and Sozen, M.A., "Effect of Beam Strength and Stiffness on Dynamic Behavior of RC Coupled Walls", Civil Engineering Studies, SRS No.444, University of Illinois, Urbana, 1977.

Mander, J.B., Priestly, M.J.N. and Park, R., "Theoretical Stress-Strain Model for Confined Concrete", Journal of Structural Engineering, ASCE, Vol.114, No.8, 1988.

Malvern, L.E., "Introduction to the Mechanics of a Continuous Medium", Prentice-Hall, Inc., 1969.

Mondkar, D.P. and Powell, G.H., "ANSR-1 - General Purpose Program for Analysis of Nonlinear Structural Response", EERC Report No.75/37, University of California, Berkeley, 1975.

Mondkar, D.P. and Powell, G.H., "ANSR-II - Analysis of Nonlinear Structural Response, User's Manual", EERC Report No.79/17, University of California, Berkeley, 1979.

Moazzami, S. and Bertero, V.V., "Three-Dimensional Inelastic Analysis of Reinforced Concrete Frame-Wall Structures", Report No.UCB/EERC/87/05, University of California, Berkeley, 1987.

Nakata, S., Sproul, T. and Penzien, J., "Mathematical Modeling of Hysteresis Loops for Reinforced Concrete Columns", Report No.UCB/EERC/78/11, University of California, Berkeley, 1978.

Newmark, N.M. and Rosenblueth, E., "Fundamentals of Earthquake Engineering", Prentice Hall, 1974.

Nigam, N.C., "Inelastic Interactions in the Dynamic Response of Structures", EERL Report, California Institute of Technology, 1967.

Oh, S., "Analysis of Shear Walls", M.S. Project, Department of Civil Engineering, State University of New York, Buffalo, 1988.

Oliveira, C.S., "Seismic Risk Analysis for a Site and a Metropolitan Area", EERC Report No.75/03, University of California, Berkeley, 1975.

Otani, S., "SAKE: A Computer Program for Inelastic Analysis of R/C Frames to Earthquakes", Civil Engineering Studies, Structural Research Series No.413, University of Illinois, Urbana, 1975.

Otani, S. and Sozen, M.A., "Behavior of Multistory Reinforced Concrete Frames During Earthquakes", Civil Engineering Studies, Structural Research Series No.392, University of Illinois, Urbana, 1972.

Ozdemir, H., "Nonlinear Transient Dynamic Analysis of Yielding Structures", Ph.D. Dissertation, University of California, Berkeley, 1976.

Padilla-Mora, R. and Schnobrich, W.C., "Nonlinear Response of Framed Strcutures to Two-Dimensional Earthquake Motion", Civil Engineering Studies, SRS No.408, University of Illinois, Urbana, 1974.

Park, R., Kent, D.C. and Sampson, R.A., "Reinforced Concrete Members with Cyclic Loading", Journal of Structural Division, ASCE, Vol.98, ST7, 1972.

Park, Y.J. and Ang, A. H-S., "Mechanistic Seismic Damage Model for Reinforced Concrete", Journal of Structural Engineering, ASCE, Vol.111, No.4, 1985, pp.722-739.

Park, Y.J., Reinhorn, A.M. and Kunnath, S.K., "IDARC: Inelastic Damage Analysis of Reinforced Concrete Frame - Shear-Wall Structures", Technical Report NCEER-87-0008, State University of New York at Buffalo, July 1987.

Park, Y.J., Reinhorn, A.M. and Kunnath, S.K., "Damageability Assessment of Reinforced Concrete Buildings Using Identified Component Properties", ASCE Spring Convention, Nashville, 1987.

Park, Y.J., Wen, Y.K. and Ang, A. H-S., "Random Vibration of Hysteretic Systems Under Bi-Directional Ground Motions", Earthquake Engineering and Structural Dynamics, Vol.14, 1986.

Pecknold, D.A., "Inelastic Structural Response to 2D Ground Motion", ASCE Journal of Engineering Mechanics Division, Vol.100, EM5, 1974.

Penzien, J. "Elasto-Plastic Response of Idealized Multistory Structures Subjected to Strong Motion Earthquake", Proceedings of 2nd WCEE, Japan, Vol.II, 1960, pp.739-760.

Powell, G.H., "Supplement to Computer Program DRAIN-2D", August 1975.

Powell, G.H. and Allahabadi, R., "Seismic Damage Prediction by Deterministic Methods: Concepts and Procedures", Earthquake Engineering and Structural Dynamics, Vol.16, 719-734, 1988.

Reinhorn, A.M., Kunnath, S.K., Bracci, J. and Mander, J.B., "Normalized Damage Index for Evaluation of Buildings", Proceedings of ASCE Structures Congress, San Francisco, 1989.

Reinhorn, A.M., Kunnath, S.K. and Panahshahi, N., "Modeling of R/C Building Structures with Flexible Floor Diaphragms (IDARC2)", Technical Report NCEER 88-0035, State University of New York at Buffalo, December 1988.

Roufaiel, M.S.L and Meyer, C., "Analytical Modeling of Hysteretic Behavior of R/C Frames", Journal of Structural Engineering, ASCE, Vol.113, No.3, 1987.

Seidel, M., "Damage Assessment of Reinforced Concrete Structures in Eastern United States", M.S. Thesis, Department of Civil Engineering, SUNY, Buffalo, 1988.

Stephens, J.E. and Yao, J.T.P., "Damage Assessment Using Response Measurement", Journal of Structural Engineering, ASCE, Vol.113, No.4, 1987.

Suharwardy, M.I.H. and Pecknold, D.A., "Inelastic Response of Reinforced Concrete Columns Subjected to Two-Dimensional Earthquake Motions", Civil Engineering Studies, SRS No.455, University of Illinois, Urbana, October 1978.

Takayanagi, T. and Schnobrich, W.C., "Computed Behavior of Coupled Shear Walls", Proceedings of 6th WCEE, New Delhi, 1977.

Takeda, T., Sozen, M.A. and Nielsen, N.N., "Reinforced Concrete Response to Simulated Earthquakes", Journal of the Structural Division, ASCE, Vol.96, ST2, 1970.

Takizawa, H., "Notes on Some Basic Problems in Inelastic Analysis of Planar R/C Structures (Parts I and II)", Trans of the Arch Inst of Japan, No.240, 1976.

Takizawa, H., "Strong Motion Response Analysis of Reinforced Concrete Buildings", (in Japanese), Concrete Journal, Japan National Council on Concrete, Vol.11, No.2, 1973.

Takizawa, H. and Aoyama, H., "Biaxial Effects in Modelling Earthquake Response of RC Structures", Earthquake Engineering and Structural Dynamics, Vol.4, 523-552, 1976.

Tani, S. and Nomura, S., "Response of Reinforced Concrete Structures Characterized by Skeleton Curve and Normalized Characteristic Loops to Ground Motion", Proceedings of the 5th WCEE, Rome, 1973.

Toridis, T.G. and Khozeimeh, K., "Inelastic Response of Frames to Dynamic Loads", Journal of Engineering Mechanics Division, ASCE, Vol.97, EM3, 1971.

Tseng, W.S. and Penzien, J., "Seismic Response of Long Multiple-Span Highway Bridges", Earthquake Engineering and Structural Dynamics, Vol.4, 1975, pp.24-48.

Umemura, H. and Takizawa, H., "Dynamic Response of Reinforced Concrete Buildings", Structural Engineering Documents 2, IABSE, 1982.

Wen, Y.K., "Approximate Method for Nonlinear Random Vibration", Journal of Engineering Mechanics Division, ASCE, Vol.101, EM4, 1975.

Wen, R.K. and Farhoomand, F., "Dynamic Analysis of Inelastic Space Frames", Journal of Engineering Mechanics Division, ASCE, Vol.96, EM5, 1970.

Wen, R.K. and Janssen, J.G., "Dynamic Analysis of Elasto-Plastic Frames", Proceedings of 3rd World Conference on Earthquake Engineering", Vol.II, New Zealand, 1965.

Wight, J.K. (Editor), "Earthquake Effects on Reinforced Concrete Structures", U.S.-Japan Research, ACI Special Publication SP-84, 1985.

Wight, J.K. and Sozen, M.A., "Shear Strength Decay in Reinforced Concrete Columns Subjected to Large Deformation Reversals", Civil Engineering Studies, Structural Research Series No.403, University of Illinois, Urbana, 1973.

Yao, J.T.P. et al., "Fundamental Concepts of Building Damage", Wiss, Janney, Elstner Assoc, Inc., Emeryville, California, August 1987.

Yao, J.T.P. and Munse, W.H., "Low-Cycle Axial Fatigue Behaviour of Mild Steel", Journal of Structural Division, ASCE, Vol.95, ST8, 1969.

Yeh, L-J., "Identification of Nonlinear Cyclic Behavior of RC Frame Components Using Three Parameter Model", M.S. Project, State University of New York at Buffalo, 1987.

Yunfei, H., Yufeng, C., Chang, S. and Bainian, H., "The Experimental Study of a Two-Bay Three-Story Reinforced Concrete Frame Under Cyclic Loading", Proc., 8th Symposium on Earthquake Engrg., Roorkee, India, 1986.

Zeris, C. and Mahin, S.A., "Analysis of Reinforced Concrete Beam-Columns under Uniaxial Excitations", Journal of Structural Engineering, ASCE, Vol.114, 4, 804-820, 1988.

APPENDIX

STIFFNESS MATRIX DEVELOPMENT

The development of a versatile and efficient member model that can be used for R/C components which experience inelastic behavior under random lateral load reversals is detailed in this Appendix. The main idea is to isolate the inelastic rotational components and formulate the incrmental instantaneous stiffness matrix in terms of these components. The resulting matrix is then incorporated into the general stiffness matrix for 3-D beam-column elements in which the remaining components of force and deformation are assumed to be elastic. Details of the general development for inelastic biaxial bending are outlined.

A distributed single component model is developed for a typical beam-column element (Fig.A.1) subjected to inelastic biaxial bending. The same model can be reduced to the special case of uniaxial flexure when only one component of bending is considered. The model is composed of a single element with two inelastic rotational springs at each member end. In the proposed model, the flexibility factor, *1/EI*, is assumed to be linearly distributed along the member between the two critical sections and the point of contraflexure (Fig.A.2). Elastic properties are given to the section at the contraflexure point. This enables the development of a model whose inflection point may vary continuously as a function of the stress history. It also enables a more realistic consideration of the inflection point lying outside the member.

Consider the R/C element shown in Fig.A.1 with components of bending in two principal directions of the coordinate axes. A relationship of the following form needs to be derived:

$$\begin{pmatrix} \Delta\theta'_{ya} \\ \Delta\theta'_{yb} \\ \Delta\theta'_{za} \\ \Delta\theta'_{zb} \end{pmatrix} = \begin{pmatrix} f_{11} & f_{12} & f_{13} & f_{14} \\ f_{21} & f_{22} & f_{23} & f_{24} \\ f_{31} & f_{32} & f_{33} & f_{34} \\ f_{41} & f_{42} & f_{43} & f_{44} \end{pmatrix} \begin{pmatrix} \Delta M'_{ya} \\ \Delta M'_{yb} \\ \Delta M'_{zb} \\ \Delta M'_{zb} \end{pmatrix} \qquad (A.1)$$

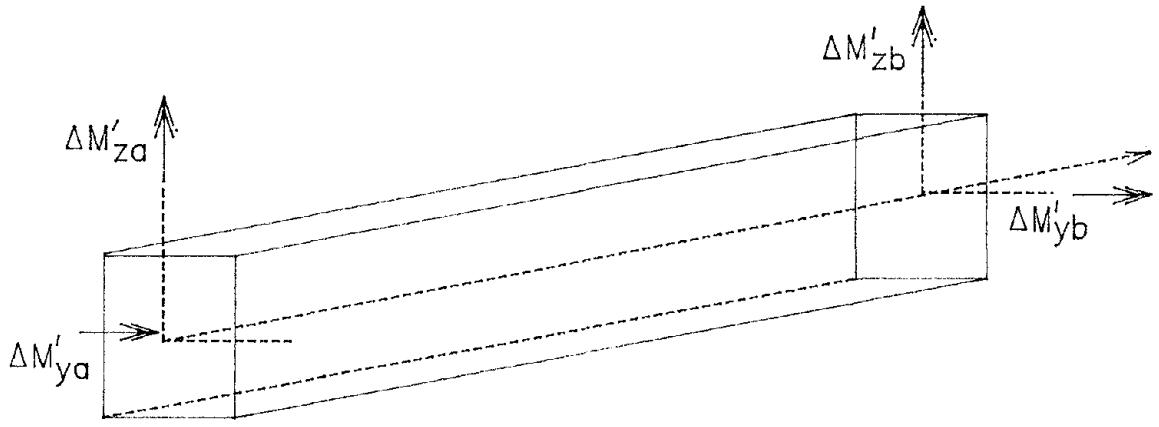

FIGURE A-1 Biaxial Components of Bending for Typical Beam-Column Element

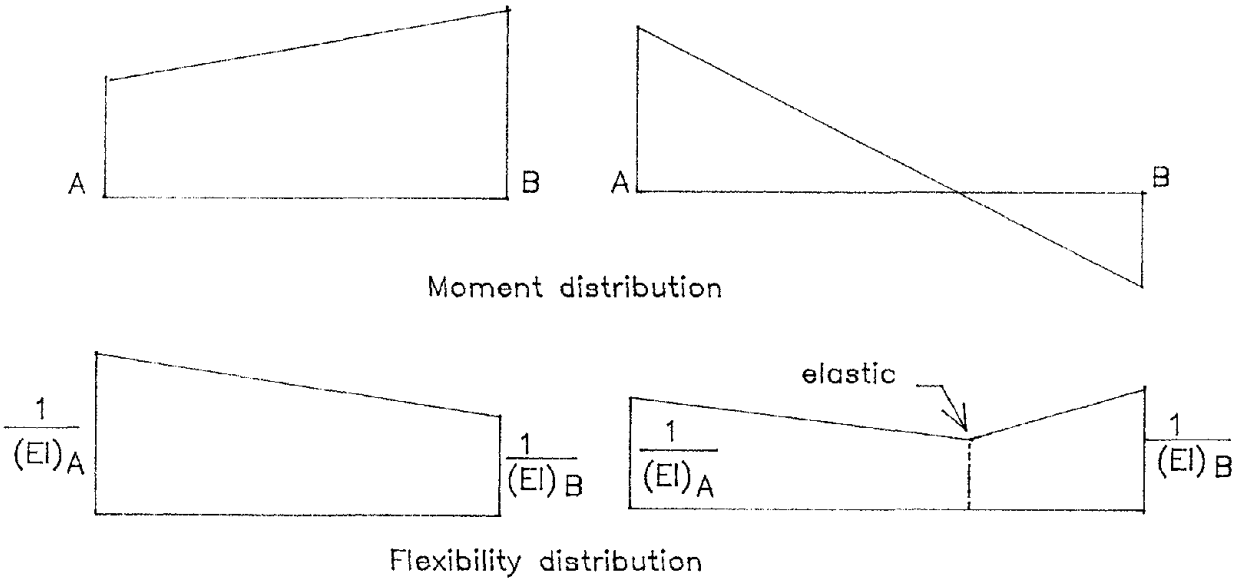

FIGURE A-2 Linear Distributed Flexibility Model

where $\Delta\theta'$ and $\Delta M'$ are the incremental rotation and corresponding moment at the interior face of the member respectively, f_{ij} are the coefficients of the flexibility matrix, subscripts y and z refer to coordinate direction, and subscripts a and b refer to the member ends.

Under the action of lateral or seismic loads, the distribution of moments across the length of the section is linear, with the point of contraflexure lying within or outside the member (see Fig.A.2). In three-dimensional moment space, when biaxial bending is considered, this can give rise to four possible moment patterns as drawn in Fig.A.3. Therefore, the construction of the incremental flexibility matrix has to account for all combinations of the moment distribution in each direction. The development of the flexibility matrix that follows is based on the principle of virtual work.

The application of Castigliano's theorem to the total complementary energy for beam flexure yields the classical *unit load* theory. To derive the element flexibility matrix using this approach, the following formulation is used:

$$f_{ij} = \int_0^l m_i m_j \frac{M_x}{EI} dx \qquad (A.2)$$

where f_{ij} is the flexibility coefficient, m_i, m_j are the unit moments applied in each principal direction under consideration, M_x is the actual moment distribution, and EI is the flexural rigidity of the member. The application of Eq.(A.2) to the moment patterns shown in Fig.A.3 produces a flexibility matrix in the following form:

$$[k_f] = L' \begin{pmatrix} f_{11} & f_{12} & 0 & 0 \\ f_{21} & f_{22} & 0 & 0 \\ 0 & 0 & f_{33} & f_{34} \\ 0 & 0 & f_{43} & f_{44} \end{pmatrix} \qquad (A.3)$$

The coefficients of the flexibility matrix for each of the four possible cases are summarised below:

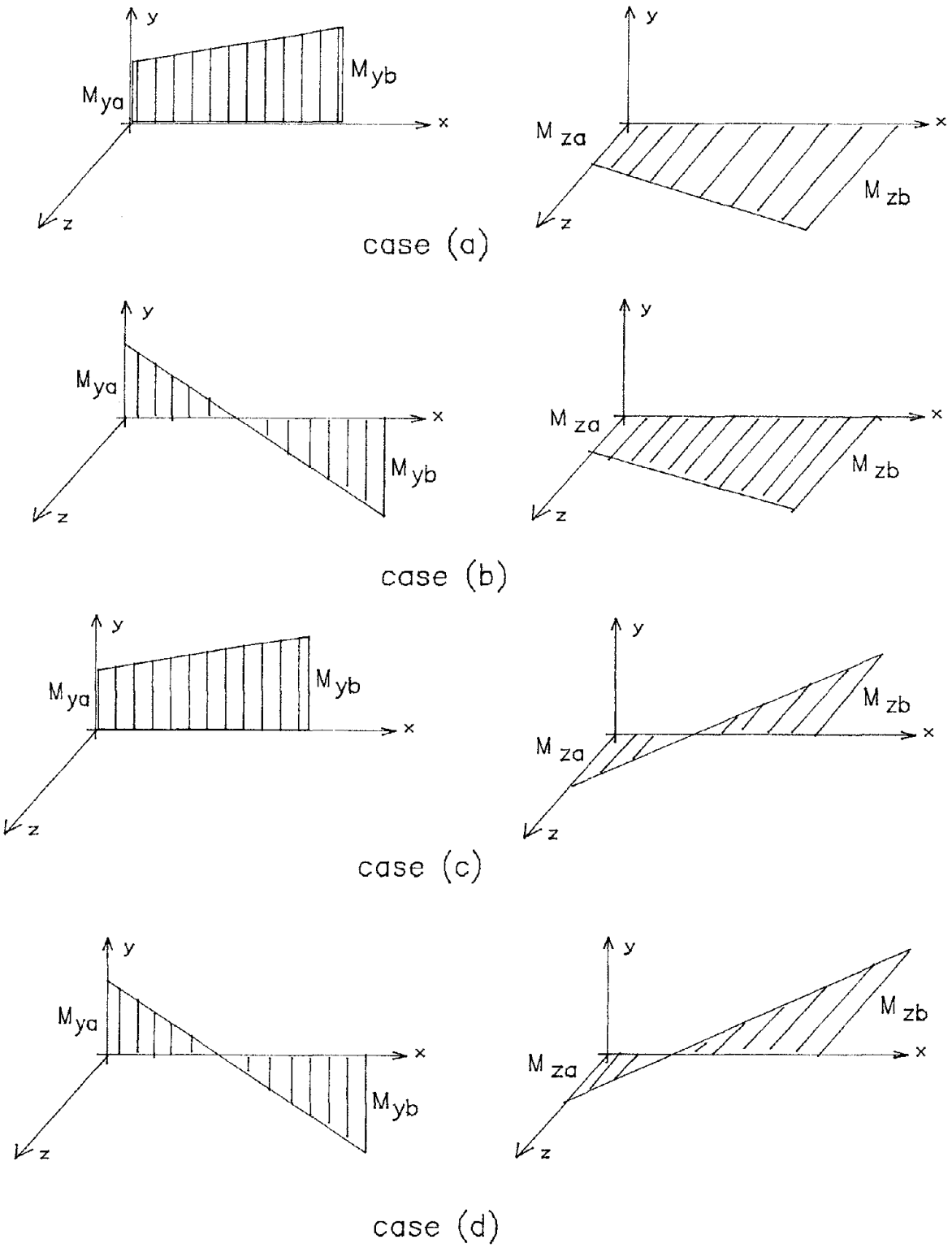

FIGURE A-3 Moment Distribution Combinations

Case (a)

$$f_{11} = \frac{l}{4(EI)_{ya}} + \frac{l}{12(EI)_{yb}}$$

$$f_{12} = f_{21} = -\frac{l}{12(EI)_{ya}} - \frac{l}{12(EI)_{yb}}$$

$$f_{22} = \frac{l}{12(EI)_{ya}} + \frac{l}{4(EI)_{yb}}$$

$$f_{33} = \frac{l}{4(EI)_{za}} + \frac{l}{12(EI)_{zb}}$$

$$f_{34} = f_{43} = -\frac{l}{12(EI)_{za}} - \frac{l}{12(EI)_{zb}}$$

$$f_{44} = \frac{l}{12(EI)_{za}} + \frac{l}{4(EI)_{zb}}$$

Case (b)

$$f_{11} = \frac{l}{12(EI)_{ya}}(6\alpha_1 - 4\alpha_1^2 + \alpha_1^3) + \frac{l}{12(EI)_{yb}}(1 - 3\alpha_1 + 3\alpha_1^2 - \alpha_1^3) + \frac{l}{12(EI)_{yo}}(3 - 3\alpha_1 + \alpha_1^2)$$

$$f_{12} = f_{21} = \frac{l}{12(EI)_{ya}}(-2\alpha_1^2 + \alpha_1^3) + \frac{l}{12(EI)_{yb}}(-1 + \alpha_1 + \alpha_1^2 - \alpha_1^3) + \frac{l}{12(EI)_{yo}}(-1 - \alpha_1 + \alpha_1^2)$$

$$f_{22} = \frac{l}{12(EI)_{ya}}\alpha_1^3 + \frac{l}{12(EI)_{yb}}(3 - \alpha_1 - \alpha_1^2 - \alpha_1^3) + \frac{l}{12(EI)_{yo}}(1 + \alpha_1 + \alpha_1^2)$$

$$f_{33} = \frac{l}{4(EI)_{za}} + \frac{l}{12(EI)_{zb}}$$

$$f_{34} = f_{43} = -\frac{l}{12(EI)_{za}} - \frac{l}{12(EI)_{zb}}$$

$$f_{44} = \frac{l}{12(EI)_{za}} + \frac{l}{4(EI)_{zb}}$$

where $\alpha_1 = \Delta M_{ya} / (\Delta M_{ya} + \Delta M_{yb})$

Case (c)

$$f_{11} = \frac{1}{4(EI)_{ya}} + \frac{1}{12(EI)_{yb}}$$

$$f_{12} = f_{21} = -\frac{1}{12(EI)_{ya}} - \frac{1}{12(EI)_{yb}}$$

$$f_{22} = \frac{1}{12(EI)_{ya}} + \frac{1}{4(EI)_{yb}}$$

$$f_{33} = \frac{1}{12(EI)_{za}}(6\alpha_2 - 4\alpha_2^2 + \alpha_2^3) + \frac{1}{12(EI)_{zb}}(1 - 3\alpha_2 + 3\alpha_2^2 - \alpha_2^3) + \frac{1}{12(EI)_{z}}(3 - 3\alpha_2 + \alpha_2^2)$$

$$f_{34} = f_{43} = \frac{1}{12(EI)_{za}}(-2\alpha_2^2 + \alpha_2^3) + \frac{1}{12(EI)_{zb}}(-1 + \alpha_2 + \alpha_2^2 - \alpha_2^3) + \frac{1}{12(EI)_{z}}(-1 - \alpha_2 + \alpha_2^2)$$

$$f_{44} = \frac{1}{12(EI)_{za}}\alpha_2^3 + \frac{1}{12(EI)_{zb}}(3 - \alpha_2 - \alpha_2^2 - \alpha_2^3) + \frac{1}{12(EI)_{z}}(1 + \alpha_2 + \alpha_2^2)$$

where $\alpha_2 = \Delta M_{za} / (\Delta M_{za} + \Delta M_{zb})$

Case (d)

$$f_{11} = \frac{1}{12(EI)_{ya}}(6\alpha_1 - 4\alpha_1^2 + \alpha_1^3) + \frac{1}{12(EI)_{yb}}(1 - 3\alpha_1 + 3\alpha_1^2 - \alpha_1^3) + \frac{1}{12(EI)_{yo}}(3 - 3\alpha_1 + \alpha_1^2)$$

$$f_{12} = f_{21} = \frac{1}{12(EI)_{ya}}(-2\alpha_1^2 + \alpha_1^3) + \frac{1}{12(EI)_{yb}}(-1 + \alpha_1 + \alpha_1^2 - \alpha_1^3) + \frac{1}{12(EI)_{yo}}(-1 - \alpha_1 + \alpha_1^2)$$

$$f_{22} = \frac{1}{12(EI)_{ya}}\alpha_1^3 + \frac{1}{12(EI)_{yb}}(3 - \alpha_1 - \alpha_1^2 - \alpha_1^3) + \frac{1}{12(EI)_{yo}}(1 + \alpha_1 + \alpha_1^2)$$

$$f_{33} = \frac{1}{12(EI)_{za}}(6\alpha_2 - 4\alpha_2^2 + \alpha_2^3) + \frac{1}{12(EI)_{zb}}(1 - 3\alpha_2 + 3\alpha_2^2 - \alpha_2^3) + \frac{1}{12(EI)_{zo}}(3 - 3\alpha_2 + \alpha_2^2)$$

$$f_{34} = f_{43} = \frac{1}{12(EI)_{za}}(-2\alpha_2^2 + \alpha_2^3) + \frac{1}{12(EI)_{zb}}(-1 + \alpha_1 + \alpha_2^2 - \alpha_2^3) + \frac{1}{12(EI)_{zo}}(-1 - \alpha_2 + \alpha_2^2)$$

$$f_{44} = \frac{1}{12(EI)_{za}}\alpha_2^3 + \frac{1}{12(EI)_{zb}}(3 - \alpha_2 - \alpha_2^2 - \alpha_2^3) + \frac{1}{12(EI)_{zo}}(1 + \alpha_2 + \alpha_2^2)$$

where α_1 and α_2 are as defined earlier.

Development of Stiffness Matrix for Elements with Finite Joints

The instantaneous flexibility matrix developed in the previous section is now incorporated into a generalized stiffness formulation. A beam-column element with rigid joints and five degrees-of-freedom per node is shown in Fig.A.4. In constructing the element stiffness matrix, a translation matrix is necessary to transfer force and deformation quantities across the rigid panel zone. The following transformations are obtained:

$$\begin{pmatrix} \Delta M_{ya} \\ \Delta M_{yb} \\ \Delta M_{za} \\ \Delta M_{zb} \end{pmatrix} = [T] \begin{pmatrix} \Delta M'_{ya} \\ \Delta M'_{yb} \\ \Delta M'_{za} \\ \Delta M'_{zb} \end{pmatrix} \qquad (A.4)$$

$$\begin{pmatrix} \Delta \theta'_{ya} \\ \Delta \theta'_{yb} \\ \Delta \theta'_{za} \\ \Delta \theta'_{zb} \end{pmatrix} = [T]^T \begin{pmatrix} \Delta \theta_{ya} \\ \Delta \theta_{yb} \\ \Delta \theta_{za} \\ \Delta \theta_{zb} \end{pmatrix} \qquad (A.5)$$

where:

$$[T] = \begin{pmatrix} \frac{(1-\lambda_b)}{\lambda_x} & \frac{\lambda_a}{\lambda_x} & 0 & 0 \\ \frac{\lambda_b}{\lambda_x} & \frac{(1-\lambda_a)}{\lambda_x} & 0 & 0 \\ 0 & 0 & \frac{(1-\lambda_b)}{\lambda_x} & \frac{\lambda_a}{\lambda_x} \\ 0 & 0 & \frac{\lambda_b}{\lambda_x} & \frac{(1-\lambda_a)}{\lambda_x} \end{pmatrix} \qquad (A.6)$$

where: $\lambda_x = 1-\lambda_a-\lambda_b$, and $\lambda_a = r_a/L$ and $\lambda_b = r_b/L$ are the rigid zone lengths at the two ends of the member.

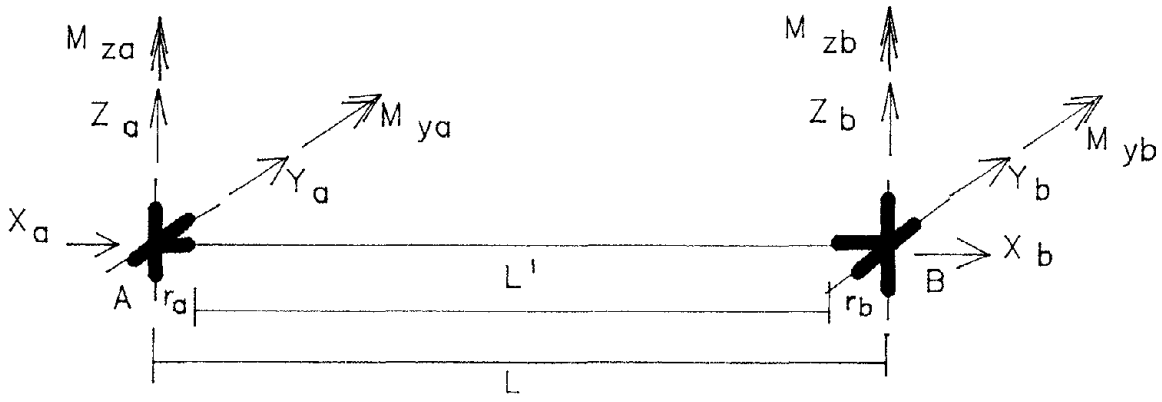

FIGURE A-4 Typical beam-column element with rigid panel zones

Substituting Eq.(A.1) and Eq.(A.5) into Eq.(A.4) after the inversion of the flexibility matrix of Eq.(A.1), the following stiffness equation relating moments and inelastic rotations is obtained:

$$\begin{pmatrix} \Delta M_{ya} \\ \Delta M_{yb} \\ \Delta M_{za} \\ \Delta M_{zb} \end{pmatrix} = [k_s] \begin{pmatrix} \Delta \theta_{ya} \\ \Delta \theta_{yb} \\ \Delta \theta_{za} \\ \Delta \theta_{zb} \end{pmatrix} \qquad (A.7)$$

where $[k_s] = [T][k_f'][T]^T$

and k_f' is the inverted flexibility matrix.

To set up the overall force-deformation relationship, consider the equilibrium of forces in the member shown in Fig.A.4. This gives:

$$\{F\} = [R] \begin{pmatrix} \Delta M_{ya} \\ \Delta M_{yb} \\ \Delta M_{za} \\ \Delta M_{zb} \end{pmatrix} \qquad (A.8)$$

where:

$$\{F\} = \begin{pmatrix} \Delta F_{ya} \\ \Delta M_{ya} \\ \Delta F_{za} \\ \Delta M_{za} \\ \Delta F_{yb} \\ \Delta M_{yb} \\ \Delta F_{zb} \\ \Delta M_{zb} \end{pmatrix} \qquad (A.8a)$$

$$[R] = \begin{pmatrix} 0 & 0 & \frac{1}{L} & \frac{1}{L} \\ 1 & 0 & 0 & 0 \\ -\frac{1}{L} & -\frac{1}{L} & 0 & 0 \\ 0 & 0 & 1 & 0 \\ 0 & 0 & -\frac{1}{L} & -\frac{1}{L} \\ 0 & 1 & 0 & 0 \\ \frac{1}{L} & \frac{1}{L} & 0 & 0 \\ 0 & 0 & 0 & 1 \end{pmatrix} \qquad (A.9)$$

Applying a similar transformation to the displacement components, it is possible to derive the following stiffness equation:

$$\begin{pmatrix} \Delta F_{ya} \\ \Delta M_{ya} \\ \Delta F_{za} \\ \Delta M_{za} \\ \Delta F_{yb} \\ \Delta M_{yb} \\ \Delta F_{zb} \\ \Delta M_{zb} \end{pmatrix} = [R][k_s][R]^T \begin{pmatrix} \Delta u_{ya} \\ \Delta \theta_{ya} \\ \Delta u_{za} \\ \Delta \theta_{za} \\ \Delta u_{yb} \\ \Delta 0_{yb} \\ \Delta u_{zb} \\ \Delta \theta_{zb} \end{pmatrix} \qquad (A.10).$$

where $[K] = [R][k_s][R]^T$ is the element stiffness matrix, and Δu_{ya}, $\Delta \theta_{ya}$, Δu_{za}, $\Delta \theta_{za}$, Δu_{yb}, $\Delta \theta_{yb}$, Δu_{zb}, $\Delta \theta_{zb}$ are the incremental displacements and rotations respectively, in each principal direction, at the two member ends. The axial stiffness term, EA/L, is included directly in the resulting stiffness matrix to enable incorporation of F_{xa} and F_{xb} in Eq.(A.10). It is possible to show that Eq.(A.10) reduces to the standard finite element stiffness matrix in the elastic range by setting the rigid zone lengths to zero and assuming the moment distribution pattern shown in case (a) of Fig.A.3.

NATIONAL CENTER FOR EARTHQUAKE ENGINEERING RESEARCH
LIST OF PUBLISHED TECHNICAL REPORTS

The National Center for Earthquake Engineering Research (NCEER) publishes technical reports on a variety of subjects related to earthquake engineering written by authors funded through NCEER. These reports are available from both NCEER's Publications Department and the National Technical Information Service (NTIS). Requests for reports should be directed to the Publications Department, National Center for Earthquake Engineering Research, State University of New York at Buffalo, Red Jacket Quadrangle, Buffalo, New York 14261. Reports can also be requested through NTIS, 5285 Port Royal Road, Springfield, Virginia 22161. NTIS accession numbers are shown in parenthesis, if available.

NCEER-87-0001 "First-Year Program in Research, Education and Technology Transfer," 3/5/87, (PB88-134275/AS).

NCEER-87-0002 "Experimental Evaluation of Instantaneous Optimal Algorithms for Structural Control," by R.C. Lin, T.T. Soong and A.M. Reinhorn, 4/20/87, (PB88-134341/AS).

NCEER-87-0003 "Experimentation Using the Earthquake Simulation Facilities at University at Buffalo," by A.M. Reinhorn and R.L. Ketter, to be published.

NCEER-87-0004 "The System Characteristics and Performance of a Shaking Table," by J.S. Hwang, K.C. Chang and G.C. Lee, 6/1/87, (PB88-134259/AS).

NCEER-87-0005 "A Finite Element Formulation for Nonlinear Viscoplastic Material Using a Q Model," by O. Gyebi and G. Dasgupta, 11/2/87, (PB88-213764/AS).

NCEER-87-0006 "Symbolic Manipulation Program (SMP) - Algebraic Codes for Two and Three Dimensional Finite Element Formulations," by X. Lee and G. Dasgupta, 11/9/87, (PB88-219522/AS).

NCEER-87-0007 "Instantaneous Optimal Control Laws for Tall Buildings Under Seismic Excitations," by J.N. Yang, A. Akbarpour and P. Ghaemmaghami, 6/10/87, (PB88-134333/AS).

NCEER-87-0008 "IDARC: Inelastic Damage Analysis of Reinforced Concrete Frame - Shear-Wall Structures," by Y.J. Park, A.M. Reinhorn and S.K. Kunnath, 7/20/87, (PB88-134325/AS).

NCEER-87-0009 "Liquefaction Potential for New York State: A Preliminary Report on Sites in Manhattan and Buffalo," by M. Budhu, V. Vijayakumar, R.F. Giese and L. Baumgras, 8/31/87, (PB88-163704/AS). This report is available only through NTIS (see address given above).

NCEER-87-0010 "Vertical and Torsional Vibration of Foundations in Inhomogeneous Media," by A.S. Veletsos and K.W. Dotson, 6/1/87, (PB88-134291/AS).

NCEER-87-0011 "Seismic Probabilistic Risk Assessment and Seismic Margins Studies for Nuclear Power Plants," by Howard H.M. Hwang, 6/15/87, (PB88-134267/AS). This report is available only through NTIS (see address given above).

NCEER-87-0012 "Parametric Studies of Frequency Response of Secondary Systems Under Ground-Acceleration Excitations," by Y. Yong and Y.K. Lin, 6/10/87, (PB88-134309/AS).

NCEER-87-0013 "Frequency Response of Secondary Systems Under Seismic Excitation," by J.A. HoLung, J. Cai and Y.K. Lin, 7/31/87, (PB88-134317/AS).

NCEER-87-0014 "Modelling Earthquake Ground Motions in Seismically Active Regions Using Parametric Time Series Methods," by G.W. Ellis and A.S. Cakmak, 8/25/87, (PB88-134283/AS).

NCEER-87-0015 "Detection and Assessment of Seismic Structural Damage," by E. DiPasquale and A.S. Cakmak, 8/25/87, (PB88-163712/AS).

NCEER-87-0016 "Pipeline Experiment at Parkfield, California," by J. Isenberg and E. Richardson, 9/15/87, (PB88-163720/AS).

NCEER-87-0017 "Digital Simulation of Seismic Ground Motion," by M. Shinozuka, G. Deodatis and T. Harada, 8/31/87, (PB88-155197/AS). This report is available only through NTIS (see address given above).

NCEER-87-0018 "Practical Considerations for Structural Control: System Uncertainty, System Time Delay and Truncation of Small Control Forces," J.N. Yang and A. Akbarpour, 8/10/87, (PB88-163738/AS).

NCEER-87-0019 "Modal Analysis of Nonclassically Damped Structural Systems Using Canonical Transformation," by J.N. Yang, S. Sarkani and F.X. Long, 9/27/87, (PB88-187851/AS).

NCEER-87-0020 "A Nonstationary Solution in Random Vibration Theory," by J.R. Red-Horse and P.D. Spanos, 11/3/87, (PB88-163746/AS).

NCEER-87-0021 "Horizontal Impedances for Radially Inhomogeneous Viscoelastic Soil Layers," by A.S. Veletsos and K.W. Dotson, 10/15/87, (PB88-150859/AS).

NCEER-87-0022 "Seismic Damage Assessment of Reinforced Concrete Members," by Y.S. Chung, C. Meyer and M. Shinozuka, 10/9/87, (PB88-150867/AS). This report is available only through NTIS (see address given above).

NCEER-87-0023 "Active Structural Control in Civil Engineering," by T.T. Soong, 11/11/87, (PB88-187778/AS).

NCEER-87-0024 Vertical and Torsional Impedances for Radially Inhomogeneous Viscoelastic Soil Layers," by K.W. Dotson and A.S. Veletsos, 12/87, (PB88-187786/AS).

NCEER-87-0025 "Proceedings from the Symposium on Seismic Hazards, Ground Motions, Soil-Liquefaction and Engineering Practice in Eastern North America," October 20-22, 1987, edited by K.H. Jacob, 12/87, (PB88-188115/AS).

NCEER-87-0026 "Report on the Whittier-Narrows, California, Earthquake of October 1, 1987," by J. Pantelic and A. Reinhorn, 11/87, (PB88-187752/AS). This report is available only through NTIS (see address given above).

NCEER-87-0027 "Design of a Modular Program for Transient Nonlinear Analysis of Large 3-D Building Structures," by S. Srivastav and J.F. Abel, 12/30/87, (PB88-187950/AS).

NCEER-87-0028 "Second-Year Program in Research, Education and Technology Transfer," 3/8/88, (PB88-219480/AS).

NCEER-88-0001 "Workshop on Seismic Computer Analysis and Design of Buildings With Interactive Graphics," by W. McGuire, J.F. Abel and C.H. Conley, 1/18/88, (PB88-187760/AS).

NCEER-88-0002 "Optimal Control of Nonlinear Flexible Structures," by J.N. Yang, F.X. Long and D. Wong, 1/22/88, (PB88-213772/AS).

NCEER-88-0003 "Substructuring Techniques in the Time Domain for Primary-Secondary Structural Systems," by G.D. Manolis and G. Juhn, 2/10/88, (PB88-213780/AS).

NCEER-88-0004 "Iterative Seismic Analysis of Primary-Secondary Systems," by A. Singhal, L.D. Lutes and P.D. Spanos, 2/23/88, (PB88-213798/AS).

NCEER-88-0005 "Stochastic Finite Element Expansion for Random Media," by P.D. Spanos and R. Ghanem, 3/14/88, (PB88-213806/AS).

NCEER-88-0006 "Combining Structural Optimization and Structural Control," by F.Y. Cheng and C.P. Pantelides, 1/10/88, (PB88-213814/AS).

NCEER-88-0007 "Seismic Performance Assessment of Code-Designed Structures," by H.H-M. Hwang, J-W. Jaw and H-J. Shau, 3/20/88, (PB88-219423/AS).

NCEER-88-0008 "Reliability Analysis of Code-Designed Structures Under Natural Hazards," by H.H-M. Hwang, H. Ushiba and M. Shinozuka, 2/29/88, (PB88-229471/AS).

NCEER-88-0009 "Seismic Fragility Analysis of Shear Wall Structures," by J-W Jaw and H.H-M. Hwang, 4/30/88, (PB89-102867/AS).

NCEER-88-0010 "Base Isolation of a Multi-Story Building Under a Harmonic Ground Motion - A Comparison of Performances of Various Systems," by F-G Fan, G. Ahmadi and I.G. Tadjbakhsh, 5/18/88, (PB89-122238/AS).

NCEER-88-0011 "Seismic Floor Response Spectra for a Combined System by Green's Functions," by F.M. Lavelle, L.A. Bergman and P.D. Spanos, 5/1/88, (PB89-102875/AS).

NCEER-88-0012 "A New Solution Technique for Randomly Excited Hysteretic Structures," by G.Q. Cai and Y.K. Lin, 5/16/88, (PB89-102883/AS).

NCEER-88-0013 "A Study of Radiation Damping and Soil-Structure Interaction Effects in the Centrifuge," by K. Weissman, supervised by J.H. Prevost, 5/24/88, (PB89-144703/AS).

NCEER-88-0014 "Parameter Identification and Implementation of a Kinematic Plasticity Model for Frictional Soils," by J.H. Prevost and D.V. Griffiths, to be published.

NCEER-88-0015 "Two- and Three- Dimensional Dynamic Finite Element Analyses of the Long Valley Dam," by D.V. Griffiths and J.H. Prevost, 6/17/88, (PB89-144711/AS).

NCEER-88-0016 "Damage Assessment of Reinforced Concrete Structures in Eastern United States," by A.M. Reinhorn, M.J. Seidel, S.K. Kunnath and Y.J. Park, 6/15/88, (PB89-122220/AS).

NCEER-88-0017 "Dynamic Compliance of Vertically Loaded Strip Foundations in Multilayered Viscoelastic Soils," by S. Ahmad and A.S.M. Israil, 6/17/88, (PB89-102891/AS).

NCEER-88-0018 "An Experimental Study of Seismic Structural Response With Added Viscoelastic Dampers," by R.C. Lin, Z. Liang, T.T. Soong and R.H. Zhang, 6/30/88, (PB89-122212/AS).

NCEER-88-0019 "Experimental Investigation of Primary - Secondary System Interaction," by G.D. Manolis, G. Juhn and A.M. Reinhorn, 5/27/88, (PB89-122204/AS).

NCEER-88-0020 "A Response Spectrum Approach For Analysis of Nonclassically Damped Structures," by J.N. Yang, S. Sarkani and F.X. Long, 4/22/88, (PB89-102909/AS).

NCEER-88-0021 "Seismic Interaction of Structures and Soils: Stochastic Approach," by A.S. Veletsos and A.M. Prasad, 7/21/88, (PB89-122196/AS).

NCEER-88-0022 "Identification of the Serviceability Limit State and Detection of Seismic Structural Damage," by E. DiPasquale and A.S. Cakmak, 6/15/88, (PB89-122188/AS).

NCEER-88-0023 "Multi-Hazard Risk Analysis: Case of a Simple Offshore Structure," by B.K. Bhartia and E.H. Vanmarcke, 7/21/88, (PB89-145213/AS).

NCEER-88-0024 "Automated Seismic Design of Reinforced Concrete Buildings," by Y.S. Chung, C. Meyer and M. Shinozuka, 7/5/88, (PB89-122170/AS).

NCEER-88-0025 "Experimental Study of Active Control of MDOF Structures Under Seismic Excitations," by L.L. Chung, R.C. Lin, T.T. Soong and A.M. Reinhorn, 7/10/88, (PB89-122600/AS).

NCEER-88-0026 "Earthquake Simulation Tests of a Low-Rise Metal Structure," by J.S. Hwang, K.C. Chang, G.C. Lee and R.L. Ketter, 8/1/88, (PB89-102917/AS).

NCEER-88-0027 "Systems Study of Urban Response and Reconstruction Due to Catastrophic Earthquakes," by F. Kozin and H.K. Zhou, 9/22/88, to be published.

NCEER-88-0028 "Seismic Fragility Analysis of Plane Frame Structures," by H.H-M. Hwang and Y.K. Low, 7/31/88, (PB89-131445/AS).

NCEER-88-0029 "Response Analysis of Stochastic Structures," by A. Kardara, C. Bucher and M. Shinozuka, 9/22/88.

NCEER-88-0030 "Nonnormal Accelerations Due to Yielding in a Primary Structure," by D.C.K. Chen and L.D. Lutes, 9/19/88, (PB89-131437/AS).

NCEER-88-0031 "Design Approaches for Soil-Structure Interaction," by A.S. Veletsos, A.M. Prasad and Y. Tang, 12/30/88.

NCEER-88-0032 "A Re-evaluation of Design Spectra for Seismic Damage Control," by C.J. Turkstra and A.G. Tallin, 11/7/88, (PB89-145221/AS).

NCEER-88-0033 "The Behavior and Design of Noncontact Lap Splices Subjected to Repeated Inelastic Tensile Loading," by V.E. Sagan, P. Gergely and R.N. White, 12/8/88.

NCEER-88-0034 "Seismic Response of Pile Foundations," by S.M. Mamoon, P.K. Banerjee and S. Ahmad, 11/1/88, (PB89-145239/AS).

NCEER-88-0035 "Modeling of R/C Building Structures With Flexible Floor Diaphragms (IDARC2)," by A.M. Reinhorn, S.K. Kunnath and N. Panahshahi, 9/7/88.

NCEER-88-0036 "Solution of the Dam-Reservoir Interaction Problem Using a Combination of FEM, BEM with Particular Integrals, Modal Analysis, and Substructuring," by C-S. Tsai, G.C. Lee and R.L. Ketter, 12/31/88.

NCEER-88-0037 "Optimal Placement of Actuators for Structural Control," by F.Y. Cheng and C.P. Pantelides, 8/15/88.

NCEER-88-0038 "Teflon Bearings in Aseismic Base Isolation: Experimental Studies and Mathematical Modeling," by A. Mokha, M.C. Constantinou and A.M. Reinhorn, 12/5/88.

NCEER-88-0039 "Seismic Behavior of Flat Slab High-Rise Buildings in the New York City Area," by P. Weidlinger and M. Ettouney, 10/15/88, to be published.

NCEER-88-0040 "Evaluation of the Earthquake Resistance of Existing Buildings in New York City," by P. Weidlinger and M. Ettouney, 10/15/88, to be published.

NCEER-88-0041 "Small-Scale Modeling Techniques for Reinforced Concrete Structures Subjected to Seismic Loads," by W. Kim, A. El-Attar and R.N. White, 11/22/88.

NCEER-88-0042 "Modeling Strong Ground Motion from Multiple Event Earthquakes," by G.W. Ellis and A.S. Cakmak, 10/15/88.

NCEER-88-0043 "Nonstationary Models of Seismic Ground Acceleration," by M. Grigoriu, S.E. Ruiz and E. Rosenblueth, 7/15/88.

NCEER-88-0044 "SARCF User's Guide: Seismic Analysis of Reinforced Concrete Frames," by Y.S. Chung, C. Meyer and M. Shinozuka, 11/9/88.

NCEER-88-0045 "First Expert Panel Meeting on Disaster Research and Planning," edited by J. Pantelic and J. Stoyle, 9/15/88.

NCEER-88-0046 "Preliminary Studies of the Effect of Degrading Infill Walls on the Nonlinear Seismic Response of Steel Frames," by C.Z. Chrysostomou, P. Gergely and J.F. Abel, 12/19/88.

NCEER-88-0047 "Reinforced Concrete Frame Component Testing Facility - Design, Construction, Instrumentation and Operation," by S.P. Pessiki, C. Conley, T. Bond, P. Gergely and R.N. White, 12/16/88.

NCEER-89-0001 "Effects of Protective Cushion and Soil Compliancy on the Response of Equipment Within a Seismically Excited Building," by J.A. HoLung, 2/16/89, (PB89-207179/AS).

NCEER-89-0002 "Statistical Evaluation of Response Modification Factors for Reinforced Concrete Structures," by H.H-M. Hwang and J-W. Jaw, 2/17/89, (PB89-207187/AS).

NCEER-89-0003 "Hysteretic Columns Under Random Excitation," by G-Q. Cai and Y.K. Lin, 1/9/89, (PB89-196513/AS).

NCEER-89-0004 "Experimental Study of 'Elephant Foot Bulge' Instability of Thin-Walled Metal Tanks," by Z-H. Jia and R.L. Ketter, 2/22/89, (PB89-207195/AS).

NCEER-89-0005 "Experiment on Performance of Buried Pipelines Across San Andreas Fault," by J. Isenberg, E. Richardson and T.D. O'Rourke, 3/10/89.

NCEER-89-0006 "A Knowledge-Based Approach to Structural Design of Earthquake-Resistant Buildings," by M. Subramani, P. Gergely, C.H. Conley, J.F. Abel and A.H. Zaghw, 1/15/89.

NCEER-89-0007 "Liquefaction Hazards and Their Effects on Buried Pipelines," by T.D. O'Rourke and P.A. Lane, 2/1/89.

NCEER-89-0008 "Fundamentals of System Identification in Structural Dynamics," by H. Imai, C-B. Yun, O. Maruyama and M. Shinozuka, 1/26/89, (PB89-207211/AS).

NCEER-89-0009 "Effects of the 1985 Michoacan Earthquake on Water Systems and Other Buried Lifelines in Mexico," by A.G. Ayala and M.J. O'Rourke, 3/8/89, (PB89-207229/AS).

NCEER-89-0010 "NCEER Bibliography of Earthquake Education Materials," by K.E.K. Ross, 3/10/89.

NCEER-89-0011 "Inelastic Three-Dimensional Response Analysis of Reinforced Concrete Building Structures (IDARC-3D), Part I - Modeling," by S.K. Kunnath and A.M. Reinhorn, 4/17/89.